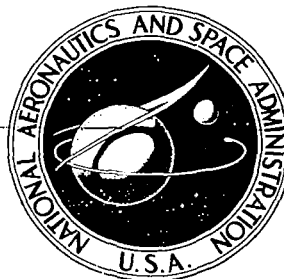


# NASA CONTRACTOR REPORT

NASA CR-1964



NASA CR-19

c.1



**LOAN COPY: RETURN TO  
AFWL (DOVL)  
KIRTLAND AFB, N. M.**

## HIGHLY LOADED MULTI-STAGE FAN DRIVE TURBINE — PLAIN BLADE CONFIGURATION DESIGN

*by D. C. Evans and G. W. Wolfmeyer*

*Prepared by*  
GENERAL ELECTRIC COMPANY  
Cincinnati, Ohio 45215  
*for Lewis Research Center*

NATIONAL AERONAUTICS AND SPACE ADMINISTRATION • WASHINGTON, D. C. • FEBRUARY 1972



0061310

1. Report No. NASA CR-1964	2. Government Accession No.	3. Recipient's Catalog No.	
4. Title and Subtitle <b>HIGHLY LOADED MULTI-STAGE FAN DRIVE TURBINE - PLAIN BLADE CONFIGURATION DESIGN</b>		5. Report Date February 1972	6. Performing Organization Code
		8. Performing Organization Report No. GE R71 AEG 242	
7. Author(s) D. C. Evans and G. W. Wolfmeyer		10. Work Unit No.	
9. Performing Organization Name and Address General Electric Company Cincinnati, Ohio 45215		11. Contract or Grant No. NAS 3-14304	
		13. Type of Report and Period Covered Contractor Report	
12. Sponsoring Agency Name and Address National Aeronautics and Space Administration Washington, D.C. 20546		14. Sponsoring Agency Code	
		15. Supplementary Notes Project Manager, Thomas P. Moffitt, Fluid System Components Division, NASA Lewis Research Center, Cleveland, Ohio	
16. Abstract The constant-inside-diameter flowpath was scaled for testing in an existing turbine test facility. Blading detailed design is discussed, and design data are summarized. Predicted performance maps are presented. Steady-state stresses and vibratory behavior are discussed and the results of the mechanical design analysis are presented.			
17. Key Words (Suggested by Author(s)) Turbine High stage loading Fan engines		18. Distribution Statement Unclassified - unlimited	
19. Security Classif. (of this report) Unclassified	20. Security Classif. (of this page) Unclassified	21. No. of Pages 113	22. Price* \$3.00

\* For sale by the National Technical Information Service, Springfield, Virginia 22151

*Turbojet engines  
Rotor blades*

*8/11/72*



## TABLE OF CONTENTS

<u>Section</u>		<u>Page</u>
I	SUMMARY	1
II	INTRODUCTION	2
III	PRELIMINARY DESIGN	4
IV	DETAILED DESIGN	5
	A. Scaling	5
	B. Streamline Slope and Curvature Effects	6
	C. Blading Aerodynamic Design	6
	1. Selection of Number of Vanes and Blades	6
	2. Blading Profile Design	6
	D. Performance	7
V	MECHANICAL DESIGN	8
	A. Vibratory Behavior	8
	B. Steady-State Behavior .	10
	C. Key Detail Drawings	10
	REFERENCES	11
	TABLES	12
	ILLUSTRATIONS	29



## LIST OF ILLUSTRATIONS

<u>Figure</u>		<u>Page</u>
1.	Effect of Flowpath Slope and Curvature on Angles, Stage One.	29
2.	Effect of Flowpath Slope and Curvature on Angles, Stage Two.	30
3.	Effect of Flowpath Slope and Curvature on Angles, Stage Three.	31
4.	Vector Diagram Nomenclature.	32
5.	Vector Diagrams.	33
6.	Aerodynamic Flowpath.	34
7.	Design Data Nomenclature.	35
8.	Stage One Vane Hub Airfoil Flowpath.	36
9.	Stage One Vane Hub Velocity Distribution.	37
10.	Stage One Vane Pitch Airfoil Flowpath.	38
11.	Stage One Vane Pitch Velocity Distribution.	39
12.	Stage One Vane Tip Airfoil Flowpath.	40
13.	Stage One Vane Tip Velocity Distribution.	41
14.	Stage One Blade Hub Airfoil Flowpath.	42
15.	Stage One Blade Hub Velocity Distribution.	43
16.	Stage One Blade Pitch Airfoil Flowpath.	44
17.	Stage One Blade Pitch Velocity Distribution.	45
18.	Stage One Blade Tip Airfoil Flowpath.	46
19.	Stage One Blade Tip Velocity Distribution.	47
20.	Stage Two Vane Hub Airfoil Flowpath.	48
21.	Stage Two Vane Hub Velocity Distribution.	49

LIST OF ILLUSTRATIONS (Continued)

<u>Figure</u>		<u>Page</u>
22.	Stage Two Vane Pitch Airfoil Flowpath.	50
23.	Stage Two Vane Pitch Velocity Distribution.	51
24.	Stage Two Vane Tip Airfoil Flowpath.	52
25.	Stage Two Vane Tip Velocity Distribution.	53
26.	Stage Two Blade Hub Airfoil Flowpath.	54
27.	Stage Two Blade Hub Velocity Distribution.	55
28.	Stage Two Blade Pitch Airfoil Flowpath.	56
29.	Stage Two Blade Pitch Velocity Distribution.	57
30.	Stage Two Blade Tip Airfoil Flowpath.	58
31.	Stage Two Blade Tip Velocity Distribution.	59
32.	Stage Three Vane Hub Airfoil Flowpath.	60
33.	Stage Three Vane Hub Velocity Distribution.	61
34.	Stage Three Vane Pitch Airfoil Flowpath.	62
35.	Stage Three Vane Pitch Velocity Distribution.	63
36.	Stage Three Vane Tip Airfoil Flowpath.	64
37.	Stage Three Vane Tip Velocity Distribution.	65
38.	Stage Three Blade Hub Airfoil Flowpath.	66
39.	Stage Three Blade Hub Velocity Distribution.	67
40.	Stage Three Blade Pitch Airfoil Flowpath.	68
41.	Stage Three Blade Pitch Velocity Distribution.	69
42.	Stage Three Blade Tip Airfoil Flowpath.	70
43.	Stage Three Blade Tip Velocity Distribution.	71

LIST OF ILLUSTRATIONS (Continued)

<u>Figure</u>		<u>Page</u>
44.	Stage One Vane Precision Master (4012241-942).	72
45.	Stage One Blade Precision Master (4012241-948).	73
46.	Stage Two Vane Precision Master (4012241-944).	74
47.	Stage Two Blade Precision Master (4012241-950).	75
48.	Stage Three Vane Precision Master (4012241-946).	76
49.	Stage Three Blade Precision Master (4012241-952).	77
50.	Stage One Vane Stackup (4012241-943).	78
51.	Stage One Blade Stackup (4012241-949).	79
52.	Stage Two Vane Stackup (4012241-945).	80
53.	Stage Two Blade Stackup (4012241-951).	81
54.	Stage Three Vane Stackup (4012241-947).	82
55.	Stage Three Blade Stackup (4012241-953).	83
56.	Equivalent Torque vs. Total-to-Total Pressure Ratio, One-Stage Configuration.	84
57.	Equivalent Weight Flow vs. Total-to-Total Pressure Ratio, One-Stage Configuration.	85
58.	Equivalent Specific Work vs. Total-to-Total Pressure Ratio, One-Stage Configuration.	86
59.	Total-to-Total Efficiency vs. Blade-Jet Speed Ratio, One-Stage Configuration.	87
60.	Equivalent Specific Work vs. Weight Flow-Speed Para- meter, One-Stage Configuration.	88
61.	Equivalent Torque vs. Total-to-Total Pressure Ratio, Two-Stage Configuration.	89
62.	Equivalent Weight Flow vs. Total-to-Total Pressure Ratio, Two-Stage Configuration.	90



LIST OF ILLUSTRATIONS (Concluded)

<u>Figure</u>		<u>Page</u>
63.	Equivalent Specific Work vs. Total-to-Total Pressure Ratio, Two-Stage Configuration.	91
64.	Total-to-Total Efficiency vs. Blade-Jet Speed Ratio, Two-Stage Configuration.	92
65.	Equivalent Specific Work vs. Weight Flow - Speed Parameter, Two-Stage Configuration.	93
66.	Equivalent Torque vs. Total-to-Total Pressure Ratio, Three-Stage Configuration.	94
67.	Equivalent Weight Flow vs. Total-to-Total Pressure Ratio, Three-Stage Configuration.	95
68.	Equivalent Specific Work vs. Total-to-Total Pressure Ratio, Three-Stage Configuration.	96
69.	Total-to-Total Efficiency vs. Blade-Jet Speed Ratio, Three-Stage Configuration.	97
70.	Equivalent Specific Work vs. Weight Flow-Speed Parameter, Three-Stage Configuration.	98
71.	Swirl Map, One-Stage Configuration.	99
72.	Swirl Map, Two-Stage Configuration.	100
73.	Swirl Map, Three-Stage Configuration.	101
74.	Most Probable Modes of Vibration, Stage One Blade.	102
75.	Most Probable Modes of Vibration, Stage Two Blade.	103
76.	Most Probable Modes of Vibration, Stage Three Blade.	104
77.	Mechanical Design Flowpath.	105

## LIST OF SYMBOLS

A	Area (in. <sup>2</sup> )
A <sub>w</sub>	Axial width (in.)
C <sub>f</sub>	Flow coefficient
D	Diameter (in.)
d <sub>o</sub>	Throat dimension (in.)
Δh	Turbine energy extraction (Btu/lbm)
h <sub>ex</sub>	Height at blade row exit (in.)
h <sub>th</sub>	Height at blade row throat (in.)
M	Mach Number
N	Rotational Speed (rev/min)
n	Number of vanes or blades
P <sub>S</sub>	Static pressure (psia)
P <sub>T</sub>	Total pressure (psia)
T <sub>HLE</sub>	Blade temperature at hub leading edge (°F)
T <sub>S</sub>	Static temperature (°R)
T <sub>T</sub>	Total temperature (°R)
t	Spacing (in.)
t <sub>e</sub>	Trailing edge thickness (in.)
t <sub>max.</sub>	Maximum thickness (in.)
U	Wheel speed (ft/sec)
W	Mass flow rate (lbm/sec)

LIST OF SYMBOLS (Continued)

$\alpha_0$	Vane inlet absolute flow angle (degrees)
$\alpha_1$	Vane exit absolute flow angle (degrees)
$\beta_1$	Blade inlet relative flow angle (degrees)
$\beta_2$	Blade exit relative flow angle (degrees)
$\Gamma$	Stage leaving swirl angle (degrees)
$\eta_B$	Blade efficiency
$\eta_{TT}$	Total-to-Total efficiency
$\eta_V$	Vane efficiency
$v$	Blade-jet speed ratio
$\sigma$	Stress (ksi)
$\sigma_C$	Centrifugal stress (ksi)
$\sigma_{LE}$	Stress at blade leading edge (ksi)
$\sigma_{TE}$	Stress at blade trailing edge (ksi)
$\sigma_{Hi-c}$	Stress at maximum distance from axis of least moment of inertia, convex surface (ksi)
$\sigma_{Midcv}$	Stress at maximum distance from axis of least moment of inertia, concave surface (ksi)
$\sigma_{lmi}$	Stress due to bending moment about axis of least moment of inertia (ksi)
$\sigma_{mmi}$	Stress due to bending moment about axis of maximum moment of inertia (ksi)
$\tau_{eq}$	Equivalent torque (ft-lbf)
$\psi_{Zwei}$	Zweifel number
$gJ\Delta h/2U^2$	Loading factor

**LIST OF SYMBOLS (Concluded)**

$E/\theta_{cr}$	Equivalent specific work (Btu/lbm)
$W\sqrt{\theta_{cr}} \epsilon/\delta$	Equivalent weight flow (lbm/sec)
$N/\sqrt{\theta_{cr}}$	Equivalent rotative speed (rev/min)
$WN\epsilon/60\delta$	Weight flow - speed parameter

## I. SUMMARY

The results of the Task III detailed design of the plain blade configuration turbine are presented. The constant-inside-diameter flowpath was scaled to a 28.4 inch exit tip diameter for testing in an existing air turbine test facility. Final vector diagram calculations were made taking into account streamline slope and curvature effects. The number of vanes and blades was selected based on Zweifel loading criteria. Vane and blade section coordinates were generated and detailed design data was summarized. Predicted turbine performance maps were generated. Steady state stresses and vibratory behavior were predicted. No stress problems are expected during air turbine testing.

## II. INTRODUCTION

The development of high-bypass-ratio turbofan engines for future aircraft propulsion schemes requires the development of fan drive turbines with increasingly higher work output. The requirements of minimized weight and size of such turbofan engines produce a need for turbines with increasingly high stage loading. In order to maintain high turbine efficiencies at high stage loading, advances are required in the technology of producing increased aerodynamic load capability in turbine blading by means of improved design techniques and high-lift devices.

The specific objectives of this program are to:

- Investigate analytically and experimentally aerodynamic means for increasing the turbine stage loading and turbine blade loading consistent with high efficiency for multistage highly loaded fan drive turbine configurations.
- Develop sufficient design information to determine the relative importance of changes in engine size, weight, and performance and give primary consideration to use of tandem rotors and stators, where applicable, to reduce weight or extend or improve the blading performance.
- Modify an existing three-stage highly loaded turbine rig and adapt the rig to an overall performance test program of sufficient extent so as to obtain blade element performance.

This is a 24-month analytical and experimental investigation program to provide a turbine high-stage-loading and high-blade-loading aerodynamic technology that will be specifically applicable to multistage fan drive turbine configurations for advanced high-bypass-ratio turbofan propulsion system application. The program will be divided into two phases encompassing nine task items of activity.

The first phase will cover Task Items I, II and III of the program which are to investigate requirements of selected advanced high-bypass-ratio turbofan systems, to carry out parametric turbine vector diagram studies, to conduct a cascade test and evaluation program, to select one design for future study, to complete a detailed aerodynamic turbine design for an existing rig, to complete the detailed blading aerodynamic design for the rig, to perform detailed blading mechanical design for the rig, to perform the turbine rig mechanical design, and to prepare the turbine rig modification drawings required to utilize the existing three-stage highly-loaded-fan turbine rig. The second phase will cover Task Items IV through IX of this proposed program to fabricate, procure, vibration bench test, fatigue endurance test, and inspect the turbine rig modifications; to instrument and calibrate the rig vehicle; to conduct a test program and to report progress, analysis, and design, as well as test and performance results.

The Task I vector diagram study results have been reported (Reference 1). Based on the results of this study, a velocity diagram was chosen for three highly loaded turbine configurations: (1) a turbine using plain blades, (2) a turbine using tandem blades and (3) another turbine using high lift devices. The purpose of this report is to present the Task III detailed design of the turbine using plain blades.

### III. PRELIMINARY DESIGN

The fan turbine to be investigated in this program have the following design requirements:

Average Pitch Loading $\frac{gJ\Delta h}{2U_p^2}$	1.5
Equivalent Specific Work	33.0 Btu/lb
Equivalent Rotative Speed	2000 rpm
Equivalent Weight Flow	70 lb/sec
Inlet Swirl Angle	0 degrees
Exit Swirl Angle Without Guide Vanes	$\cong$ 5 degrees
Maximum Tip Diameter	45.0 inches
Number of Stages	3
$W\sqrt{T_T}/P_T$ at Inlet	108.4
$\Delta h/T_T$	0.0635
$N/\sqrt{T_T}$	87.7

The results of the Task I Vector Diagram Study indicated that the most promising turbine for these requirements would be a constant-inside-diameter flowpath with a stage energy split ( $\Delta h_{\text{stage}}/\Delta h_{\text{turbine}}$ ) of 11.7% on stage one, 38.3% on stage two, and 20.0% on stage three. The corresponding stage aerodynamic loading, ( $gJ\Delta h/2U^2$ ), would be 2.1, 1.75, and 0.82 at the pitch on stages one, two, and three, respectively. This was the type of vector diagram calculation which was pursued in the Task III plain blading detailed design of the Highly Loaded Multi-Stage Fan Drive Turbine Program.



#### IV. DETAILED DESIGN

##### A. SCALING TO AIR TURBINE RIG

The design requirements described above were based on engine fan drive turbine requirements and specifications. A plan was formulated to modify an existing three stage highly loaded fan turbine rotating rig for the test and performance phase of this program. The constant-inside-diameter flowpath selected was scaled to an exit tip diameter of 28.4 inches.

In order to maintain performance similarity between the full scale turbine and the scaled air turbine, appropriate scaling factors were applied to the design requirements to assure geometric and dynamic similarity. The parameters used for scaling were

$$\frac{ND}{\sqrt{\theta_{cr}}}, \quad \frac{\Delta h}{\theta_{cr}}, \quad \text{and} \quad \frac{W_{\sqrt{\theta_{cr}}} \epsilon}{\delta A}$$

Thus, the scaled fan turbines to be investigated have the following design requirements:

Average Pitch Loading $\frac{gJ\Delta h}{2U_p^2}$	1.5
Equivalent Specific Work	33.0 Btu/lb
Equivalent Rotative Speed	3169.0 rpm
Equivalent Weight Flow	28.0 lb/sec
Inlet Swirl Angle	0 degrees
Exit Swirl Angle Without Guide Vanes	≅ 5 degrees
Maximum Tip Diameter	28.4 inches
Number of Stages	3
$W_{\sqrt{T_T}}/P_T$ at Inlet	43.16
$\Delta h/T_T$	0.0635
$N/\sqrt{T_T}$	138.98

## B. STREAMLINE SLOPE AND CURVATURE EFFECTS

Having determined the most promising stage energy distribution for the constant-inside-diameter flowpath, final axisymmetric calculations were performed using a computer program which accounts for the radial variation in streamline slope and curvature. The vector diagram angles obtained by accounting for streamline slope and curvature are compared to the vector diagram angles obtained from the preliminary design free vortex calculation in Figures 1, 2, and 3. The variation in streamline slope and curvature effected an increase in the tip inlet and exit angles, and a decrease in the hub inlet and exit angles.

The blading aerodynamic design proceeded using the vector diagram angles which accounted for the streamline slope and curvature effect. The vector diagram nomenclature and the final design vector diagrams are shown in Figures 4 and 5. A summary of the vector diagram calculation results is shown in Table I.

## C. BLADING AERODYNAMIC DESIGN

### 1. Selection of Number of Vanes and Blades

Vane and blade solidities were determined through selection of Zweifel Numbers based on General Electric design experience using the Zweifel loading criteria. The vane and blade axial widths and the number of vanes and blades were set such that no performance loss would be expected due to trailing edge blockage.

After the vane and blade axial widths had been determined, the aerodynamic flowpath was finalized and is presented in Figure 6.

### 2. Blading Profile Design

The vane and blade throat openings were calculated using the following equations:

$$nd_{OV} = \pi D \cos \alpha_1 (\sqrt{\eta V} / C_f) \frac{h_{ex}}{h_{th}} \quad \text{and}$$

$$nd_{OB} = \pi D \cos \beta_2 (\sqrt{\eta_B} / C_f) \frac{h_{ex}}{h_{th}}$$

These equations were the result of applying the law of conservation of mass between the throat and downstream of each blade row. The terms for these equations are shown in Figure 7.

The vane and blade hub, pitch, and tip profiles were then generated with the aid of a computer program in which the section coordinates are developed from a small number of numerical inputs. An analysis of flow conditions through each blade section passage was conducted

## C. 2. CONTINUED

using a potential flow cascade analysis computer program. Design iterations on the vane and blade section profiles were made until satisfactory velocity distributions around each profile were obtained. The vane hub, pitch, and tip sections were stacked on the trailing edge.

The center of gravity was calculated for each blade hub, pitch, and tip section, and the stacking axis was located to pass through each section c.g.. A summary of parameters describing the blading design is presented in Tables II through VII. Figure 7 defines these parameters. The final vane and blade hub, pitch, and tip airfoil flowpaths and velocity distributions are presented in Figures 8 through 43.

A computer program was employed to generate the coordinates of the sections intermediate to the hub, pitch, and tip. Sections were interpolated at 10%, 30%, 70%, and 90% trailing edge height for each vane and blade. These coordinates were then used to generate the precision masters required for the fabrication of the vanes and blades. Reduced copies of the vane and blade precision masters are presented in Figures 44 through 49. Figures 50 through 55 show the stacked vane and blade sections for each blade row.

## D. PERFORMANCE

The performance of the one-stage, two-stage, and three-stage configurations was predicted with the aid of the "Analytical Procedure and Computer Program for Determining the Off-Design Performance of Axial Flow Turbines" (Reference 2).

Turbine performance maps for each configuration are presented in Figures 56 through 70 in the following format:

- 1) Equivalent torque vs. total-to-total pressure ratio
- 2) Equivalent weight flow vs. total-to-total pressure ratio
- 3) Equivalent specific work vs. total-to-total pressure ratio
- 4) Total-to-total efficiency vs. blade-jet speed ratio
- 5) Equivalent specific work vs. weight flow speed parameter with lines of constant total-to-total pressure ratio, constant speed and with efficiency contours.

The turbine exit swirl maps shown in Figures 71 through 73 are based on calculations derived from the rotor blade exit vector diagram analysis. The swirl angle is presented as a function of the exit flow function,  $(W\sqrt{T_{T2}}/P)$  and speed parameter,  $(N\sqrt{T_{T2}})$ .

## V. MECHANICAL DESIGN

### A. VIBRATORY BEHAVIOR

In the analysis of a tip shrouded blade, the fundamental question becomes one of choosing the appropriate shroud boundary conditions for both vibratory and steady-state operation. Conditions are generally chosen on the basis of such factors as blade length versus disc stiffness, shroud configuration, etc. Thus, several sets of conditions were chosen in an attempt to simulate various modes of behavior. From those conditions, the modes which seemed most likely to occur were extracted and are described below.

1. Cantilevered Mode - Cantilevered at the base of the shank, free at the tip shroud. This condition was used only to determine the amount of steady-state tip shroud twist or untwist and to obtain lower bounds on certain resonant frequencies.
2. Out of Phase Mode - Fixed at the base of the shank, pinned at the tip shroud. The flexure and torsion modes obtained for these conditions will probably exist under operating conditions.
3. Wheel Mode - Fixed at the base of the shank, restrained at the tip shroud in all directions except axially. Simulates blade behavior in a wheel mode. The flexure, axial, and torsion modes obtained for these conditions will exist under operating conditions.
4. Free Slip Mode - Fixed at the base of the shank, adjacent tip shrouds allowed to slip relative to each other. The axial and torsion modes obtained for these conditions may exist during turbine operation. Steady stresses obtained for this set of conditions are probably the most realistic.

Although the above four conditions appear to yield values covering a wide range of frequencies, the results are quite consistent and have been reduced to a set of "Most Probable Frequencies of Vibration" as shown on Campbell Diagrams in Figures 74 through 76 and tabulated below. The most probable frequencies of vibration represent frequencies at the design speed, and small differences resulting from the various tip shroud boundary conditions have been averaged out.

#### Most Probable Frequencies of Vibration

<u>Mode</u>	<u>Stage 1</u>	<u>Stage 2</u>	<u>Stage 3</u>	<u>Modes Used To Obtain Averages</u>
First Flexure	3656 cps	2191 cps	1242 cps	2, 3
First Axial	1402	849	514	1, 3, 4
First Torsional	4194	2573	1741	2, 3, 4
Second Flexure	Above	7068	4635	2, 3
Second Torsional	Operating Range	4951	3387	2, 3, 4

## A. CONTINUED

Frequencies were calculated only at the design speed, and frequency versus RPM curves are represented on Figures 74 through 76 as straight lines through these points. Most of the modes will exhibit a change in frequency with RPM due to the temperature effect and centrifugal stiffening, but these effects will not change the conclusions discussed below and thus have been ignored. Estimated vibratory capabilities are summarized in Table VIII.

It does not appear that there will be any significant resonances, particularly of the lower order vibratory modes (First Flex, First Axial, First Torsion, and Second Flex), within the operating speed range for the stage two blade.

The stage one blade First Flex natural frequency has a nozzle passing resonance (64/rev) near the design speed. In addition, the First Torsion mode is within 5% of being resonant at design speed. However, uncorrected gas bending stresses, traditionally an indicator of the level of separated flow vibratory response, are lower than those encountered in certain engine design experience. This fact would indicate substantial margin, within the realm of design practice, to account for any aerodynamic peculiarities which may be present near resonance in the air turbine. Also included in this margin would be possible differences from full-scale engines in calculated limits due to materials, temperatures, and loading. The primary concern is generally given to the possibility of lower order resonances (1-10 cycles per revolution). The analysis showed no such resonances among the "Most Probable Modes of Vibration" for the stage one blade. See Figure 74. On the basis of this information, it is expected that no serious vibratory stress problems will be encountered during air turbine testing.

The stage three blade has a "Most Probable First Axial" mode with a 10 cycle per revolution resonance at approximately 80% design speed. See Figure 76. As noted above, lower order resonances are generally of major importance. Concern for this particular resonance can be minimized when one notes that the stimuli are 10 struts approximately 15 inches forward of the stage three blades, with three stages of vanes and two stages of blades in between to weaken the stimuli.

## B. STEADY-STATE BEHAVIOR

Steady-state mechanical stresses were calculated for the Free Slip tip shroud boundary conditions. These conditions were felt to be the most realistic for steady-state operation. The stresses (centrifugal and gas bending) were found to be quite low for all three stages. The

## B. CONTINUED

steady-state stress results are presented in Table VIII. The results of the analysis showed that the shrouds on all three stages lock up throughout the entire operating range of speed.

## C. KEY DETAIL DRAWINGS

The mechanical design flowpath for the air turbine test rig is shown in Figure 77. Key detail drawings used for the assembly of the test rig are listed in Table IX.

## REFERENCES

1. Evans, D.C., "Investigation of a Highly Loaded Multistage Fan Drive Turbine, Report for Task I - Vector Diagram Study," NASA CR-1862, July, 1971.
2. Flagg, E.E., "Analytical Procedure and Computer Program for Determining the Off-Design Performance of Axial-Flow Turbines," NASA CR-710, March, 1966.

Table I. Vector Diagram Calculation Results

NASA TURBINE COMPUTER PROGRAM  
 NAME G W WOLFMEYER 2-10-71 SCALED FLOWPATH 28.4/45  
 TITLE NASA HLMSFT PERFORMANCE MAP

CASE 1, 2  
 STAGE PERFORMANCE

	STAGE 1	STAGE 2	STAGE 3
TT 0	700.0	624.5	553.3
PT 0	30.000	18.895	11.620
WG 0	49.389	49.389	49.389
DEL H	18.185	17.084	9.188
WRT/P 1	43.557	65.323	99.983
DH/T 1	0.02598	0.02735	0.01660
N/RT 1	138.977	147.133	156.314
ETA TT	0.87470	0.87912	0.88672
ETA TS	0.59854	0.60630	0.64783
ETA AT	0.71035	0.73602	0.88487
PT0/PS1	1.7525	1.6692	1.4360
PT0/PT2	1.5877	1.6261	1.3287
PT0/PS2	2.0396	2.1097	1.4847
PIR1A/PS2	1.6137	1.6647	1.2.73
TT2/TT0	0.89220	0.88599	0.93075
TIR1/TT0	0.93998	0.93851	0.95182
PS 1	17.118	11.335	8.102
YTR 1	658.0	586.1	526.7
PTR 1	23.694	14.875	9.664
PS 2	14.709	8.956	7.826
TT 2	624.5	553.3	515.0
PT 2	18.895	11.620	8.745
UP/VI	0.26879	0.29331	0.43614
UR/VI	0.23144	0.23999	0.33838
PSI P	2.06944	1.75550	0.84890
PSI R	2.79126	2.62228	1.41026
RX P	0.19620	0.29220	0.08276
RX R	0.08264	0.14544	-0.19428
ALPHA 0	0.	44.434	40.342
I STATOR	0.	-0.315	0.312
BETA 1A	48.650	45.210	29.284
I ROTOR	-0.549	-0.039	1.084
ALPHA 2	44.434	40.342	3.206
DBETA R	112.768	110.511	80.584
M 1	0.91668	0.87252	0.72544
M1 RT	1.02092	1.00829	0.84787
MR 1A	0.67277	0.61423	0.48057
MR1A RT	0.80070	0.78089	0.62731
MR 2	0.83164	0.85943	0.54472
MR2 TIP	0.80763	0.83624	0.56808
MF 2A	0.42353	0.45915	0.40735
E/TH CR	13.493	14.196	8.612
N/RTH CR	3167.3	3351.9	3559.8
WRTWCRE/D	28.1	42.2	64.5

OVRALL PERFORMANCE

PSI B	1.51511	RSI R	2.27460	DEL H	44.45695
WRT/P	43.55717	N/RT	138.97716	DELH/T	0.06351
PT0/PT2	3.43040	RT0/PS2	3.83315	PT/PAT2	3.41889
ETA TT	0.89147	ETA TS	0.83010	ETA TAT	0.89110
WNE/60D	1485.38728	N/RTH CR	3167.33063	E/TH CR	32.98690

TURBINE COMPUTER PROGRAM  
 NAME G W WOLFMEYER 2-10-71 SCALED FLOWPATH 28.4/45  
 TITLE NASA WLMST PERFORMANCE MAP

CASE 1. 2  
 INTER-STAGE PERFORMANCE

STA 0	STATOR	INLET	STAGE 1.				
DIAM 0	17.800	17.811	18.529	19.945	21.361	22.079	22.090
YT 0	700.0	700.0	700.0	700.0	700.0	700.0	700.0
PT 0	30.000	30.000	30.000	30.000	30.000	30.000	30.000
ALPHA 0	0.	0.	0.	0.	0.	0.	0.
I STA 0	0.	0.	0.	0.	0.	0.	0.
V 0	501.624	501.624	501.624	501.624	501.624	501.624	501.624
VU 0	0.	0.	0.	0.	0.	0.	0.
VZ 0	501.624	501.624	501.624	501.624	501.624	501.624	501.624
YS 0	679.2	679.2	679.2	679.2	679.2	679.2	679.2
PS 0	26.975	26.975	26.975	26.975	26.975	26.975	26.975
DENS 0	0.10719	0.10719	0.10719	0.10719	0.10719	0.10719	0.10719
M 0	0.39327	0.39327	0.39327	0.39327	0.39327	0.39327	0.39289

STA 1	STATOR	EXIT					
DIAM 1	17.800	17.813	18.677	20.380	22.083	22.947	22.960
YT 1	700.0	700.0	700.0	700.0	700.0	700.0	700.0
ALPHA 1	61.047	61.029	60.099	58.869	59.099	60.099	60.085
DEL A	61.047	61.029	60.099	58.869	59.099	60.099	60.085
V 1	1203.999	1203.332	1164.273	1099.483	1034.197	1005.312	1004.888
VU 1	1053.516	1052.753	1009.295	941.144	887.399	871.493	871.003
VZ 1	582.854	582.854	580.394	568.429	531.118	501.151	501.151
YS 1	580.0	580.1	587.8	599.9	611.5	616.3	616.4
PS 1	15.134	15.146	15.298	17.118	18.349	18.887	18.895
DENS 1	0.07043	0.07047	0.07296	0.07702	0.08100	0.08271	0.08274
M 1	1.02092	1.02024	0.98067	0.91668	0.85408	0.82693	0.82654
ZWI INC	-0.8472	-0.8475	-0.8643	-0.8851	-0.8813	-0.8643	-0.8645
CP S	0.8264	0.8262	0.8144	0.7918	0.7647	0.7510	0.7508

	STATOR FORCES						
AVG DIA	17.800	17.812	18.603	20.163	21.722	22.513	22.525
FTAN/IN	-597.9	-597.9	-603.4	-618.1	-635.2	-649.9	-649.9
			R TAN	-601.7			
FAX/IN	704.5	703.7	663.7	593.2	527.4	504.9	504.3
			F AX	1408.7			
F DRUM	0.						-706.0



TURBINE COMPUTER PROGRAM  
 NAME G W WOLFMEYER 3-10-71 SCALED FLOWPATH 28.4/45  
 TITLE NASA HLMSFT PERFORMANCE MAP

CASE 1, 2  
 INTER-STAGE PERFORMANCE

STA 1A	ROTOR INLET		STAGE 1				
DIAM 1A	17.800	17.813	18.713	20.485	22.557	23.157	23.170
ITR 1A	656.9	656.9	657.4	658.0	658.5	658.3	658.3
PTR 1A	23.457	23.458	23.555	23.694	23.816	23.808	23.810
BETA 1A	54.225	54.189	52.179	48.650	46.390	46.301	46.259
I ROTOR	-0.776	-0.780	-0.601	-0.549	0.171	1.502	1.502
R 1A	946.532	945.713	893.200	809.474	722.817	680.638	680.121
RU 1A	767.934	766.925	707.142	607.661	523.359	492.088	491.372
MR 1A	0.80071	0.79992	0.75197	0.67277	0.59510	0.55825	0.55779
U 1A	285.581	285.796	308.228	328.659	357.090	371.521	371.737

STA 2	ROTOR EXIT						
DIAM 2	17.800	17.815	18.840	20.860	22.880	23.905	23.920
BETA 2	58.586	58.579	58.029	57.599	58.749	60.139	60.138
DBETA	112.811	112.768	110.208	106.249	105.139	106.440	106.397
R 2	1005.990	1005.779	999.345	980.034	964.365	955.613	955.579
RU 2	858.538	858.292	844.367	827.461	824.438	828.742	828.702
MR 2	0.85787	0.85766	0.84708	0.83164	0.81601	0.80767	0.80763
U 2	285.581	285.827	302.273	334.675	367.078	383.524	383.770
RX	0.08299	0.08365	0.12512	0.19620	0.26704	0.29880	0.29926
DEL H	17.810	17.810	17.880	18.123	18.493	18.850	18.850
PSI	5.46750	5.45868	4.93261	4.12452	3.53082	3.31046	3.30642
ETA TT	0.86190	0.86190	0.86655	0.87418	0.88188	0.88553	0.88553
ETA TS	0.55491	0.55491	0.56928	0.59603	0.62690	0.64629	0.64629
ETA AT	0.65681	0.65681	0.67722	0.71145	0.73861	0.74999	0.74999
ZWI INC	-1.6437	-1.6431	-1.6207	-1.5573	-1.4521	-1.3824	-1.3817
CP R	0.1147	0.1159	0.1911	0.3178	0.4382	0.4927	0.4934

	ROTOR FORCES						
AVG DIA	17.800	17.814	18.777	20.673	22.568	23.531	23.545
F TAN/IN	720.5	720.4	722.5	731.1	744.9	758.8	758.8
			F TAN	2108.0			
F AX/IN	146.3	146.0	163.9	196.9	234.5	253.5	253.8
			F AX	570.5			
F DRUM	0.						-475.6

STA 2A	STAGE EXIT						
DIAM 2A	17.800	17.816	18.876	20.965	23.054	24.114	24.130
PI 2A	18.951	18.951	18.965	18.921	18.814	18.673	18.673
TT 2A	626.1	626.1	625.8	624.8	623.3	621.8	621.8
V 2A	762.346	761.964	739.464	700.367	657.259	631.645	631.443
VU 2A	572.957	572.448	541.069	490.318	453.903	441.350	441.061
ALPH 2A	48.727	48.701	47.029	44.434	43.678	44.325	44.306
MF 2A	0.42817	0.42815	0.42820	0.42353	0.40145	0.38123	0.38122
VZ 2A	502.883	502.883	504.035	500.103	475.354	451.869	451.869
TS 2A	574.8	574.9	577.4	581.0	584.2	585.4	585.4
PS 2A	14.283	14.287	14.542	14.918	15.265	15.394	15.396
DENS 2A	0.06707	0.06708	0.06798	0.06931	0.07052	0.07097	0.07098
M 2A	0.64908	0.64872	0.62820	0.59313	0.55507	0.53290	0.53272

TURBINE COMPUTER PROGRAM.  
 NAME G W WOLFMEYER 2-10-71 SCALED FLOWPATH 28.4/45  
 TITLE NASA HLMSFT PERFORMANCE MAP

CASE 1. 2  
 INTER-STAGE PERFORMANCE

STA 0	STATOR INLET		STAGE 2.				
DIAM 0	17.800	17.816	18.876	20.965	23.854	24.114	24.130
IT 0	626.1	626.1	625.8	624.8	623.3	621.8	621.8
PT 0	18.951	18.951	18.965	18.921	18.814	18.673	18.673
ALPHA 0	48.727	48.701	47.029	44.434	43.678	44.325	44.306
I SPA 0	-0.548	-0.548	-0.420	-0.315	0.128	1.026	1.026
V 0	762.346	761.964	739.464	700.367	657.259	631.645	631.443
VU 0	572.957	572.448	541.069	490.318	453.903	441.350	441.061
VZ 0	502.883	502.883	504.035	500.103	475.354	451.869	451.869
YS 0	577.9	574.9	577.4	581.0	584.2	585.4	588.7
PS 0	14.554	14.287	14.542	14.918	15.265	15.394	15.699
DENS 0	0.06798	0.06708	0.06798	0.06931	0.07052	0.07097	0.07198
M 0	0.64734	0.64872	0.62820	0.59313	0.55507	0.53290	0.53081

STA 1	STATOR EXIT						
DIAM 1	17.800	17.818	19.043	21.455	23.867	25.092	25.110
IT 1	626.1	626.1	625.8	624.8	623.3	621.8	621.8
ALPHA 1	61.344	61.319	59.919	58.529	58.149	58.199	58.180
DEL A	110.070	110.020	106.948	102.963	101.827	102.524	102.487
V 1	1127.347	1126.457	1076.782	995.862	909.570	867.620	867.164
VU 1	989.261	988.247	931.758	849.376	772.610	737.377	736.840
VZ 1	540.624	540.624	539.709	519.906	479.991	457.210	457.210
YS 1	520.4	520.6	529.4	542.4	554.3	559.2	559.3
PS 1	9.701	9.712	10.347	11.335	12.823	12.719	12.724
DENS 1	0.05031	0.05035	0.05275	0.05641	0.05998	0.06139	0.06141
M 1	1.00829	1.00733	0.95486	0.87252	0.78814	0.74862	0.74818
ZWL INC	-1.3657	-1.3665	-1.4068	-1.4250	-1.4283	-1.4382	-1.4387
CP S	0.5427	0.5424	0.5284	0.5054	0.4778	0.4700	0.4698

	STATOR FORCES						
AVG DIA	17.800	17.817	18.959	21.210	23.461	24.603	24.620
FTAN/IN	-588.5	-588.5	-592.3	-605.0	-614.4	-619.9	-619.9
			F TAN	-593.7			
FAX/IN	322.3	307.7	283.5	242.1	188.7	158.9	180.0
			F AX	810.4			
F DRUM	0.						-538.6

TURBINE COMPUTER PROGRAM.  
 NAME G W WOLFMEYER 2-10-71 SCALED FLOWPATH 28.4748  
 TITLE NASA HLMSFT PERFORMANCE MAP

CASE 1: 2  
 INTER-STAGE PERFORMANCE

STA 1A - ROTOR INLET		STAGE 2					
DIAM 1A	17.800	17.819	19.082	21.570	24.058	25.321	25.340
YTR 1A	585.9	585.9	986.3	586.1	584.5	586.1	586.2
PTR 1A	14.692	14.693	14.792	14.879	14.997	14.999	15.001
BETA 1A	53.565	53.512	50.371	45.210	39.828	36.758	36.686
I ROTOR	-0.682	-0.687	-0.598	-0.039	0.229	0.208	0.205
R 1A	874.651	873.566	809.798	702.808	594.070	542.159	541.653
RU 1A	703.680	702.331	623.703	498.781	380.493	324.446	323.600
MR 1A	0.78089	0.77980	0.71654	0.61423	0.51355	0.46676	0.46629
U 1A	285.581	285.884	306.146	346.067	385.987	406.250	406.552

STA 2 ROTOR EXIT							
DIAM 2	17.800	17.821	19.208	21.940	24.672	26.059	26.080
BETA 2	57.008	56.999	56.299	55.799	57.149	58.069	58.070
DB, YA	110.573	110.511	106.671	101.009	96.977	94.827	94.756
R 2	980.706	980.461	969.515	952.446	938.682	930.300	930.331
RU 2	822.567	822.275	806.583	787.741	788.068	789.532	789.570
MR 2	0.88941	0.88914	0.87728	0.85943	0.84410	0.83622	0.83624
U 2	285.581	285.913	308.164	352.003	395.841	418.092	418.424
RX	0.14586	0.14679	0.20212	0.29220	0.38416	0.42560	0.42609
DEL H	16.713	16.713	16.805	17.092	17.297	17.337	17.337
PSI	5.13058	5.11920	4.45951	3.51235	2.83350	2.55447	2.55054
EYA YT	0.86400	0.86400	0.86967	0.87883	0.88676	0.88998	0.88998
EYA YS	0.55366	0.55366	0.57123	0.60439	0.63803	0.65503	0.65503
EYA AT	0.66838	0.66838	0.69459	0.73834	0.76907	0.78263	0.78263
ZWI INC	-1.7167	-1.7157	-1.6668	-1.5663	-1.4622	-1.3156	-1.3145
CP R	0.2046	0.2062	0.3023	0.4555	0.5990	0.6604	0.6610

ROTOR FORCES							
AVG DIA	17.800	17.820	19.145	21.755	24.365	25.690	25.710
FYAN/IN	466.5	466.5	668.6	475.9	480.9	481.8	481.8
			F TAN	1878.7			
FAX/IN	106.1	106.5	128.2	167.1	215.5	238.6	238.8
			F AX	673.9			
F DRUM	0.						-331.0

STA 2A STAGE EXIT							
DIAM 2A	17.800	17.821	19.252	22.070	24.888	26.319	26.340
PT 2A	11.699	11.699	11.711	11.635	11.536	11.443	11.443
YT 2A	556.5	556.5	955.8	553.6	551.2	549.5	549.5
V 2A	742.713	742.248	715.913	669.152	620.575	594.713	594.529
VU 2A	536.986	536.342	497.275	433.172	388.826	367.780	367.482
ALPH 2A	46.303	46.269	43.996	40.342	38.797	38.201	38.178
MF 2A	0.46450	0.46447	0.46507	0.45915	0.43424	0.41921	0.41920
VZ 2A	513.097	513.097	515.023	510.026	483.660	467.356	467.356
TS 2A	507.6	507.7	510.2	513.3	514.1	517.1	517.1
PS 2A	8.640	8.644	8.842	9.104	9.343	9.427	9.429
DENS 2A	0.04594	0.04596	0.04678	0.04787	0.04886	0.04921	0.04922
M 2A	0.67237	0.67191	0.64647	0.60240	0.55716	0.53344	0.53327

TURBINE COMPUTER PROGRAM  
 NAME G W WOLFMEYER 2-10-71 SCALED FLOWPATH 28.4/45  
 TITLE NASA HLMSFT PERFORMANCE MAP

CASE 1. 2  
 INTER-STAGE PERFORMANCE

STA 0	STATOR INLET		STAGE 3				
DIAM 0	17.800	17.821	19.252	22.070	24.888	26.319	26.340
YT 0	556.5	556.5	955.8	553.6	551.2	549.5	549.5
PT 0	11.699	11.699	11.711	11.635	11.536	11.443	11.443
ALPHA 0	46.303	46.269	43.996	40.342	38.797	38.201	38.178
I STA 0	0.200	0.200	0.336	0.312	0.577	0.181	0.181
Y 0	742.713	742.248	715.913	669.152	620.575	594.713	594.529
VU 0	536.986	536.342	497.275	433.172	388.826	367.780	367.482
VZ 0	513.097	513.097	519.023	510.026	483.660	467.356	467.356
YS 0	510.5	507.7	510.2	513.3	516.1	517.1	520.1
PS 0	8.814	8.644	8.842	9.104	9.343	9.427	9.622
DENS 0	0.04660	0.04596	0.04678	0.04787	0.04886	0.04921	0.04994
M 0	0.67046	0.67191	0.64647	0.60240	0.55716	0.53344	0.53153

STA 1	STATOR EXIT						
DIAM 1	17.800	17.824	19.435	22.610	25.785	27.396	27.420
YT 1	556.5	556.5	955.8	553.6	551.2	549.5	549.5
ALPHA 1	56.934	56.899	54.799	52.199	51.499	51.599	51.575
DEL A	103.238	103.168	98.795	92.541	90.296	89.800	89.753
V 1	916.956	916.087	870.270	796.069	715.573	677.741	677.376
VU 1	768.452	767.415	711.129	629.010	560.006	531.135	530.669
VZ 1	500.290	500.290	501.663	487.926	445.463	420.986	420.986
YS 1	486.4	486.5	492.6	500.7	508.5	511.3	511.3
FS 1	7.196	7.202	7.578	8.102	8.625	8.819	8.822
DELS 1	0.03993	0.03996	0.04152	0.04367	0.04578	0.04656	0.04657
M 1	0.84787	0.84695	0.79955	0.72544	0.64709	0.61123	0.61088
ZWI INC	-1.5375	-1.5385	-1.5837	-1.6067	-1.5975	-1.5808	-1.5812
CP S	0.3439	0.3435	0.3230	0.2934	0.2479	0.2300	0.2297

	STATOR FORCES						
AVG DIA	17.800	17.823	19.344	22.340	25.336	26.857	26.880
FTAN/IN	-351.0	-351.0	-353.6	-359.9	-365.4	-367.3	-367.3
			F TAN	-355.2			
FAX/IN	136.6	127.2	111.5	84.1	52.1	37.5	52.5
			F AX	375.3			
F DRUM	0.						-420.5

TURBINE COMPUTER PROGRAM.  
 NAME G W WOLFMEYER 2-10-71 SCALED FLOWPATH 28.4/45  
 TITLE NASA\_HLMSFT PERFORMANCE MAP

CASE 1. 2  
 INTER-STAGE PERFORMANCE

STA 1A	ROTOR INLET		STAGE 3				
DIAM 1A	17.800	17.825	19.495	22.785	26.675	27.745	27.770
YTR 1A	526.7	526.7	527.0	526.7	527.2	527.1	527.2
PTR 1A	9.503	9.505	9.589	9.664	9.780	9.811	9.813
BETA 1A	45.272	45.184	39.704	29.284	17.869	11.305	11.184
I ROTOR	-0.059	-0.065	0.105	1.084	1.769	2.505	2.503
R 1A	679.664	678.617	620.175	528.729	441.351	404.603	404.433
RU 1A	482.870	481.396	396.184	258.619	135.422	79.313	78.442
MR 1A	0.62731	0.62626	0.56849	0.48057	0.39818	0.36411	0.36394
U 1A	285.581	285.981	312.774	365.560	418.346	445.139	445.539

STA 2	ROTOR EXIT		STAGE 3				
DIAM 2	17.800	17.826	19.602	23.100	26.598	28.374	28.400
BETA 2	35.370	35.399	37.099	41.599	48.699	57.799	57.817
DBETA	80.642	80.584	76.834	70.883	66.568	69.104	69.001
R 2	569.878	570.086	583.337	595.816	614.406	620.088	620.393
RU 2	329.876	330.235	351.868	395.572	461.726	524.709	525.069
MR 2	0.51986	0.52005	0.53262	0.54472	0.56259	0.56780	0.56808
U 2	285.581	286.006	314.492	370.614	426.735	455.221	455.646
RX	-0.19419	-0.19202	-0.07484	0.08276	0.24000	0.30233	0.30305
DEL.H	8.900	8.900	8.953	9.104	9.456	10.164	10.164
PSI	2.73210	2.72422	2.27881	1.68220	1.32581	1.25554	1.25324
EYA TY	0.87468	0.87469	0.87890	0.88614	0.89352	0.90020	0.90020
EYA YS	0.61400	0.61400	0.61714	0.63999	0.68157	0.74986	0.74986
EYA AT	0.87136	0.87136	0.87651	0.88508	0.89148	0.89262	0.89262
ZWI INC	-2.2866	-2.2818	-2.0187	-1.6202	-1.2725	-1.0154	-1.0138
CP.R	-0.4224	-0.4170	-0.1303	0.2125	0.4843	0.5743	0.5750

	ROTOR FORCES		STAGE 3				
AVG DIA	17.800	17.826	19.548	22.943	26.337	28.059	28.085
FX/IN	181.8	181.8	182.5	184.8	191.5	205.7	205.7
				R TAN	963.9		
FAX/IN	-6.3	-5.9	9.5	36.8	71.3	105.5	105.8
			F AX	210.0			
F DRUM	0.						-231.4

STA 2A	STAGE EXIT		STAGE 3				
DIAM 2A	17.800	17.826	19.602	23.100	26.598	28.374	28.400
PI 2A	8.864	8.864	8.868	8.778	8.616	8.365	8.365
TY 2A	519.3	519.3	518.4	515.6	511.7	507.1	507.1
Y 2A	466.802	466.796	466.783	446.253	407.154	337.666	337.653
VU 2A	44.295	44.229	37.376	24.958	34.991	69.488	69.423
ALPH 2A	5.445	5.437	4.593	3.206	4.930	11.876	11.865
MF 2A	0.42391	0.42391	0.42481	0.40735	0.37129	0.30258	0.30258
VZ 2A	464.696	464.696	469.264	445.555	405.648	330.439	330.439
TS 2A	499.6	499.6	498.7	497.4	496.2	495.8	495.8
PS 2A	7.824	7.824	7.826	7.826	7.827	7.828	7.828
DENS 2A	0.04227	0.04227	0.04236	0.04247	0.04257	0.04261	0.04261
M 2A	0.42583	0.42583	0.42618	0.40799	0.37267	0.30919	0.30919

Table II. STAGE ONE VANE DESIGN DATA

<u>Parameter</u>	<u>Hub</u>	<u>Pitch</u>	<u>Tip</u>
Diameter (trailing edge, in.)	17.8	20.38	22.96
$\alpha_1$ , (degrees)	61.13	58.87	60.17
$\psi$ $Z_{wei}$ , incompressible	.748	.763	.733
$A_w$ , (in.)	.99	1.16	1.33
$t$ , (in.)	.874	1.0	1.127
$n$		64	
$nd_o$ ( $C_f = .975$ $\eta_V = .97$ )	28.16	34.50	37.38
$d_o = nd_o/n$ , (in.)	.440	.539	.584
$t_e$ , (in.)	.020	.020	.020
$t_e/(t_e + d_o)$	.043	.036	.033
Chord, (in.)	1.316	1.476	1.721
$t_{max}$ , max thickness (in.)	.153	.179	.205
Unguided turning (degrees)	10.8	10.0	9.8
Overturning (degrees)	0	1.0	1.6
Wedge angle (degrees)	6.5	7.0	8.5
Precision Master No. 4012241-942			

Table III. STAGE TWO VANE DESIGN DATA

<u>Parameter</u>	<u>Hub</u>	<u>Pitch</u>	<u>Tip</u>
Diameter (trailing edge, in.)	17.8	21.455	25.11
$\alpha_1$ , (degrees)	61.37	58.53	58.23
$\psi_{Zwei}$ , incompressible	.777	.757	.730
$A_w$ , (in.)	.91	1.175	1.44
$t$ , (in.)	.518	.6241	.730
$n$		108	
$nd_o$ ( $C_f = .975$ $\eta_V = .97$ )	27.43	36.07	42.55
$d_o = nd_o/n$ , (in.)	.254	.334	.394
$t_e$ , (in.)	.020	.020	.020
$t_e/(t_e + d_o)$	.073	.056	.048
Chord, (in.)	.991	1.278	1.556
$t_{max}$ , max thickness (in.)	.087	.104	.122
Unguided turning (degrees)	9.0	9.0	8.2
Overturning (degrees)	0	-.3	0
Wedge angle (degrees)	4.5	5.0	4.6
Precision Master No. 4012241-944			

TABLE IV. STAGE THREE VANE DESIGN DATA

<u>Parameter</u>	<u>Hub</u>	<u>Pitch</u>	<u>Tip</u>
Diameter (trailing edge, in)	17.8	22.61	27.42
$\alpha_1$ , (degrees)	56.99	52.2	51.65
$\psi_{Zwei}$ , incompressible	.860	.879	.852
$A_w$ , (in.)	1.0	1.3	1.6
$t$ , (in.)	.559	.710	.861
$n$		100	
$nd_o$ ( $C_f = .975$ $\eta_V = .97$ )	31.2	44.5	54.6
$d_o = nd_o/n$ (in.)	.312	.445	.546
$t_e$ , (in.)	.020	.020	.020
$t_e/(t_e + d_o)$	.060	.043	.035
Chord, (in.)	1.062	1.374	1.681
$t_{max}$ , max thickness (in.)	.09	.109	.128
Unguided turning (degrees)	8.8	8.1	6.4
Overturning (degrees)	.7	1.0	2.8
Wedge angle (degrees)	5.5	5.3	5.0
Precision Master No. 4012241-946			



TABLE V. STAGE ONE BLADE DESIGN DATA

<u>Parameter</u>	<u>Hub</u>	<u>Pitch</u>	<u>Tip</u>
Diameter (trailing edge, in.)	17.8	20.86	23.92
$\beta_1$ (degrees)	55.0	48.63	43.60
$\beta_2$ (degrees)	58.60	57.6	60.15
$\Delta\beta$ (degrees)	113.595	106.23	103.75
$\psi_{Zwei}$ , incompressible	.953	1.003	.970
$A_w$ , (in.)	.91	.96	1.01
$t$ , (in.)	.528	.61824	.709
$n$		106	
$nd_o$ ( $C_f = .97$ $\eta_B = .95$ )	29.89	35.93	38.27
$d_o = nd_o/n$ , (in.)	.282	.339	.361
$t_e$ , (in.)	.020	.020	.020
$t_e/(t_e + d_o)$	.066	.056	.052
Chord, (in.)	.925	1.004	1.113
$t_{max}$ , max thickness (in.)	.117	.104	.09
Unguided turning (degrees)	12.0	11.3	11.1
Overturning (degrees)	1.2	1.0	1.6
Wedge angle (degrees)	6.5	5.0	3.7
Precision Master No. 4012241-948			

Table VI. STAGE TWO BLADE DESIGN DATA

<u>Parameter</u>	<u>Hub</u>	<u>Pitch</u>	<u>Tip</u>
Diameter (trailing edge, in.)	17.8	21.94	26.08
$\beta_1$ (degrees)	54.24	44.3	34.6
$\beta_2$ (degrees)	57.02	55.8	58.11
$\Delta\beta$ (degrees)	111.26	100.1	92.71
$\psi_{Zwei}$ , incompressible	.961	1.028	.978
$A_w$ , (in.)	.98	1.03	1.08
$t$ , (in.)	.548	.676	.803
$n$		102	
$nd_o$ ( $C_f = .97$ $\eta_B = .95$ )	31.01	39.37	43.96
$d_o = nd_o/n$ , (in.)	.304	.386	.431
$t_e$ , (in.)	.020	.020	.020
$t_e/(t_e + d_o)$	.062	.049	.044
Chord, (in.)	.996	1.085	1.207
$t_{max}$ , max thickness (in.)	.101	.096	.091
Unguided turning (degrees)	10.5	11.0	11.1
Overturning (degrees)	1.6	2.5	3.3
Wedge angle (degrees)	5.5	5.0	4.0
Precision Master No. 4012241-950			

Table VII. STAGE THREE BLADE DESIGN DATA

<u>Parameter</u>	<u>Hub</u>	<u>Pitch</u>	<u>Tip</u>
Diameter (trailing edge, in.)	17.8	23.1	28.4
$\beta_1$ (degrees)	45.45	27.1	5.6
$\beta_2$ (degrees)	35.31	41.6	58.06
$\Delta\beta$ (degrees)	80.762	68.7	63.66
$\psi_{Zwei}$ , incompressible	.937	1.001	.919
$A_w$ , (in.)	1.22	1.05	.88
$t$ , (in.)	.499	.648	.797
$n$		112	
$nd_o$ ( $C_f = .97$ $\eta_B = .95$ )	46.26	55.10	47.82
$d_o = nd_o/n$ , (in.)	.413	.492	.427
$t_e$ , (in.)	.020	.020	.020
$t_e/(t_e + d_o)$	.046	.039	.045
Chord, (in.)	1.24	1.084	1.128
$t_{max}$ , max thickness (in.)	.090	.075	.06
Unguided turning (degrees)	9.8	10.0	10.0
Overturning (degrees)	-2.2	1.0	3.4
Wedge angle (degrees)	7.2	5.2	3.0
Precision Master No. 4012241-952			

Table VIII. STEADY-STATE MECHANICAL STRESSES AND ESTIMATED VIBRATORY CAPABILITIES

<u>Mechanical Stresses (ksi)</u>	<u>Stage 1</u>	<u>Stage 2</u>	<u>Stage 3</u>
<b>Airfoil Hub</b>			
$\sigma$ centrifugal	6.27	9.60	9.41
$\sigma$ maximum gas bending (LE)	16.91	27.66	14.43
$\sigma$ resultant span wise stress (free slip mode)			
LE	23.31	37.49	23.79
TE	22.40	32.27	18.68
Hi-c	-3.81	-5.02	2.39
Midcv	3.47	4.47	8.07
$\sigma$ uncorrected gas bending (1 m i and m m i, free slip mode)			
LE	13.03	17.55	14.18
TE	13.15	16.06	14.77
Hi-c	-7.98	-9.74	-8.33
Midcv	-2.18	-3.38	-1.63
$\sigma$ corrected gas bending (1 m i and m m i, free slip mode)			
LE	12.63	16.36	11.41
TE	12.75	14.95	11.58
Hi-c	-7.73	-9.08	-6.62
Midcv	-2.11	-3.15	-1.30
<b>Under Tip Shroud</b>			
$\sigma$ centrifugal	3.55	4.85	7.18
$\sigma$ resultant span wise stress (free slip mode)			
LE	8.75	21.44	27.56
TE	6.84	18.46	22.54
Hi-c	1.11	-3.33	- .84
Midcv	2.68	1.37	2.17
<b><u>Estimated Vibratory Capabilities</u></b>			
$\sigma_{\text{mean}} = \sigma_c + \sigma_{\text{limi}} + \sigma_{\text{mmi}}$ (ksi) at Hub LE ( $\sigma_{\text{thermal}}$ neglected)	23.18	37.26	23.84
Estimated $T_{\text{HLE}}$ ( $^{\circ}\text{F}$ )	256	176	113
Estimated Minimum Margin Vibratory Allowable Stress (ksisa) (Based on AISI 410 Stainless steel average strength less three standard deviations)	33.5	28.4	36.3

Table IX. KEY DETAIL DRAWING SUMMARY

<u>Drawing No.</u>	<u>Title</u>
4013097-726	Spacer, Outer Housing - Stage 2
-727	Housing, Inner Inlet
-728	Spacer, Outer Housing - Stage 3
-731	Housing, Outer Inlet
-734	Ring, Seal-Stage 1
-735	Ring, Back Up - Stage 1
-736	Ring, Back Up - Stages 2 & 3
-737	Shroud, Vane - Inner Stages 2 & 3
-738	Vane, Turbine - Stage 1
-739	Vane, Turbine - Stage 2
-740	Vane, Turbine - Stage 3
-741	Shroud, Blade - Outer, Stage 1
-742	Shroud, Blade - Outer, Stage 2
-743	Shroud, Outer-Blade, Stage 3
-744	Blade, Turbine - Stage 1
-745	Blade, Turbine - Stage 2
-746	Blade, Turbine - Stage 3
-747	Shroud, Turbine Blade - Stage 1
-748	Shroud, Turbine Blade - Stage 2
-749	Shroud, Turbine Blade - Stage 3
-750	Blade Assembly, Turbine - Stage 1
-751	Blade Assembly, Turbine - Stage 2
-752	Blade Assembly, Turbine - Stage 3
-753	Housing, Instrumentation - Inner
-754	Spacer
-755	Adapter - Bearing Housing
-756	Housing Assembly - Stage 1
-757	Housing Assembly - Stage 2
-758	Housing Assembly - Stage 3

Table IX. KEY DETAIL DRAWING SUMMARY (Concluded)

<u>Drawing No.</u>	<u>Title</u>
4013097-760	Shroud, Vane, Stage 1
-761	Shroud, Vane, Stage 2
-762	Shroud, Vane, Stage 3
-763	Vane Assembly, Stage 1
-764	Vane Assembly, Stage 2
-765	Vane Assembly, Stage 3
-767	Test Assembly, Conventional Blading
-768	Instrumentation, 3 Stage NASA HLFT
-769	3 Stage NASA HLFT Test Assembly Build-Up Conventional Blading

<u>Precision Master No.</u>	<u>Title</u>
4012241-942	Vane, Turbine, Stage 1
-943	Stackup, Vane, Stage 1
-944	Vane, Turbine, Stage 2
-945	Stackup, Vane, Stage 2
-946	Vane, Turbine, Stage 3
-947	Stackup, Vane, Stage 3
-948	Blade, Turbine, Stage 1
-949	Stackup, Blade, Stage 1
-950	Blade, Turbine, Stage 2
-951	Stackup, Blade, Stage 2
-952	Blade, Turbine, Stage 3
-953	Stackup, Blade, Stage 3

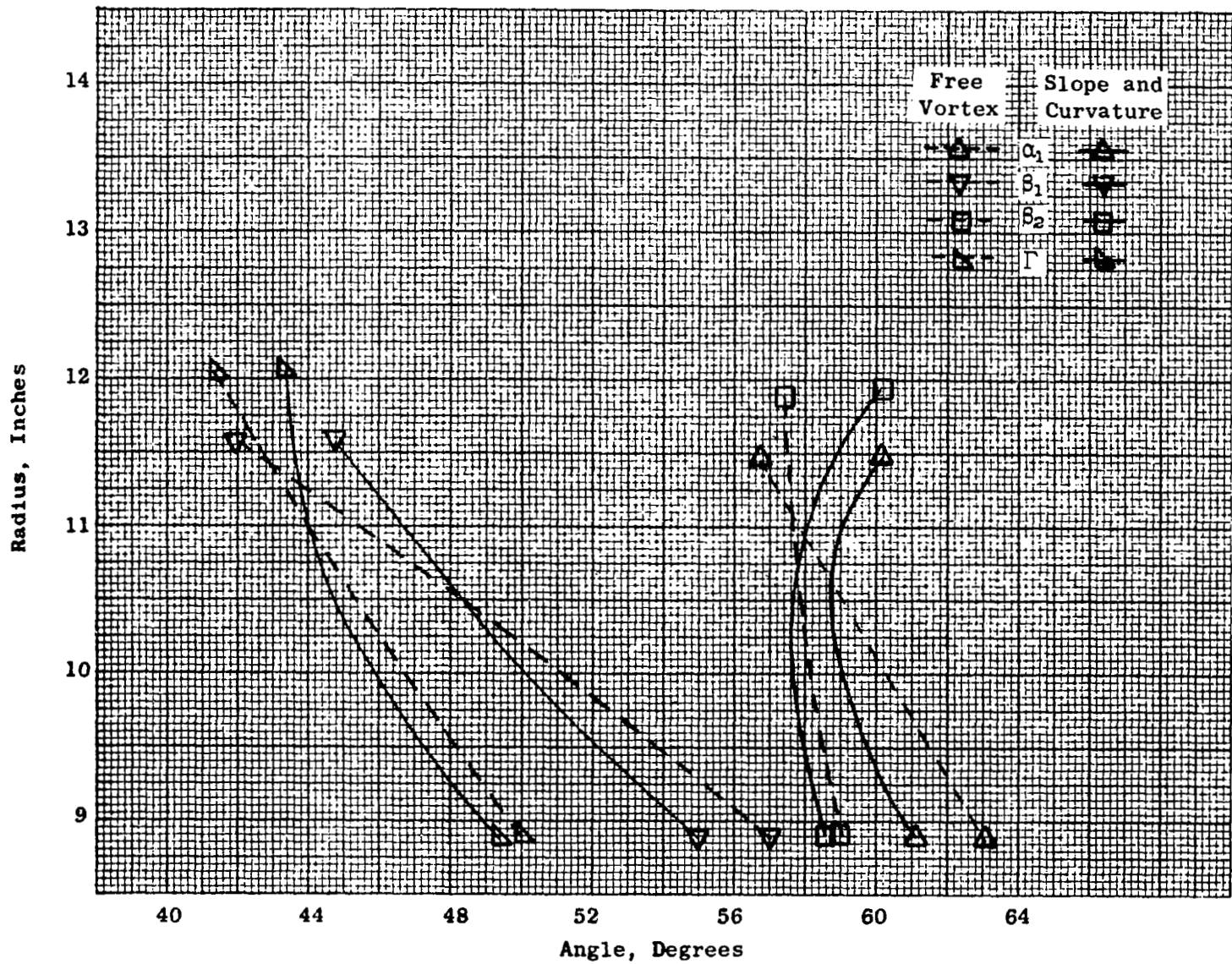


Figure 1. Effect of Flowpath Slope and Curvature on Angles, Stage One.

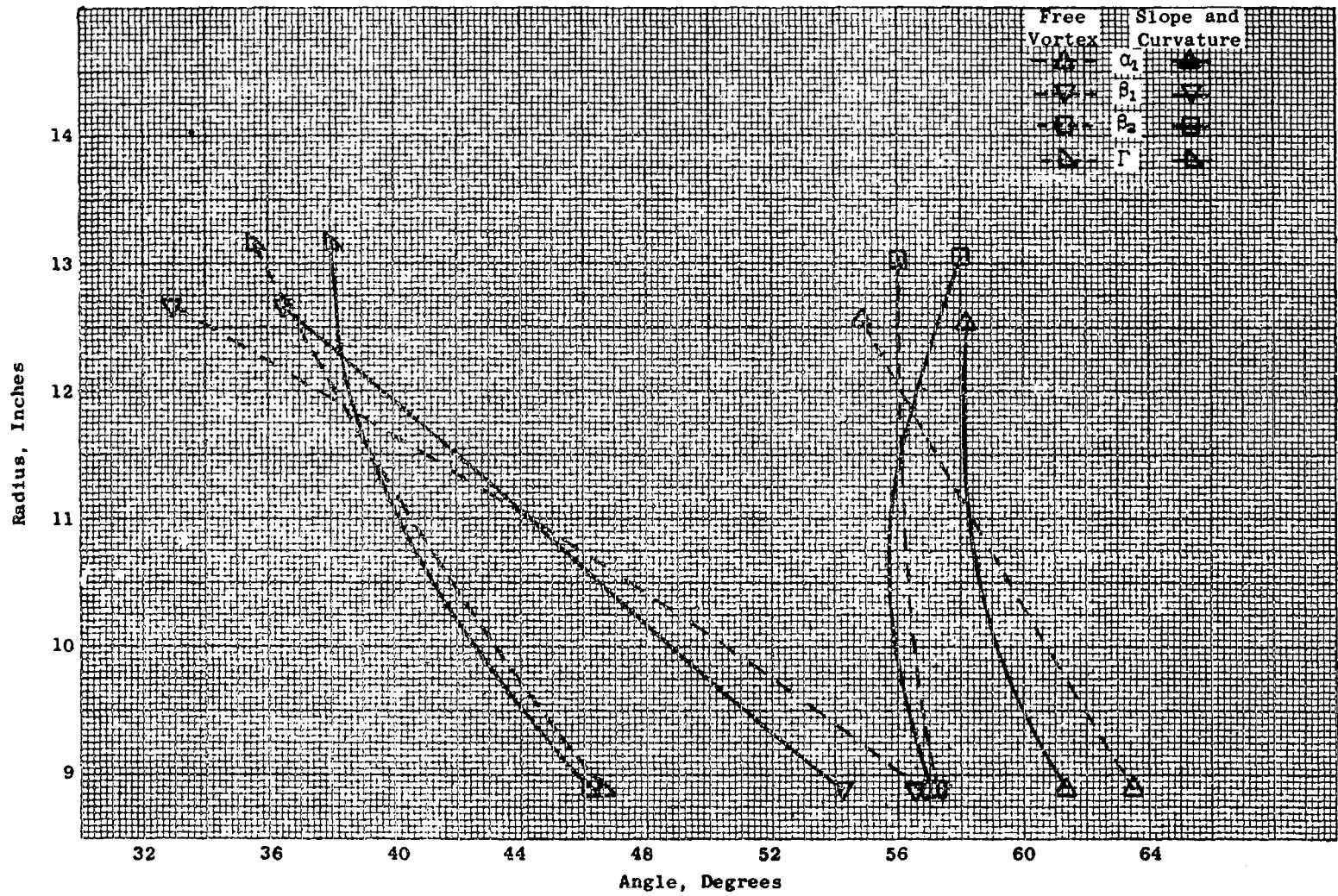


Figure 2. Effect of Flowpath Slope and Curvature on Angles, Stage Two.



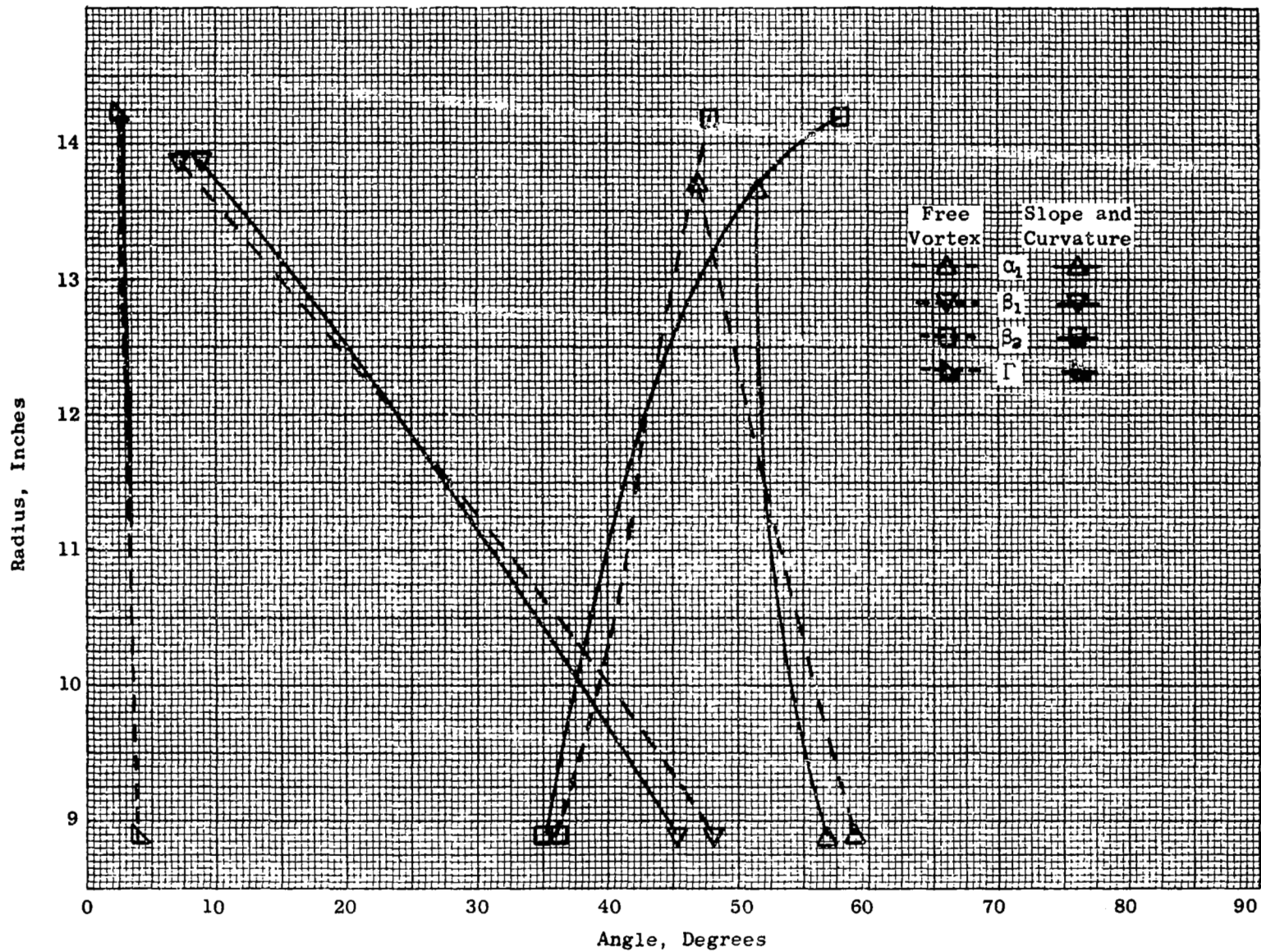


Figure 3. Effect of Flowpath Slope and Curvature on Angles, Stage Three.

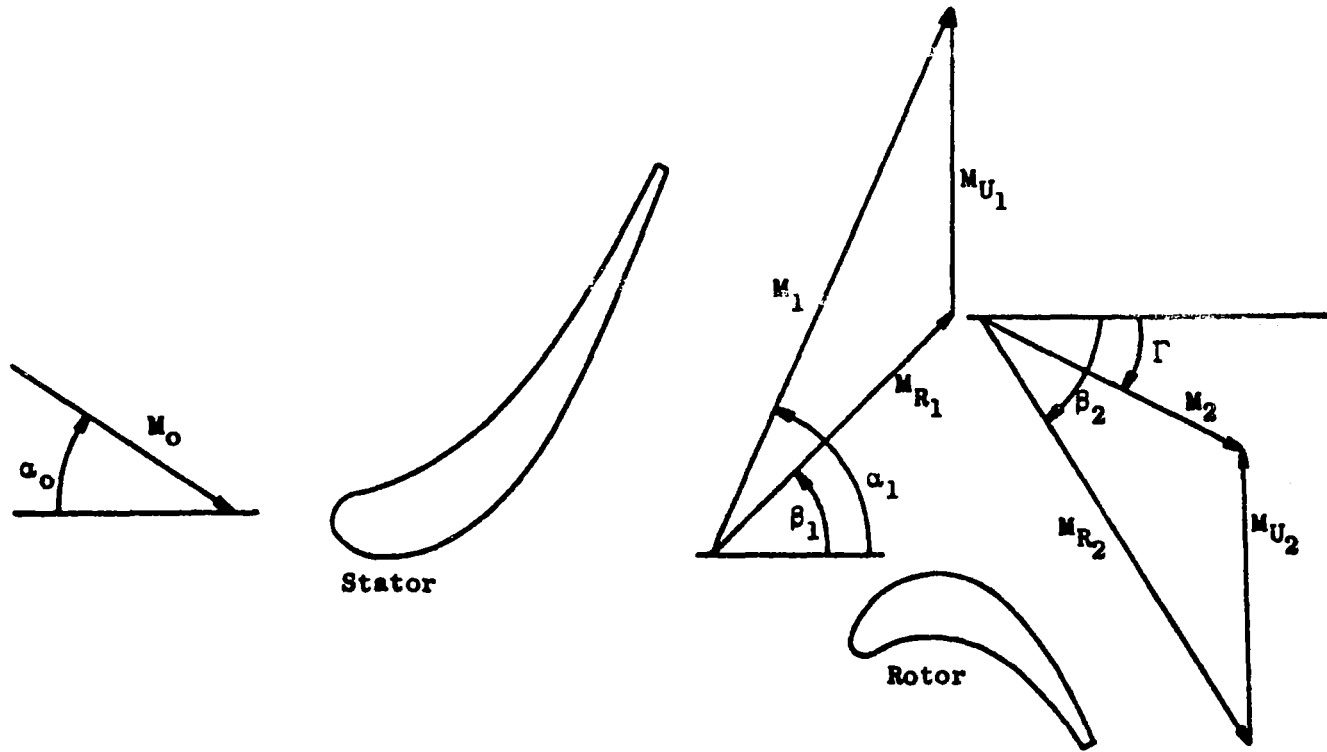
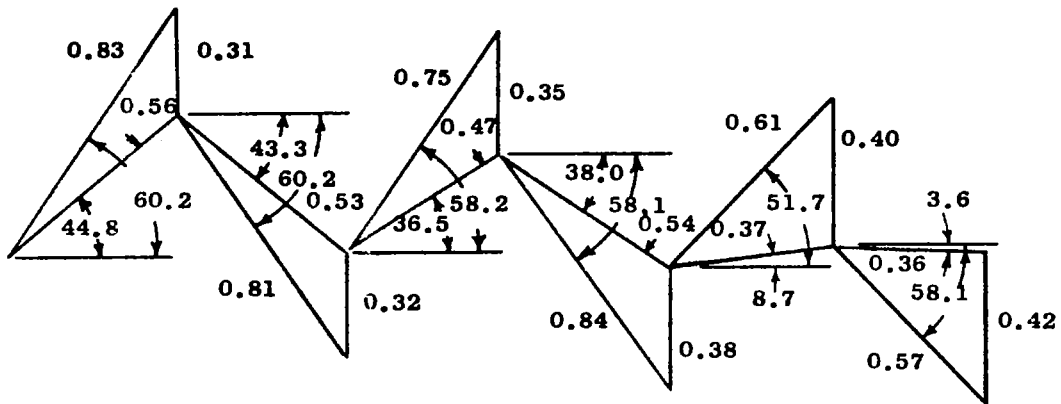
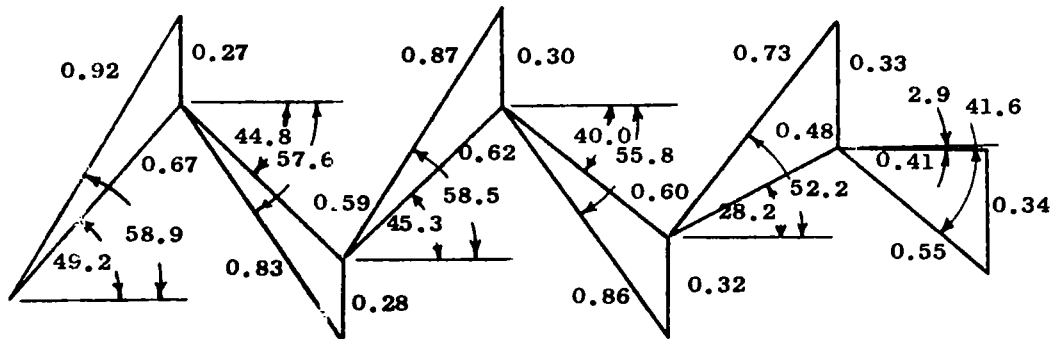


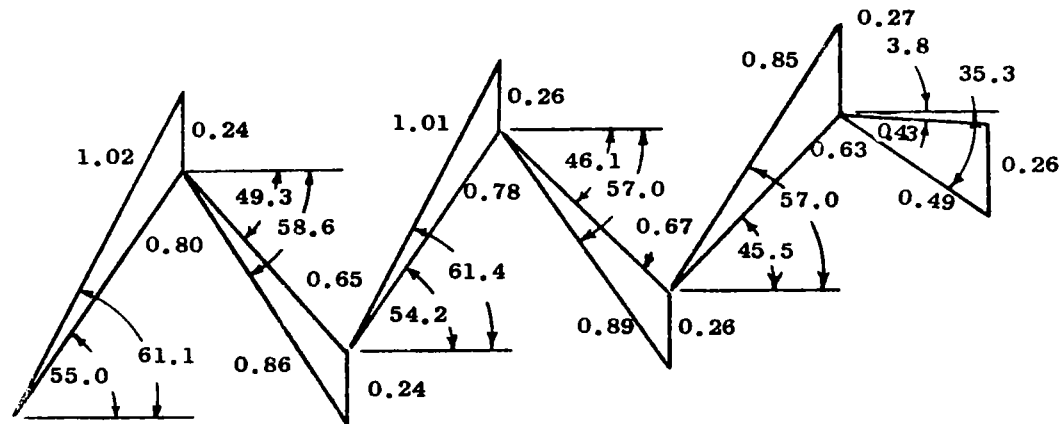
Figure 4. Vector Diagram Nomenclature.



TIP



PITCH



HUB

Numbers Shown on Vector Diagrams are Angles in Degrees and Mach Numbers

Figure 5. Vector Diagrams.

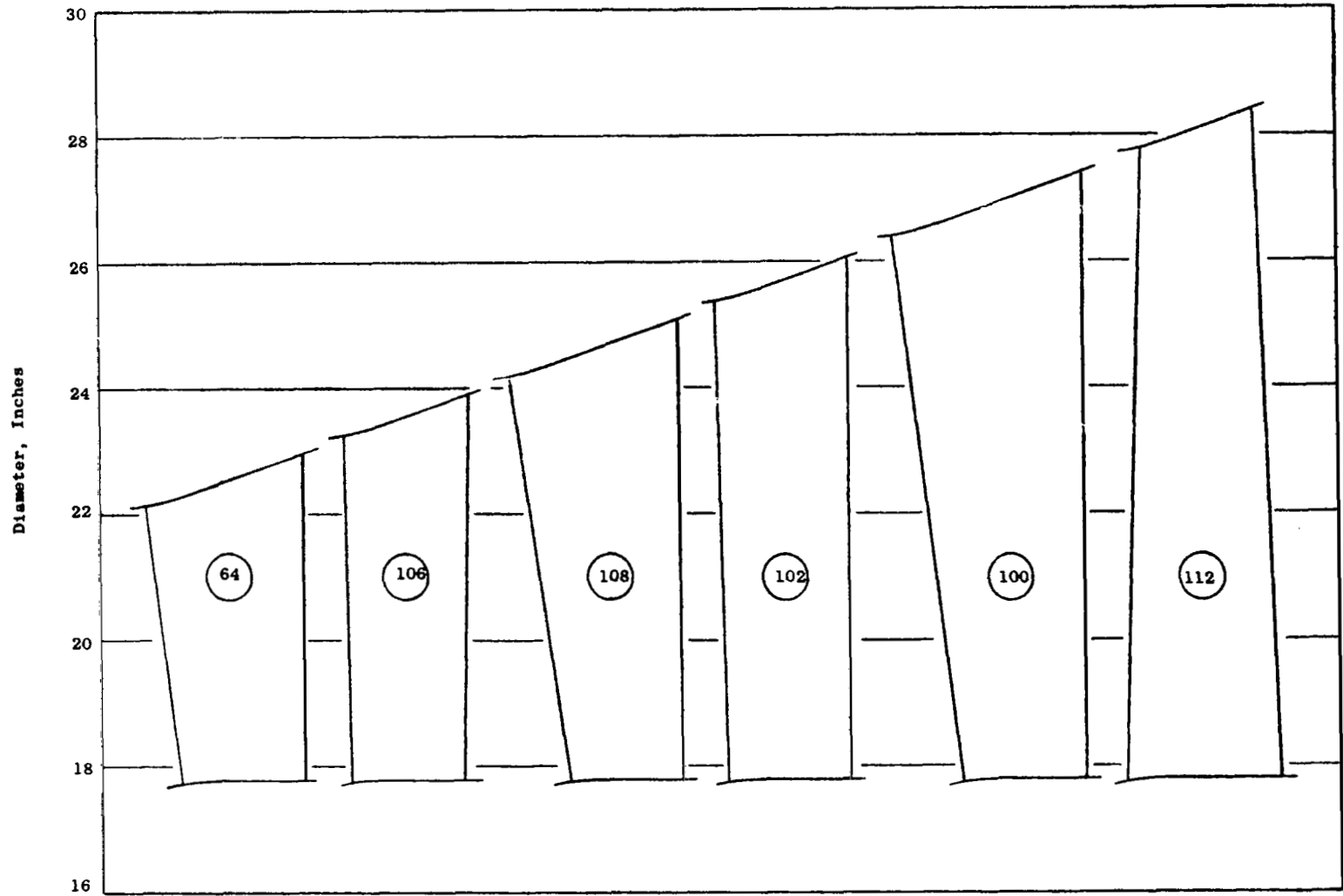


Figure 6. Aerodynamic Flowpath.

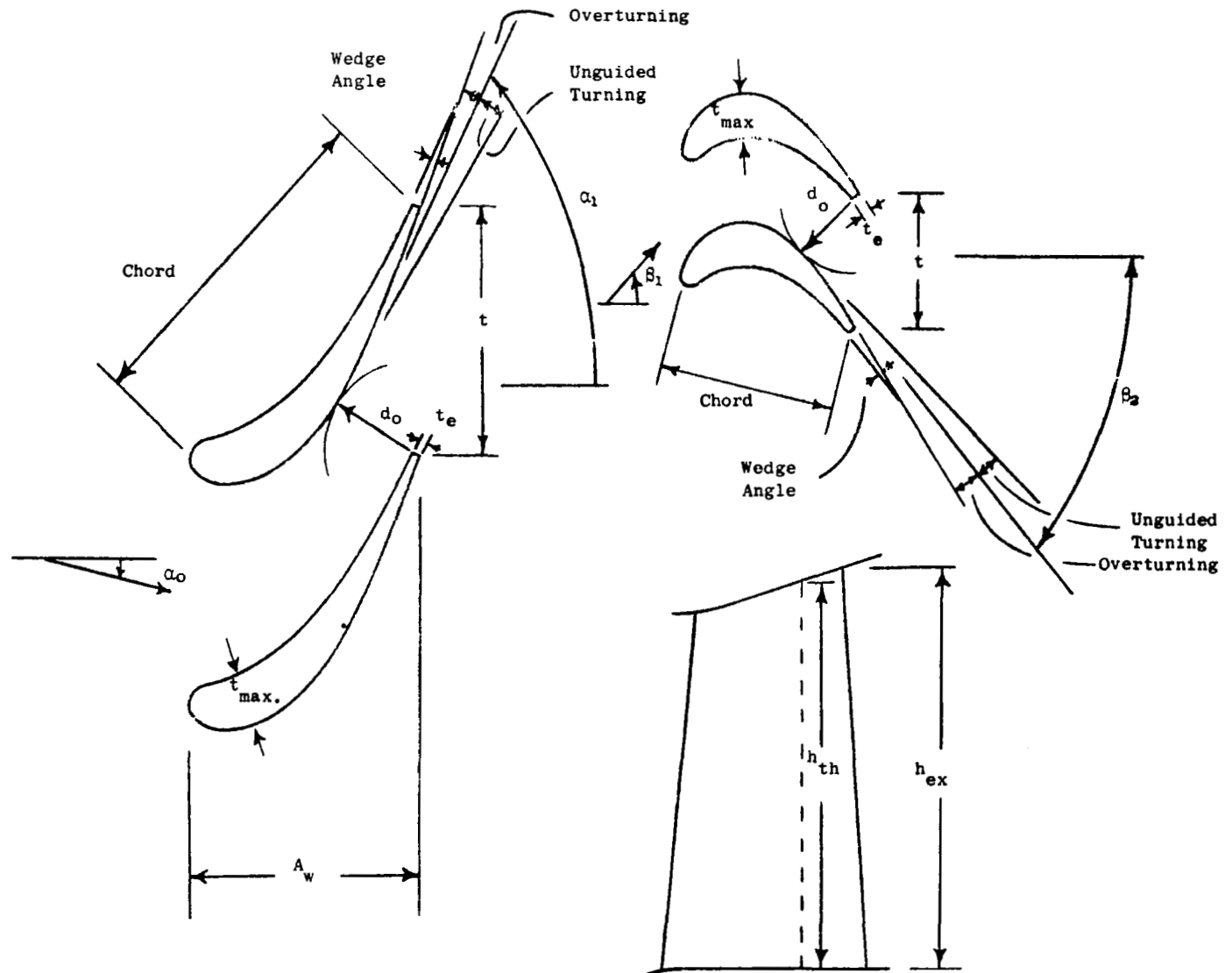


Figure 7. Design Data Nomenclature.

NASA HLMSFT SCALED N1R3 FINAL

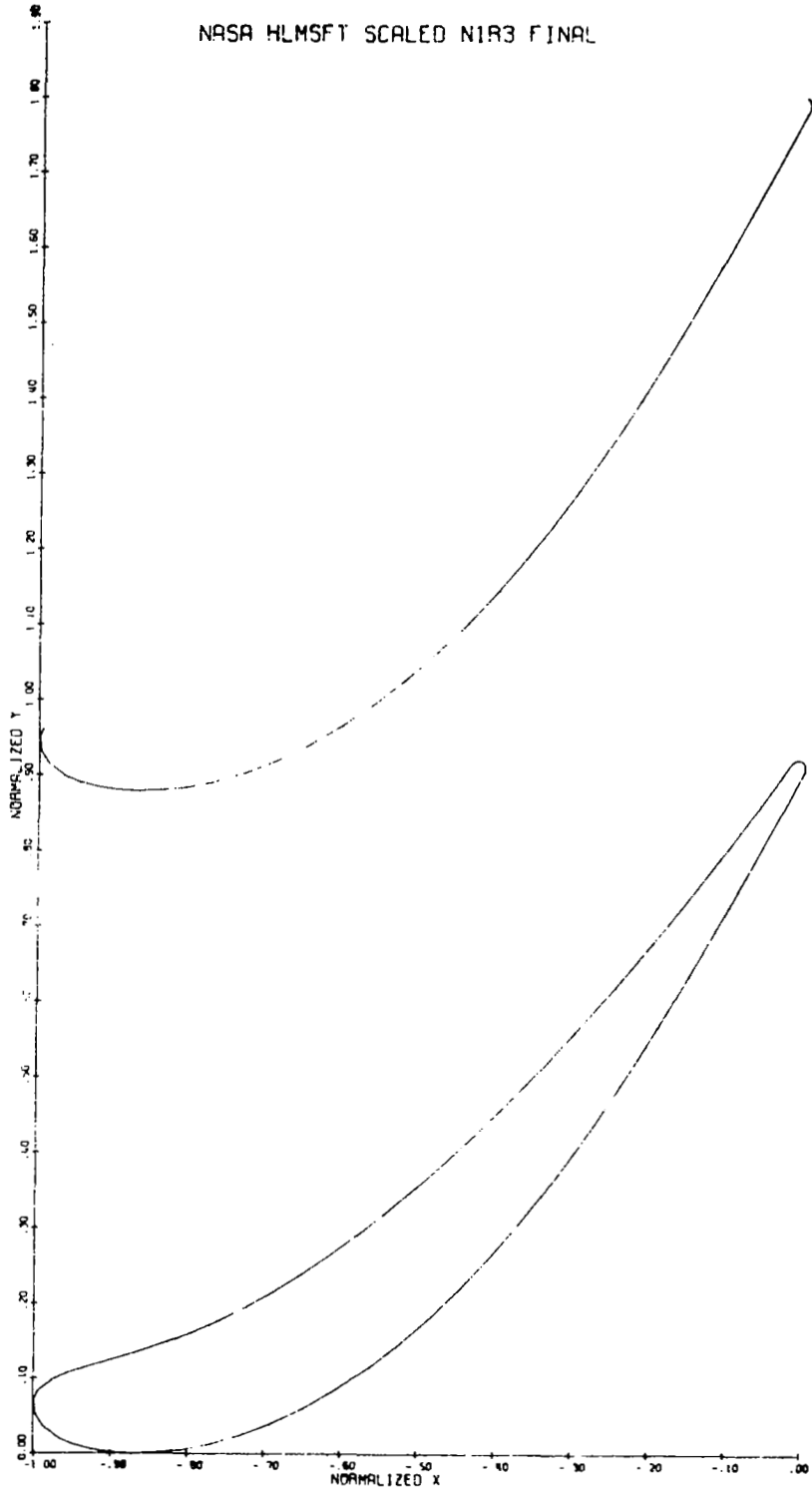


Figure 8. Stage One Vane Hub Airfoil Flowpath.

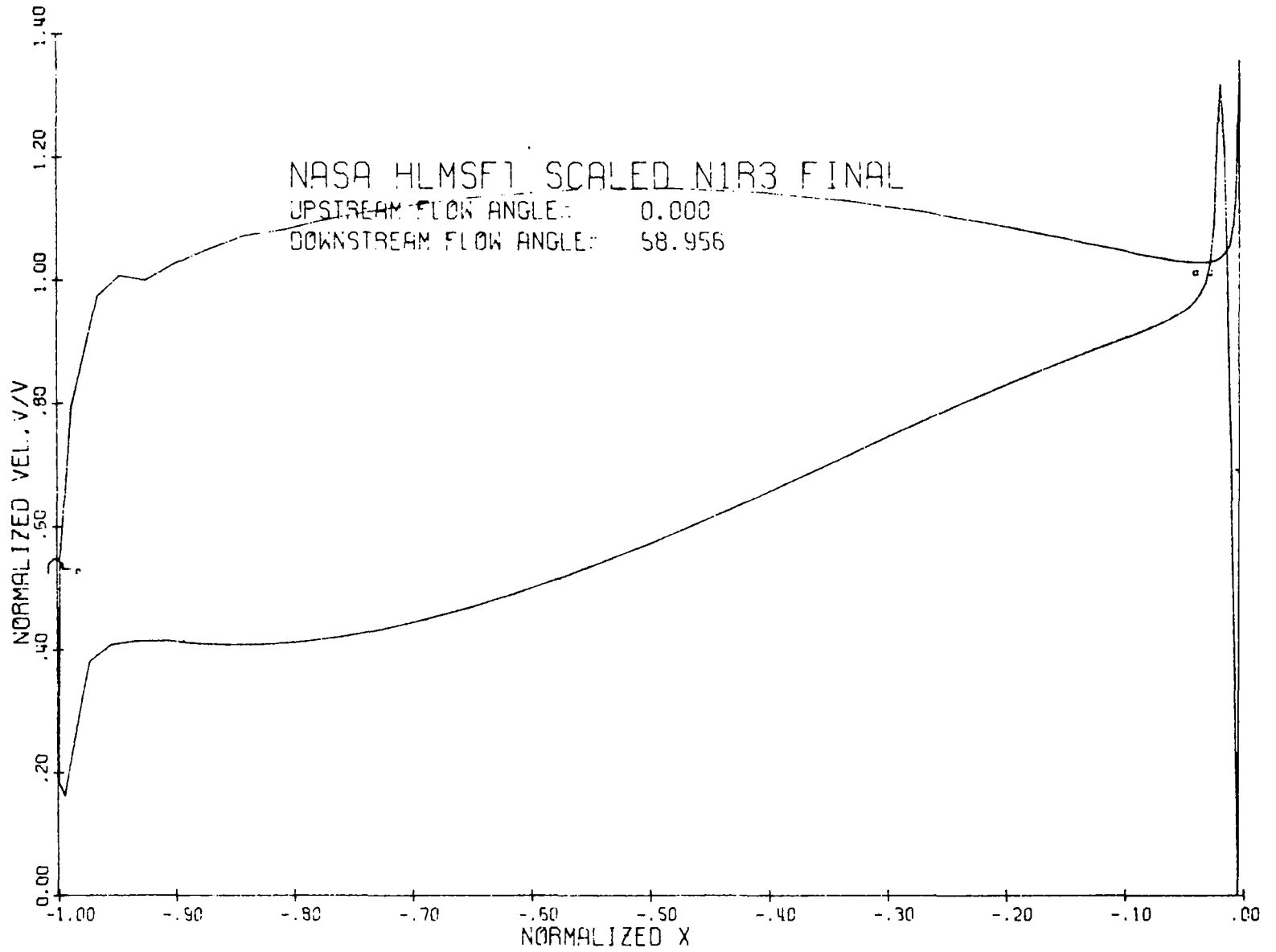


Figure 9. Stage One Vane Hub Velocity Distribution.

NASA HLMSFT SCALED N1P1 FINAL

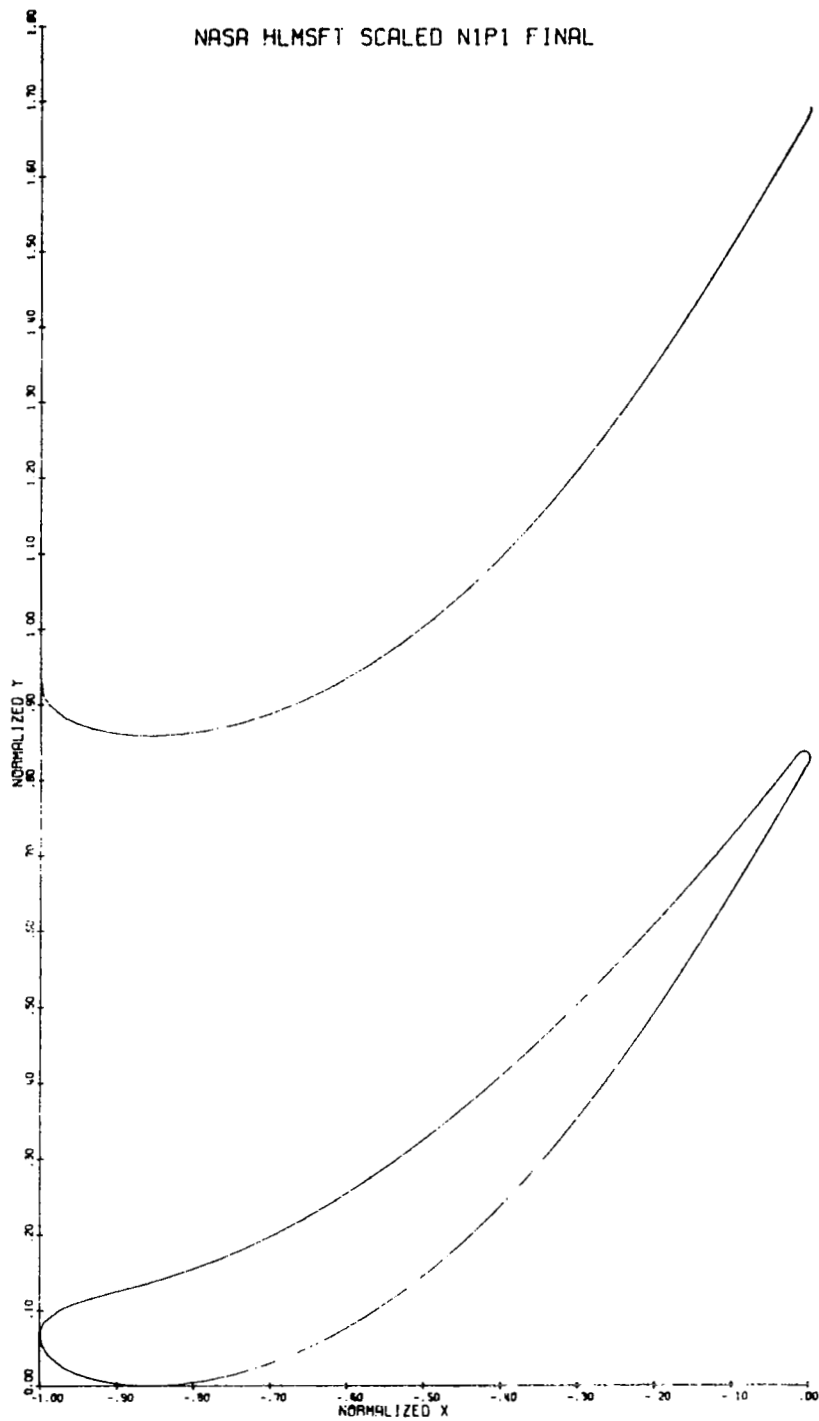


Figure 10. Stage One Vane Pitch Airfoil Flowpath.



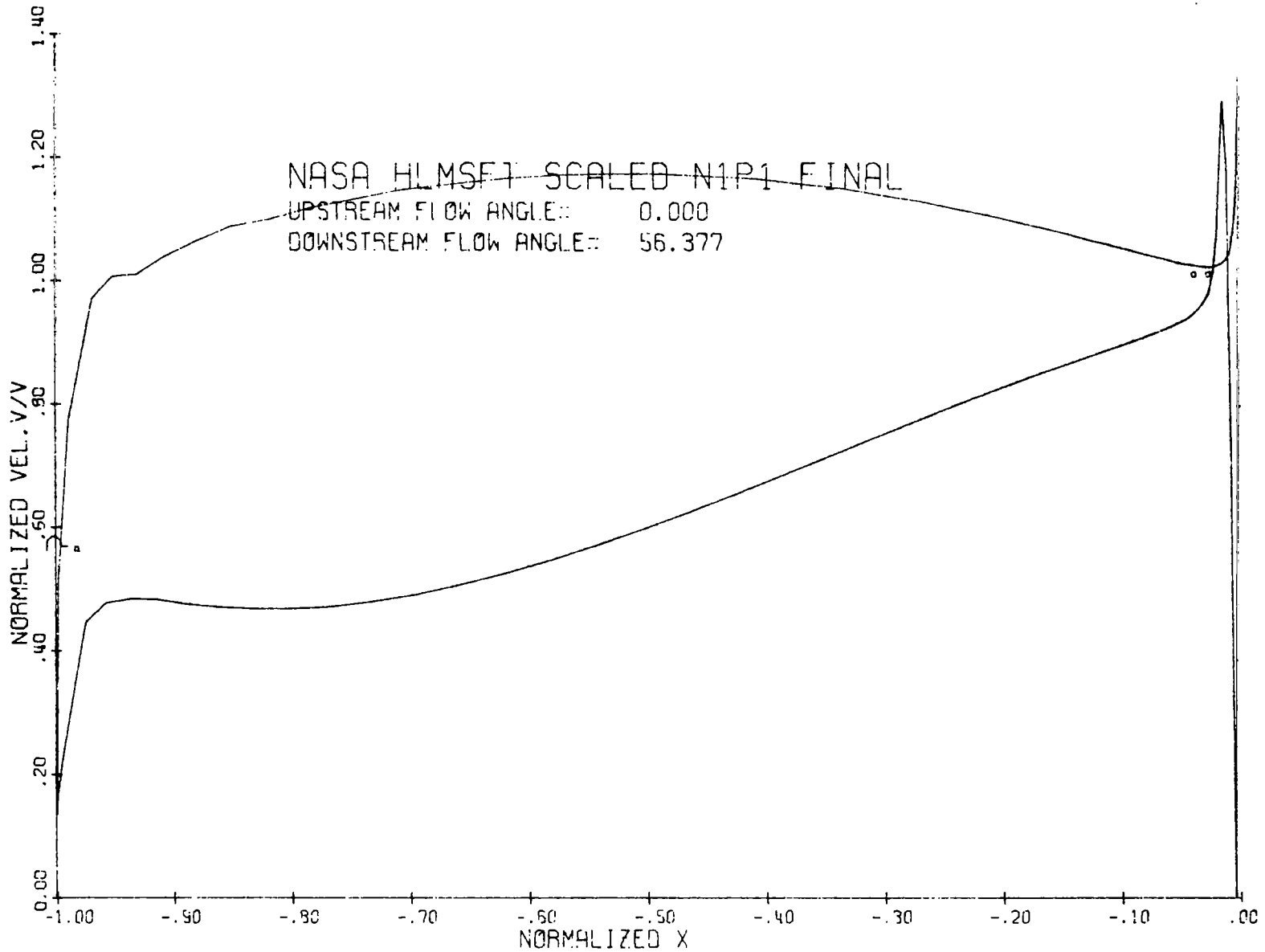


Figure 11. Stage One Vane Pitch Velocity Distribution.

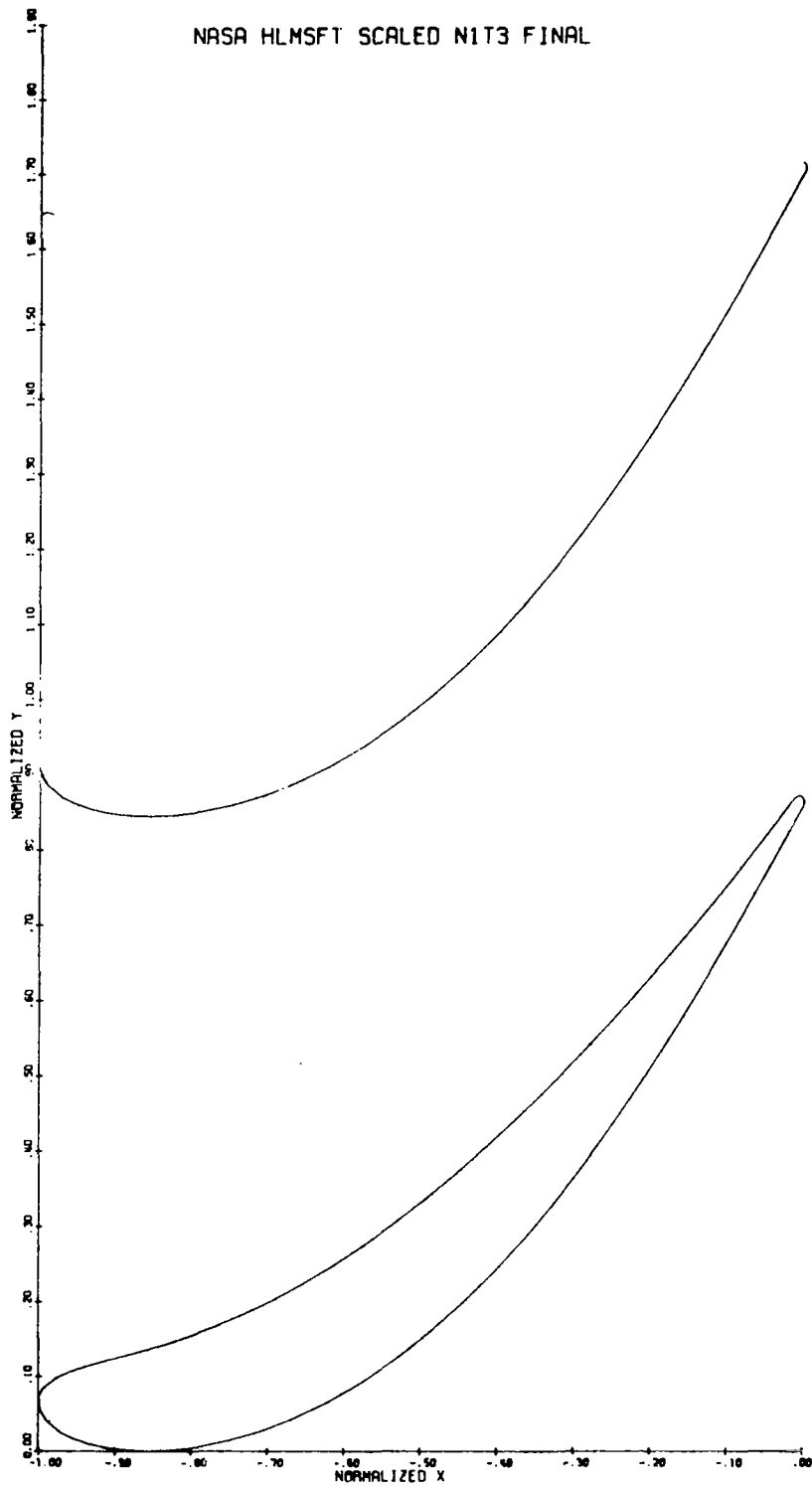


Figure 12. Stage One Vane Tip Airfoil Flowpath.

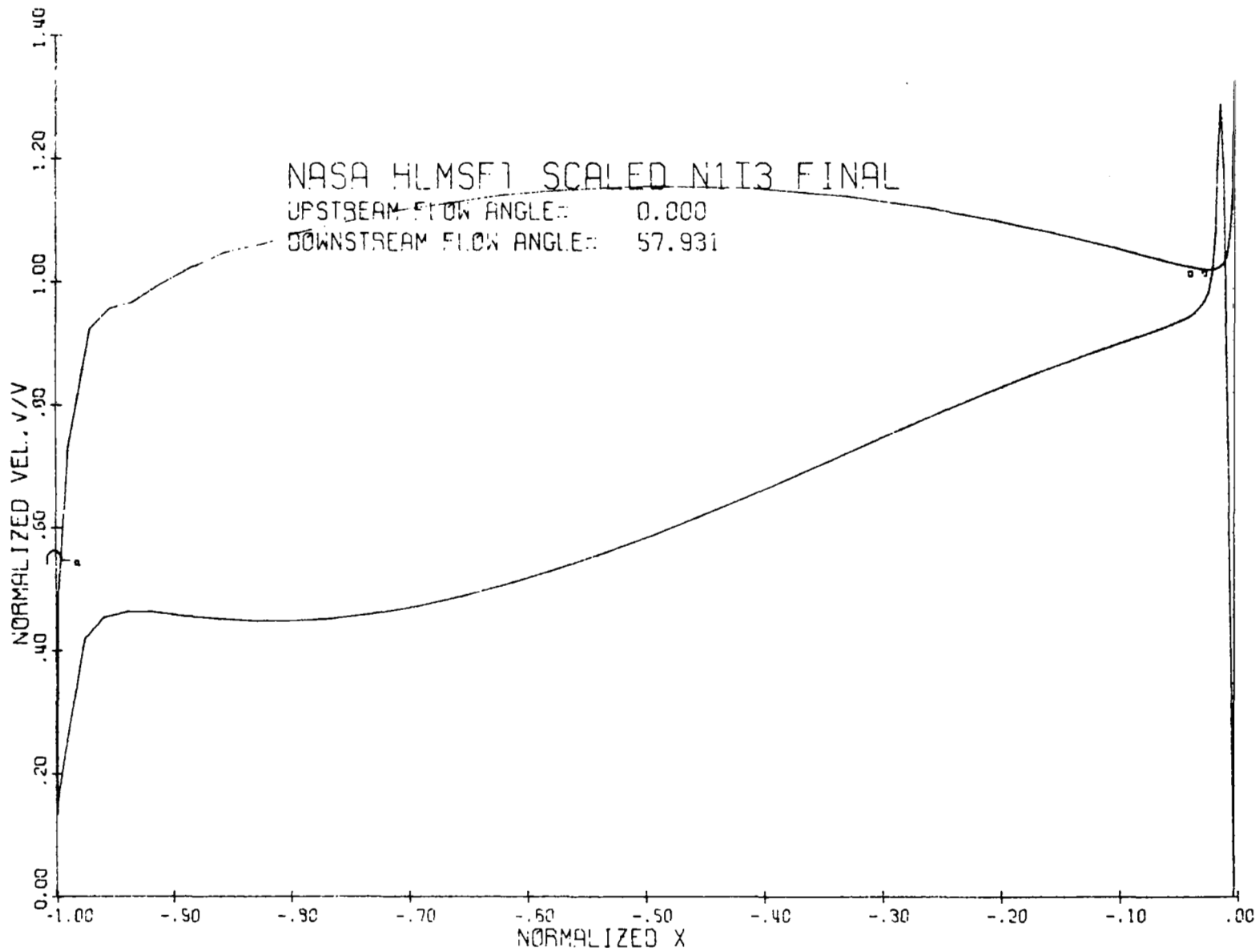


Figure 13. Stage One Vane Tip Velocity Distribution.

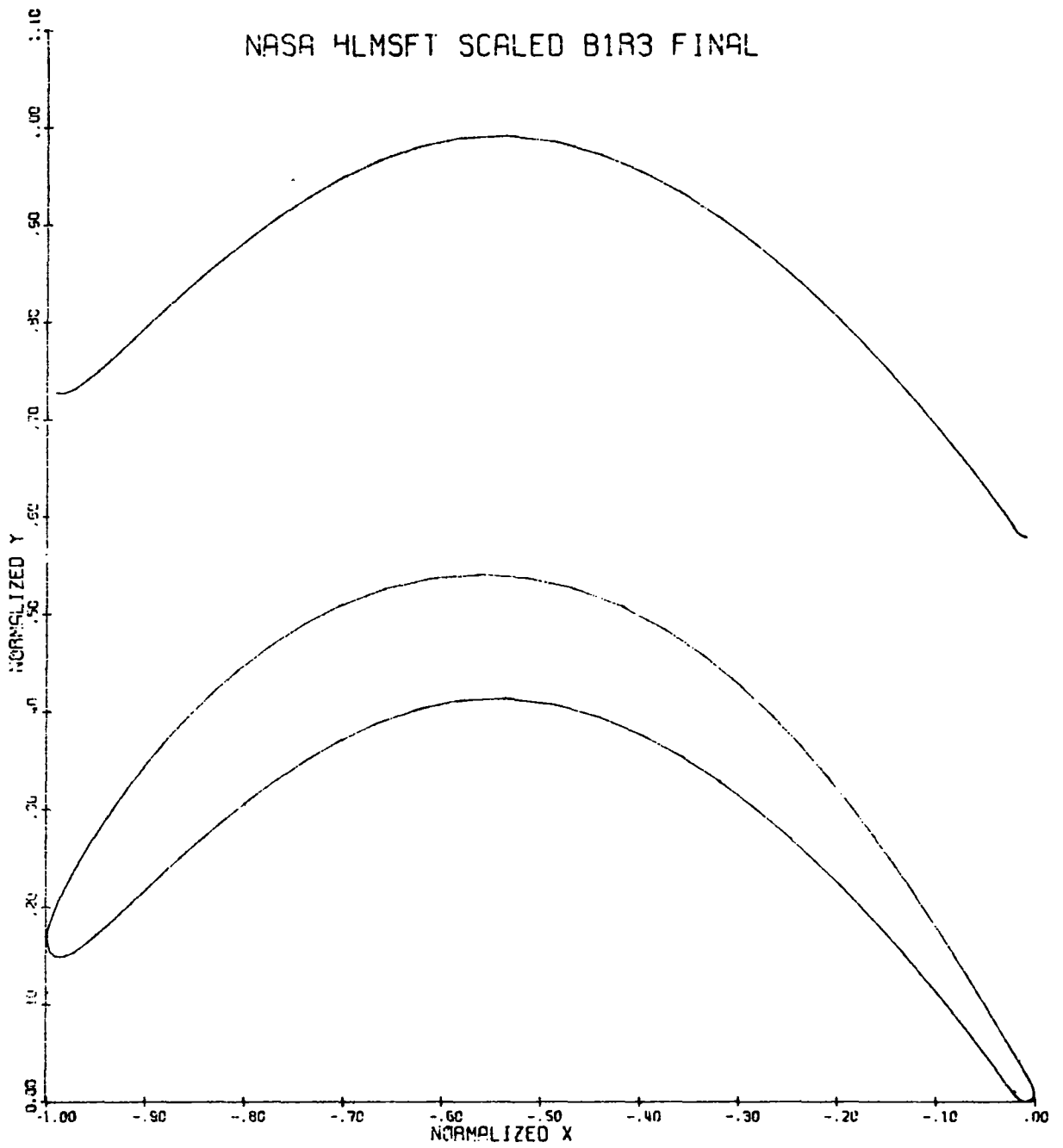


Figure 14. Stage One Blade Hub Airfoil Flowpath.

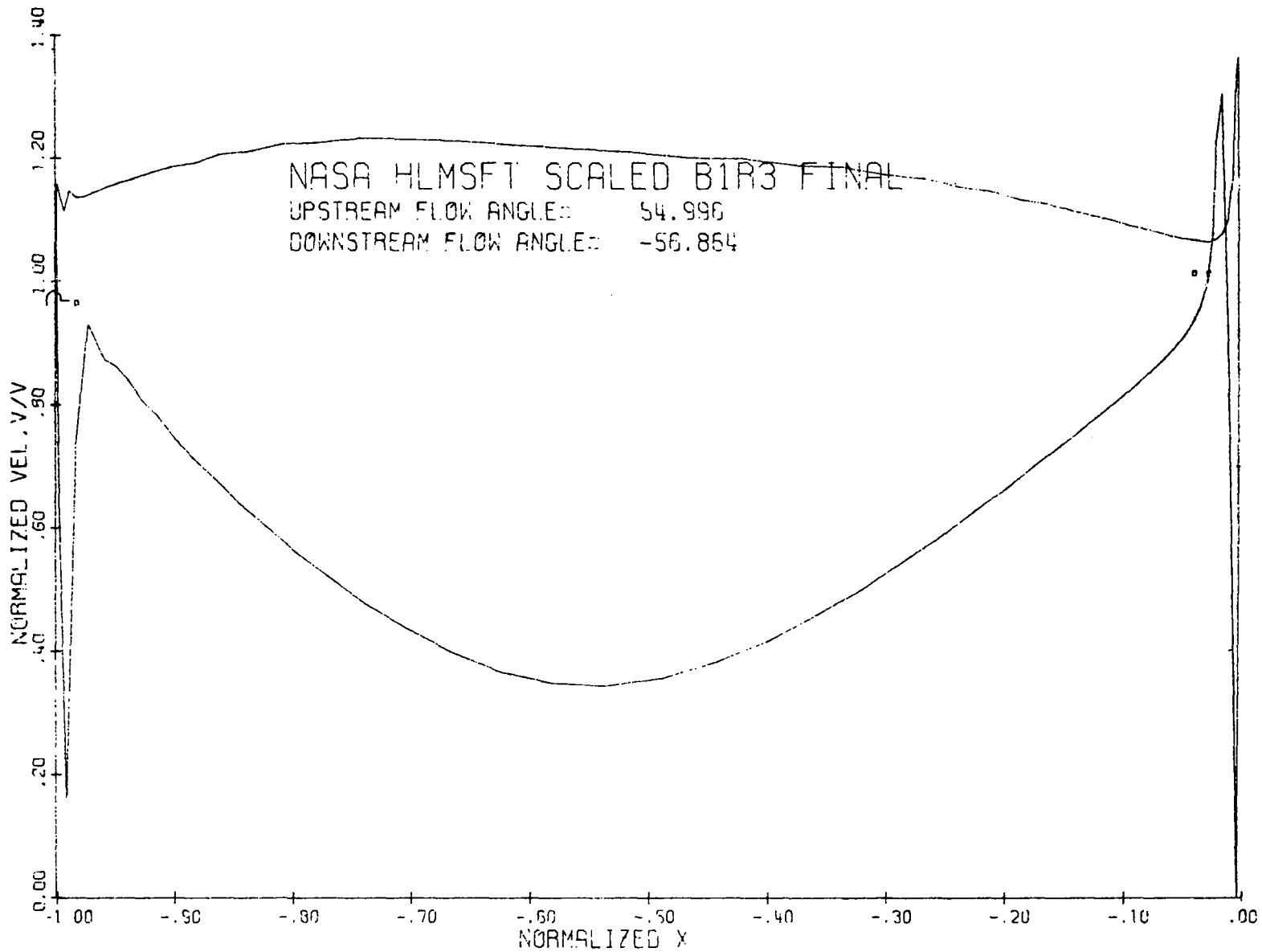


Figure 15. Stage One Blade Hub Velocity Distribution.

NASA HLMSFT SCALED B1P2 FINAL

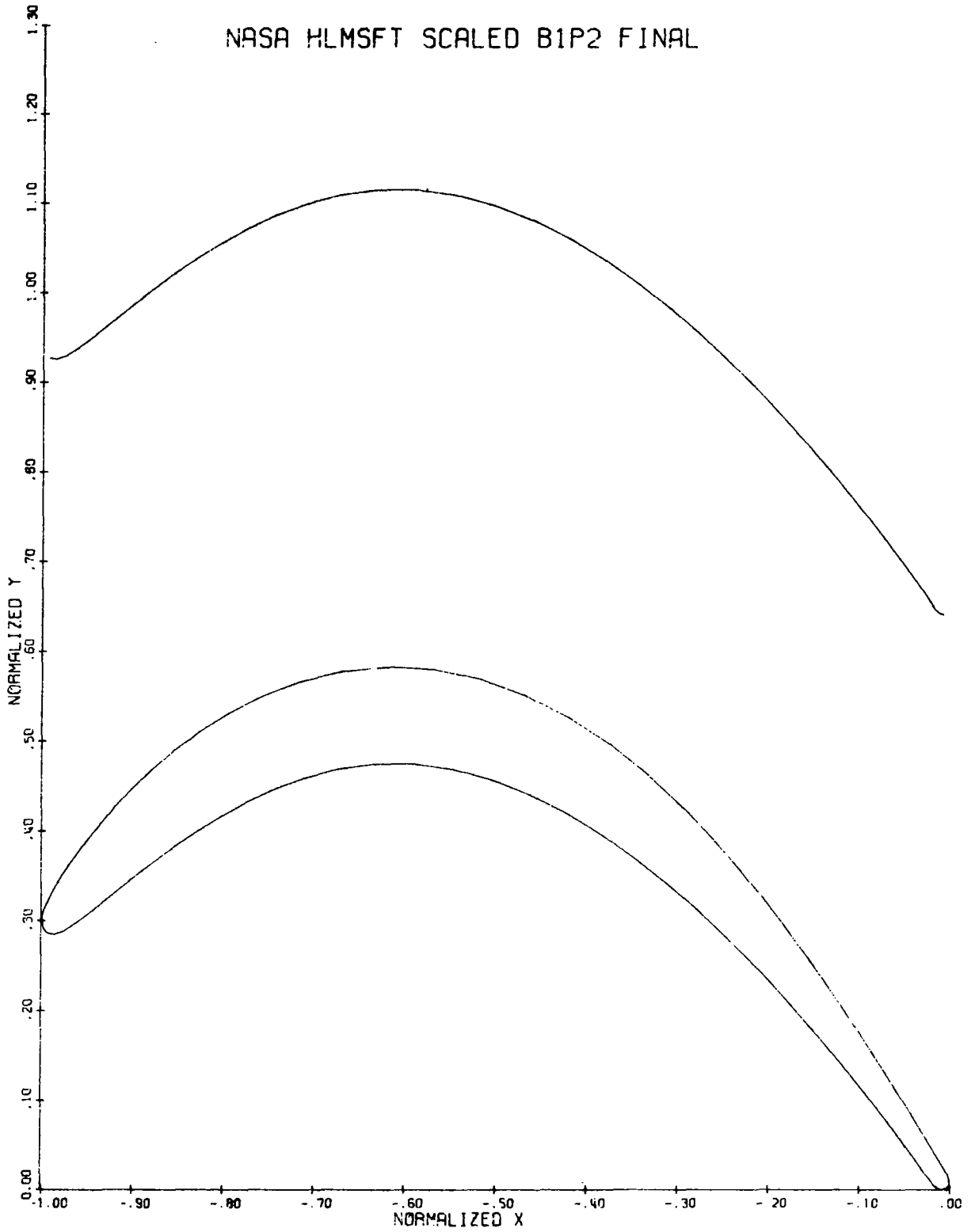


Figure 16. Stage One Blade Pitch Airfoil Flowpath.

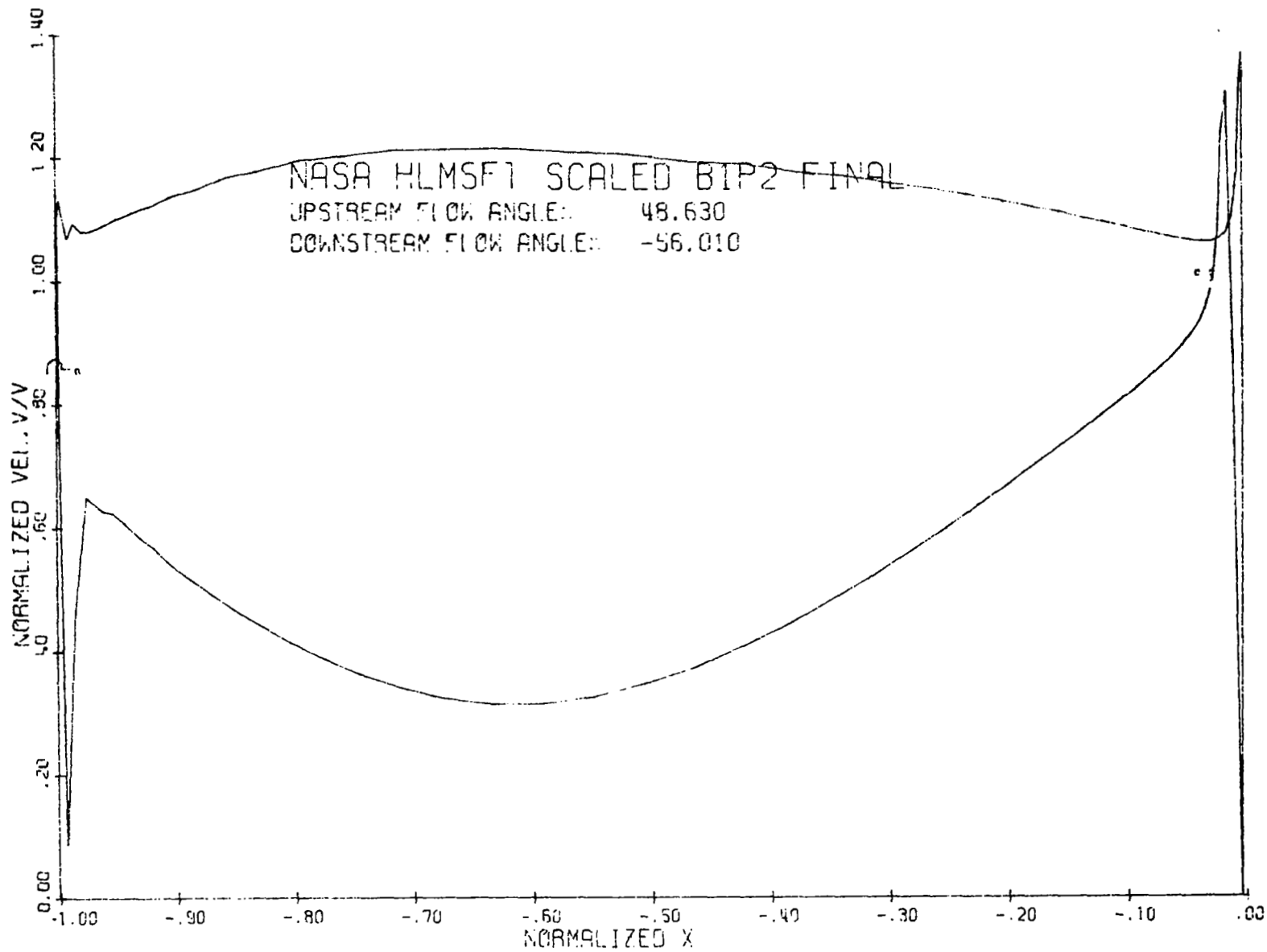


Figure 17. Stage One Blade Pitch Velocity Distribution.

NASA HLMSFT SCALED B1T3 FINAL

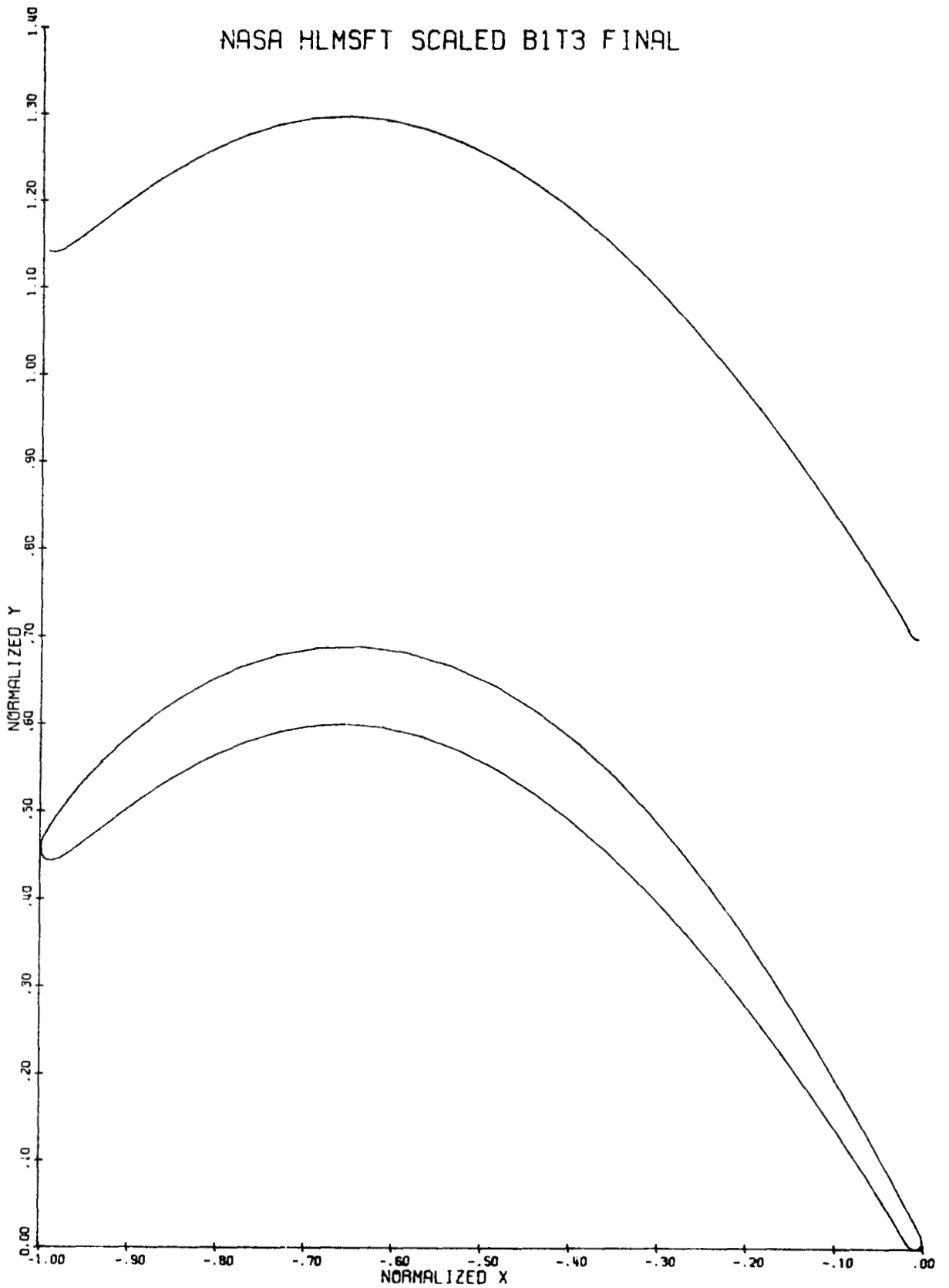


Figure 18. Stage One Blade Tip Airfoil Flowpath.



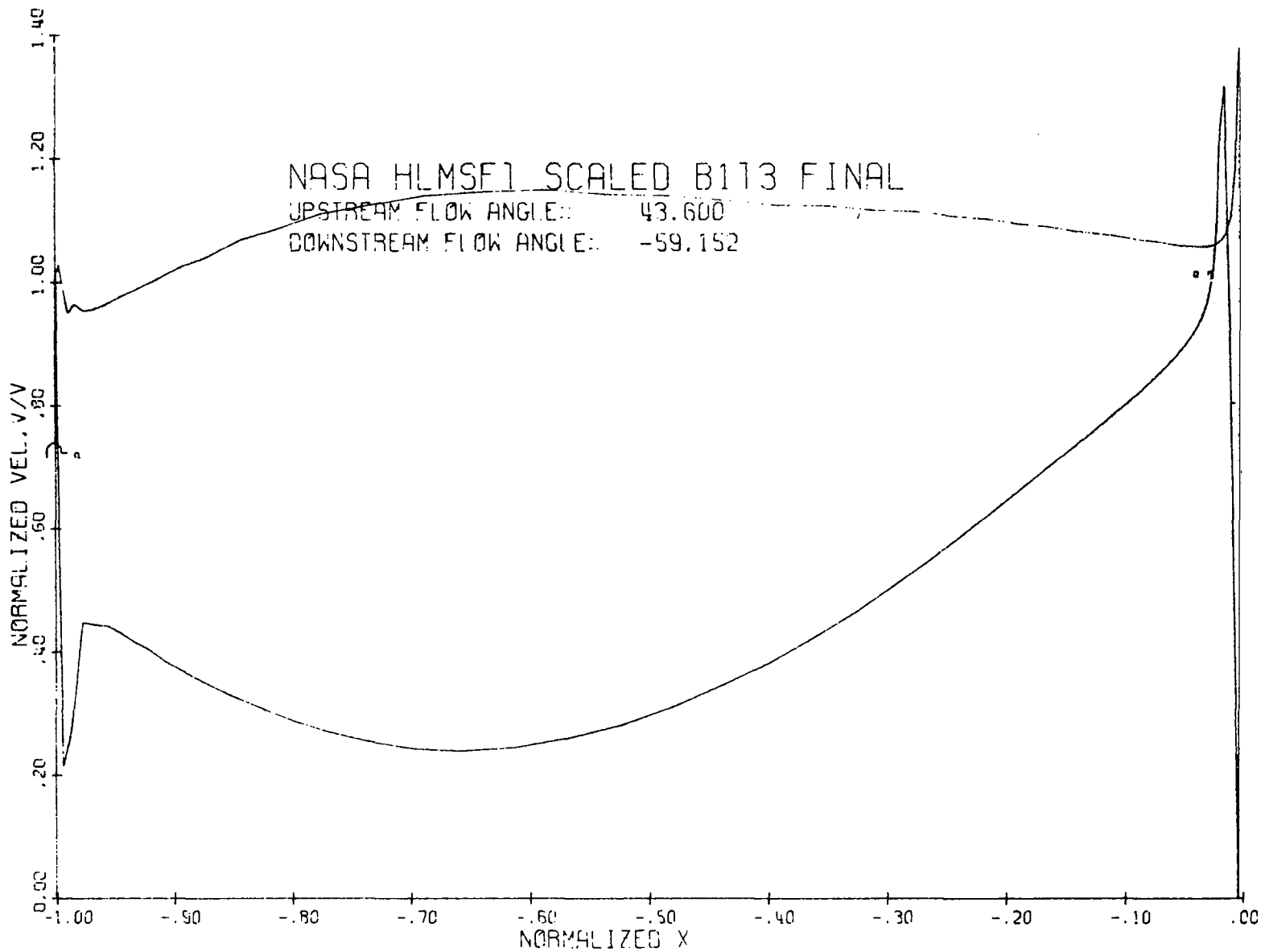


Figure 19. Stage One Blade Tip Velocity Distribution.

NASA HLMSFT SCALED N2R3 FINAL

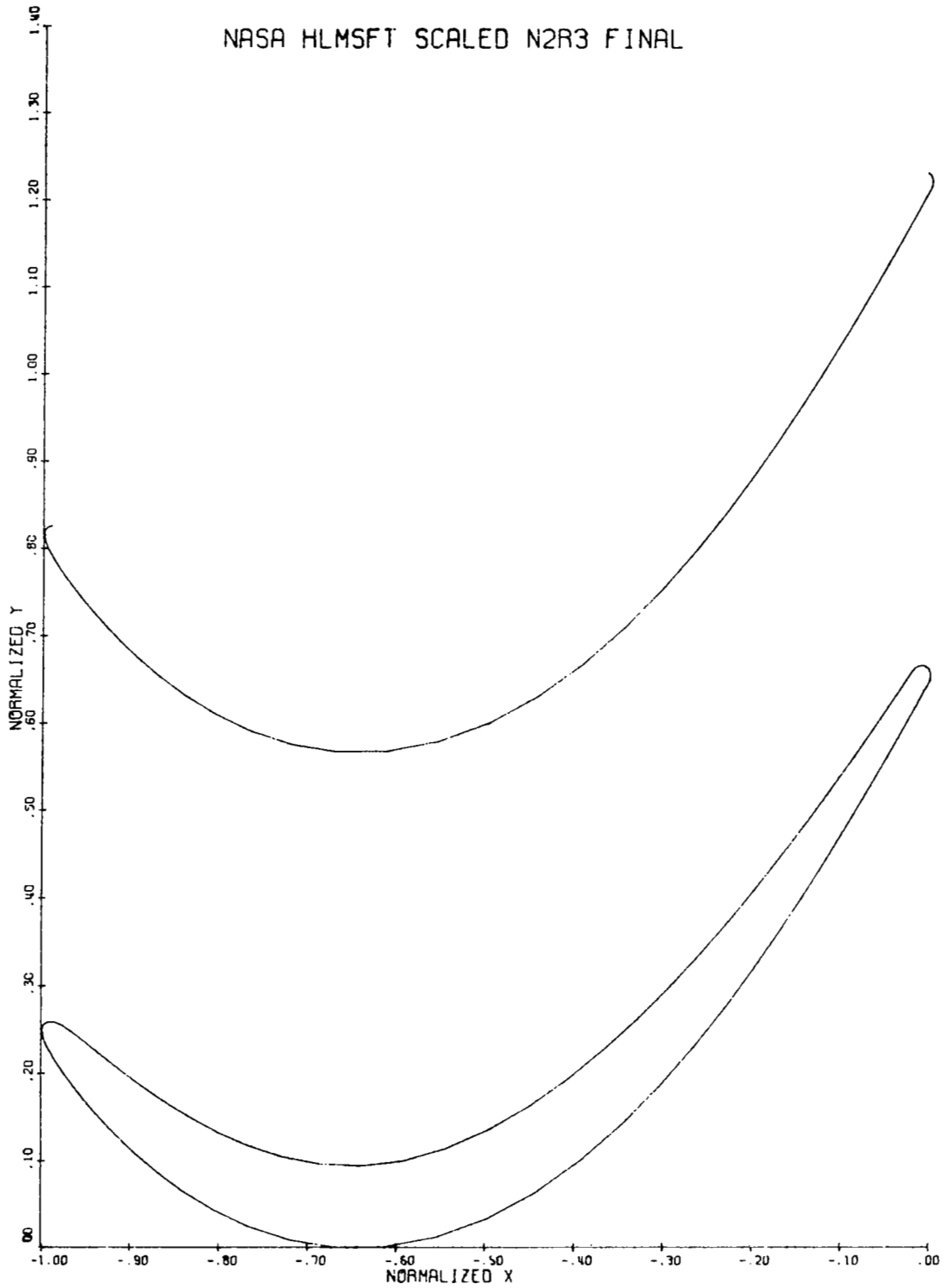


Figure 20. Stage Two Vane Hub Airfoil Flowpath.

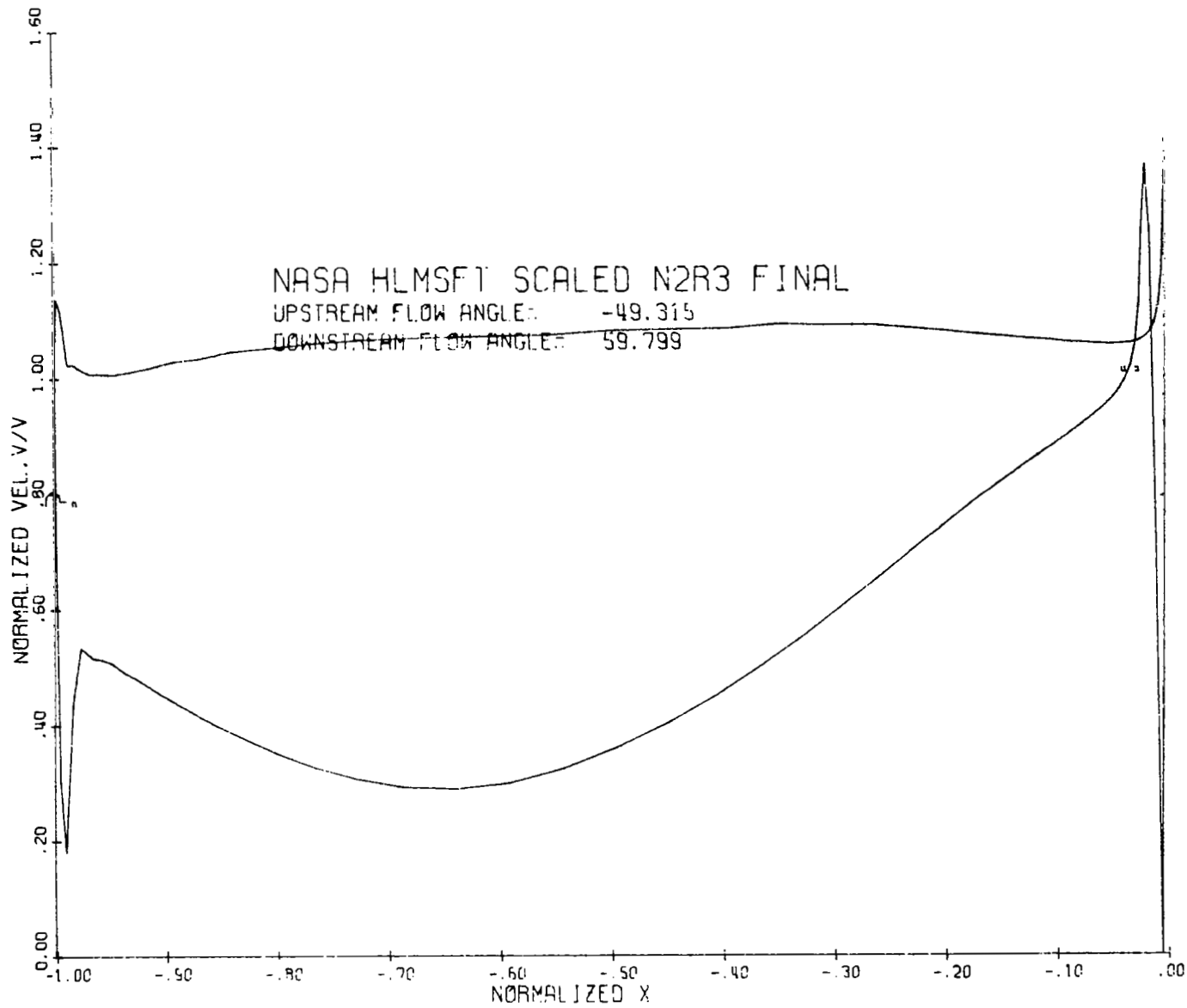


Figure 21. Stage Two Vane Hub Velocity Distribution.

NASA HLMSFT SCALED N2P2 FINAL

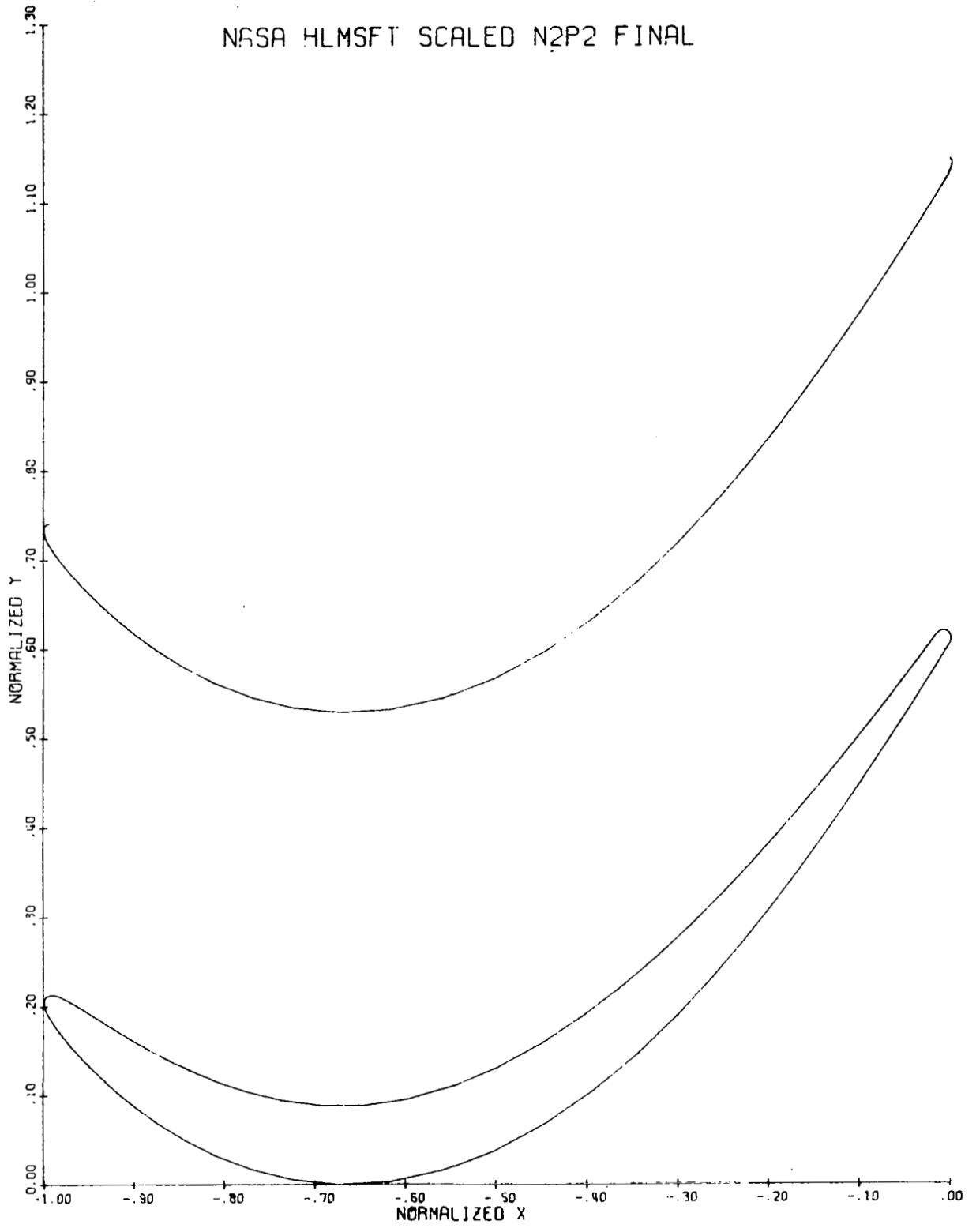


Figure 22. Stage Two Vane Pitch Airfoil Flowpath.

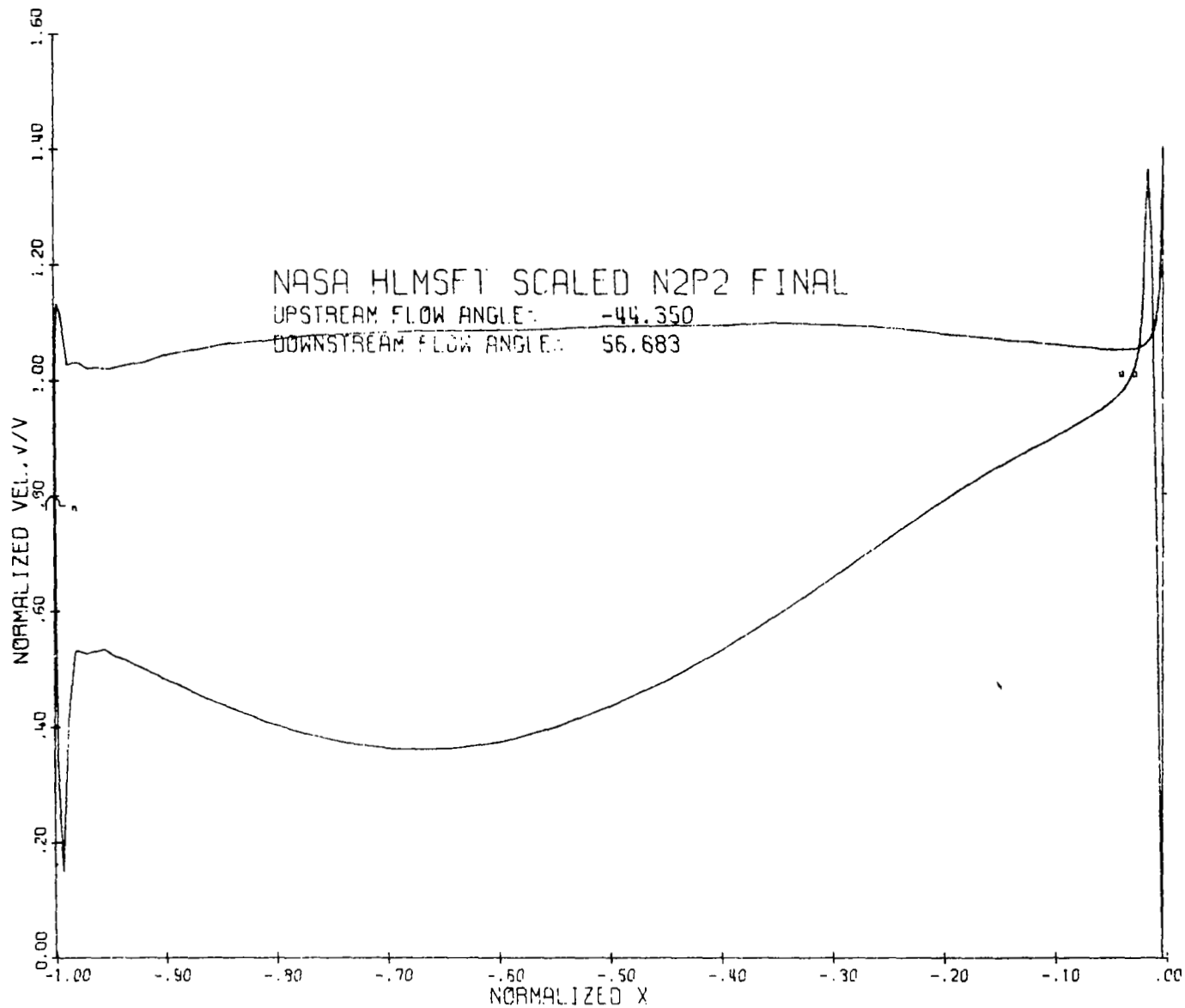


Figure 23. Stage Two Vane Pitch Velocity Distribution.

NASA HLMSFT SCALED N2T3 FINAL

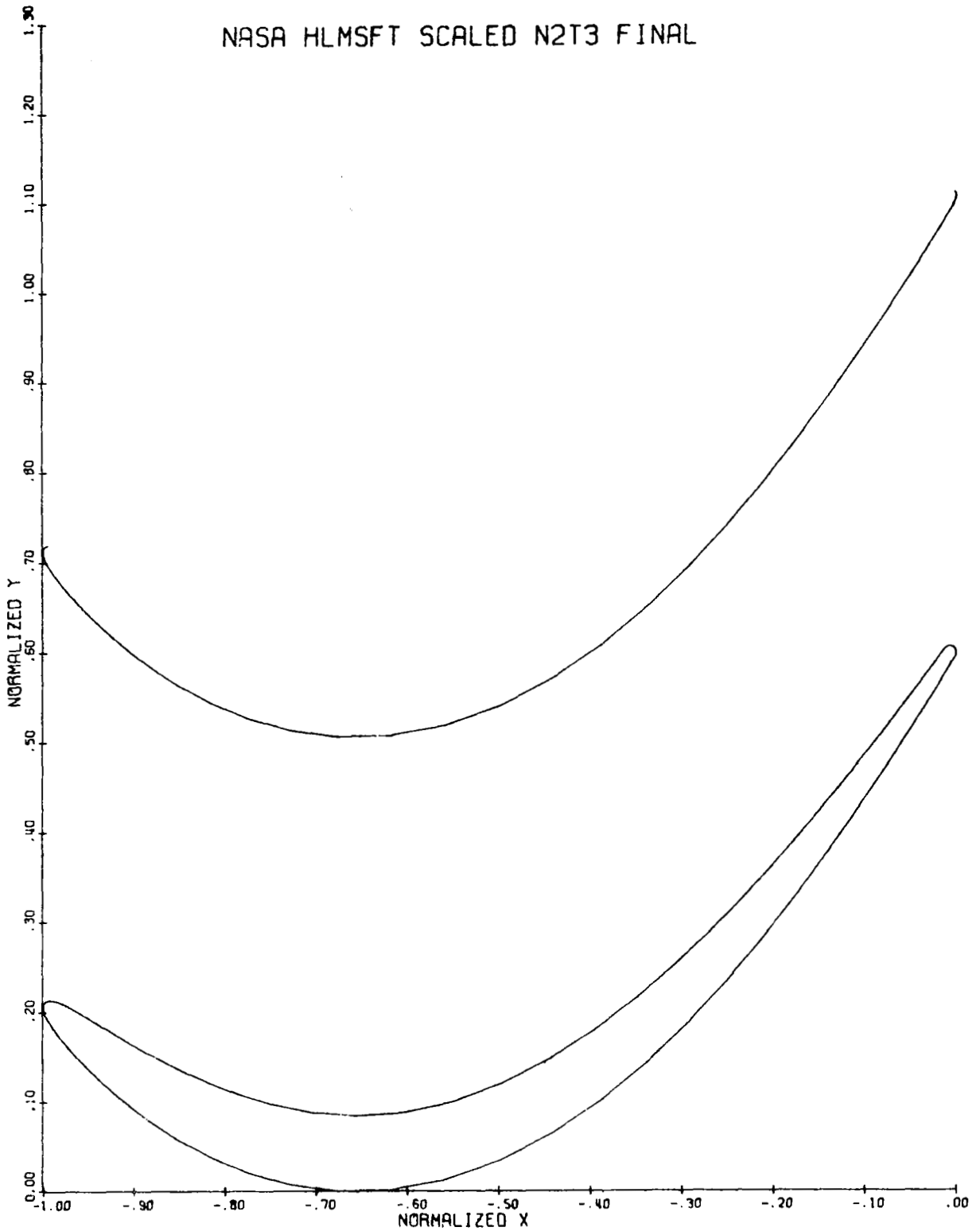


Figure 24. Stage Two Vane Tip Airfoil Flowpath.

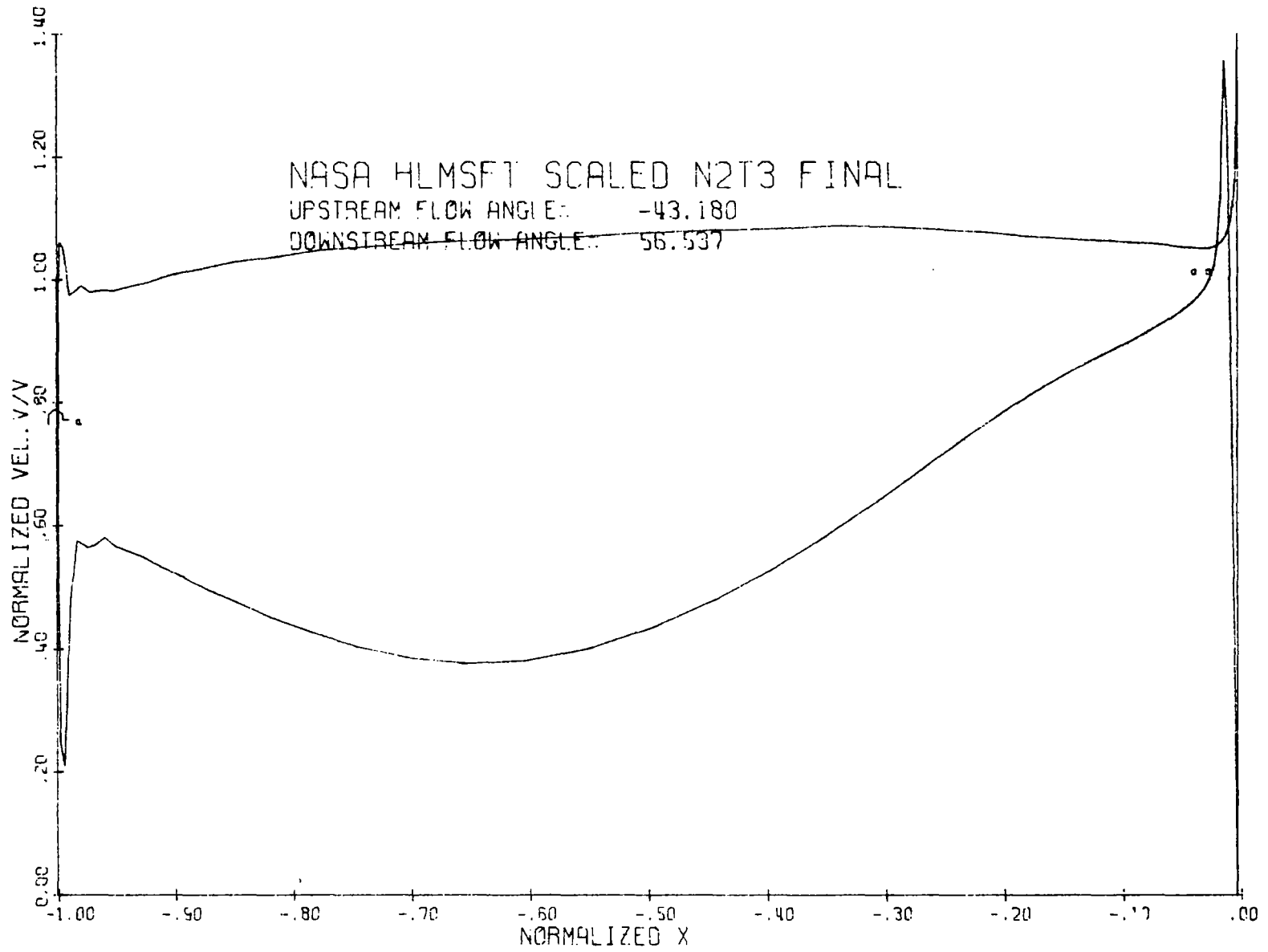


Figure 25. Stage Two Vane Tip Velocity Distribution

NASA HLMSFT SCALED B2R3 FINAL

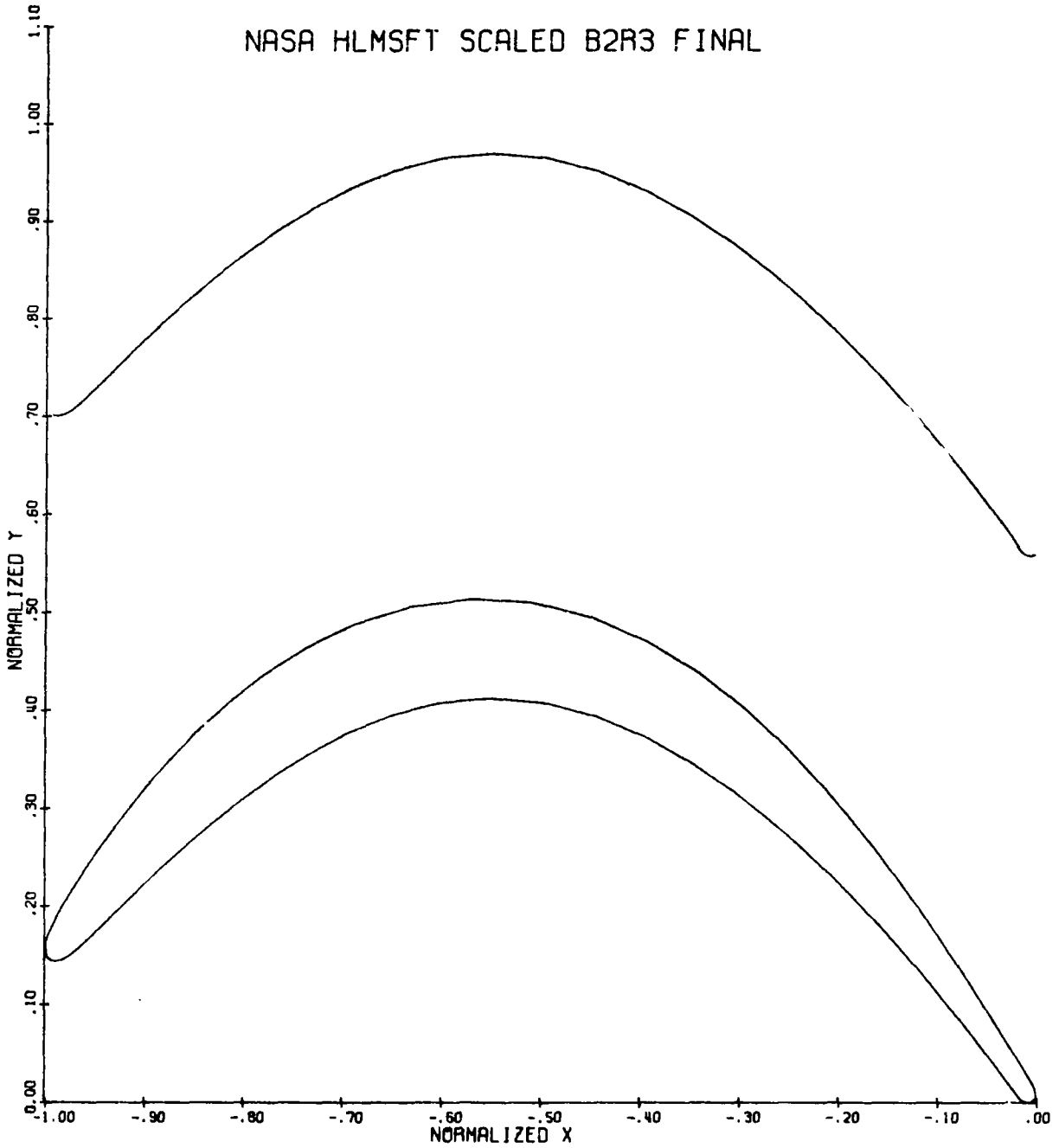


Figure 26. Stage Two Blade Hub Airfoil Flowpath.



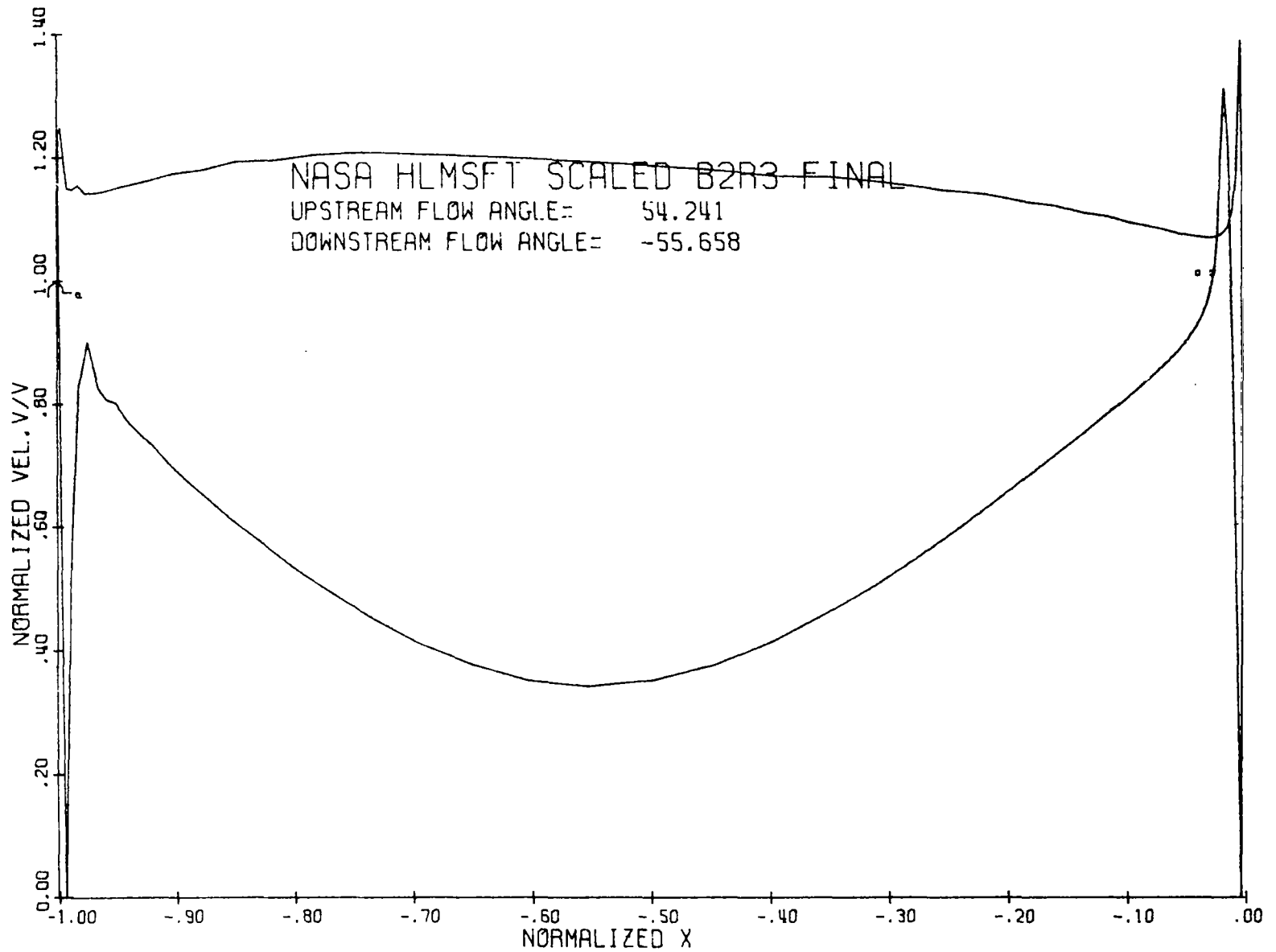


Figure 27. Stage Two Blade Hub Velocity Distribution.

NASA HLMSFT SCALED B2P2 FINAL

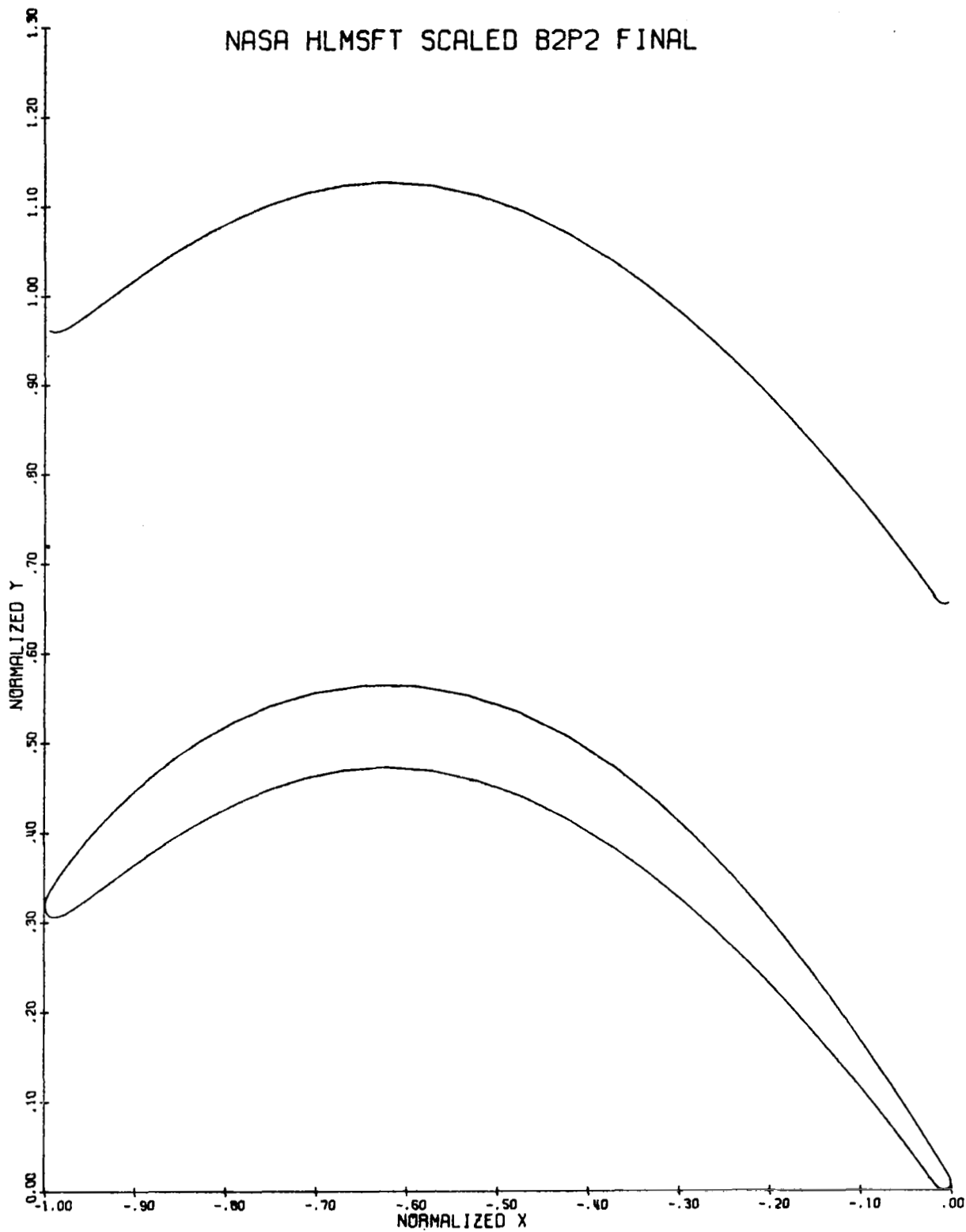


Figure 28. Stage Two Blade Pitch Airfoil Flowpath.

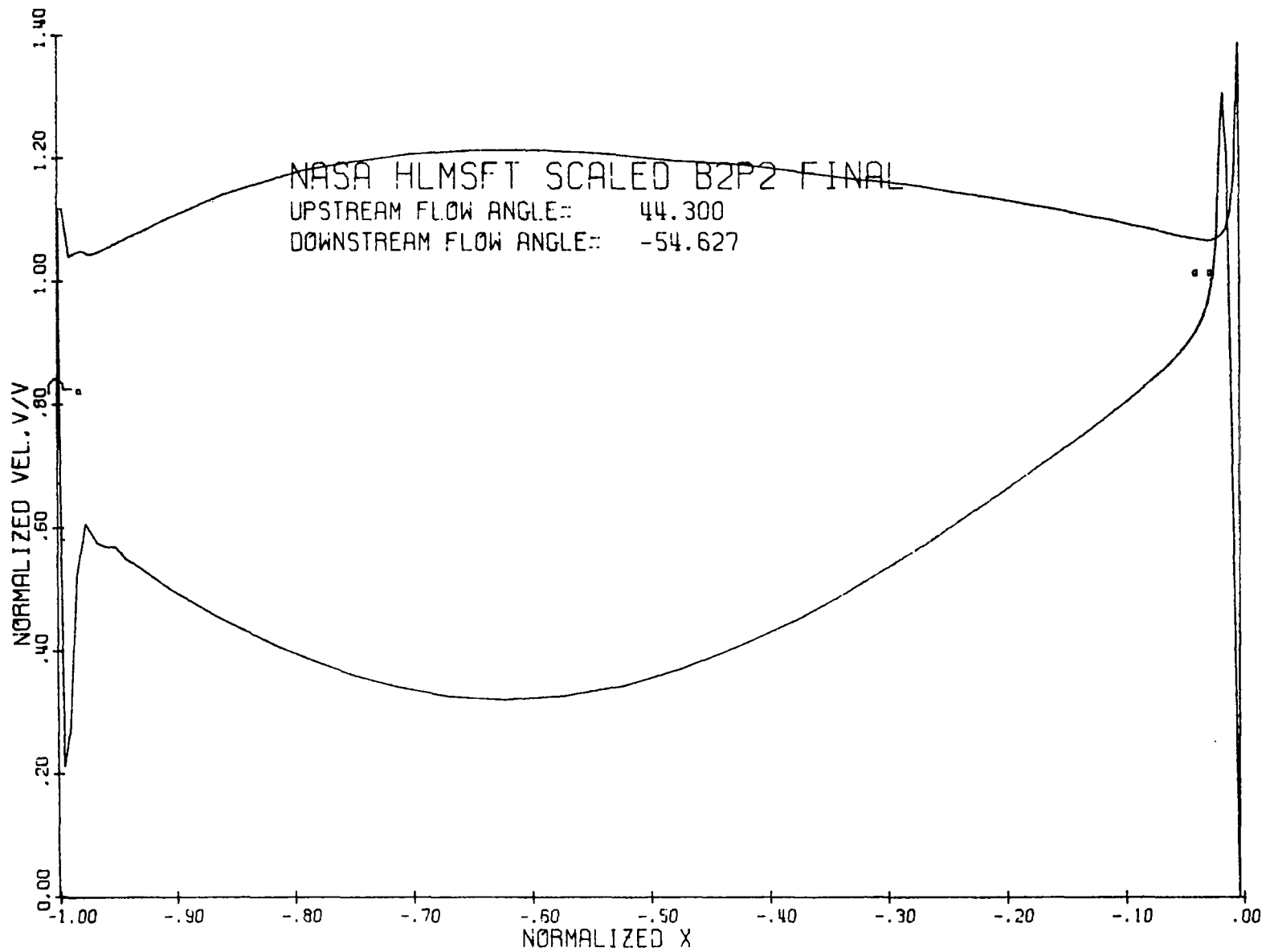


Figure 29. Stage Two Blade Pitch Velocity Distribution.

NASA HLMSFT SCALED B2T3 FINAL

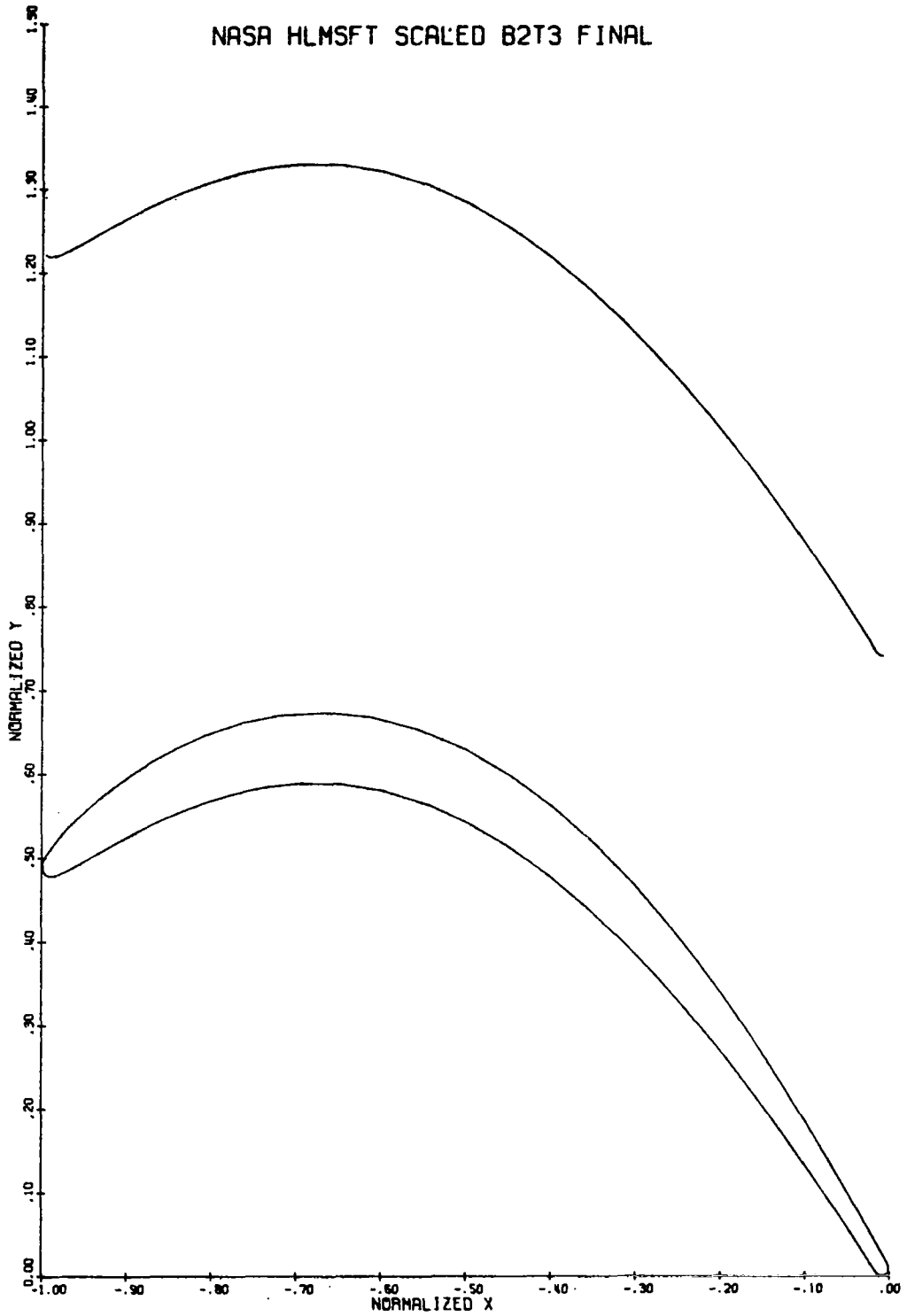


Figure 30. Stage Two Blade Tip Airfoil Flowpath.

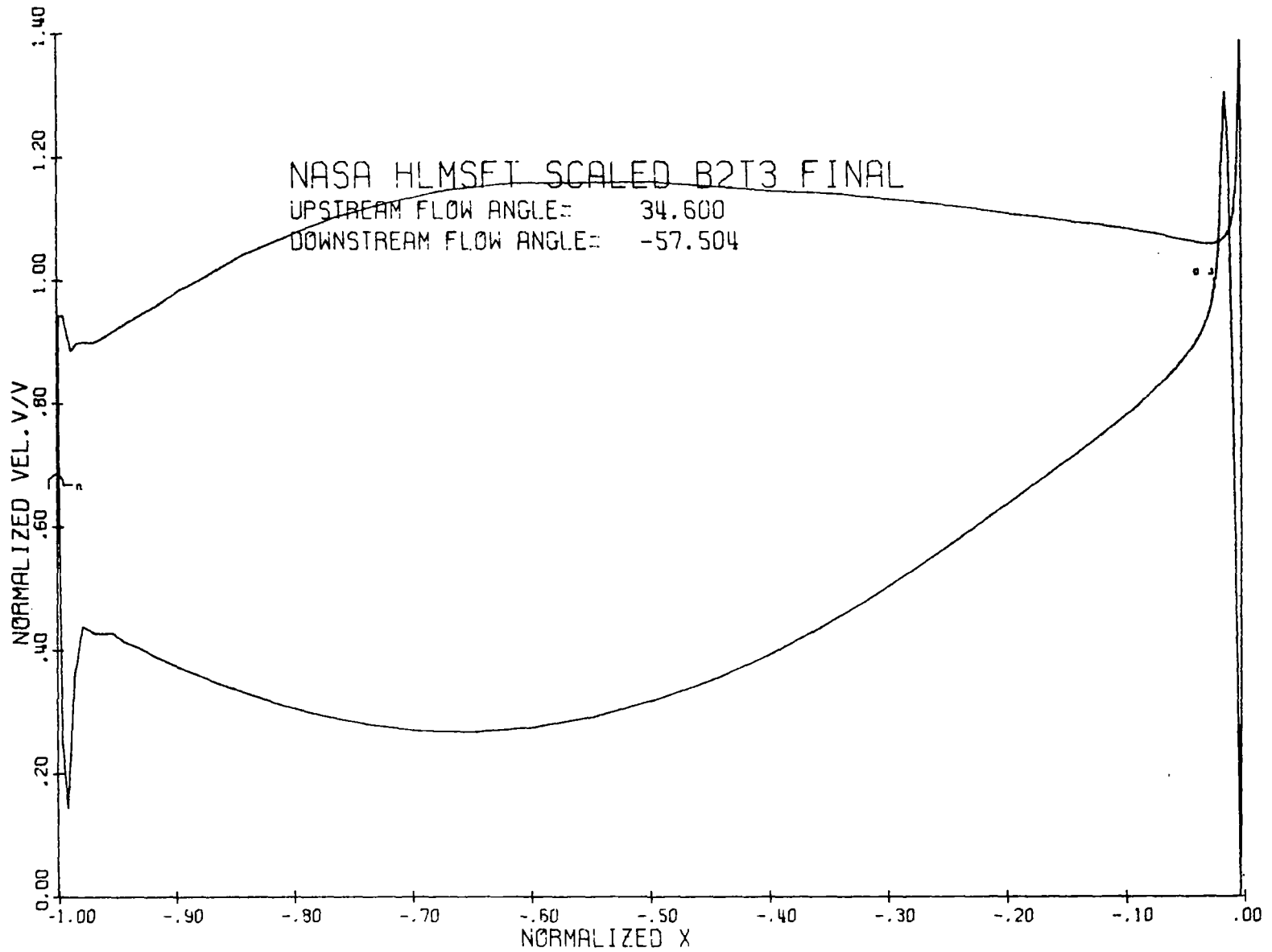


Figure 31. Stage Two Blade Tip Velocity Distribution.

NASA HLMSFT SCALED N3R3 FINAL

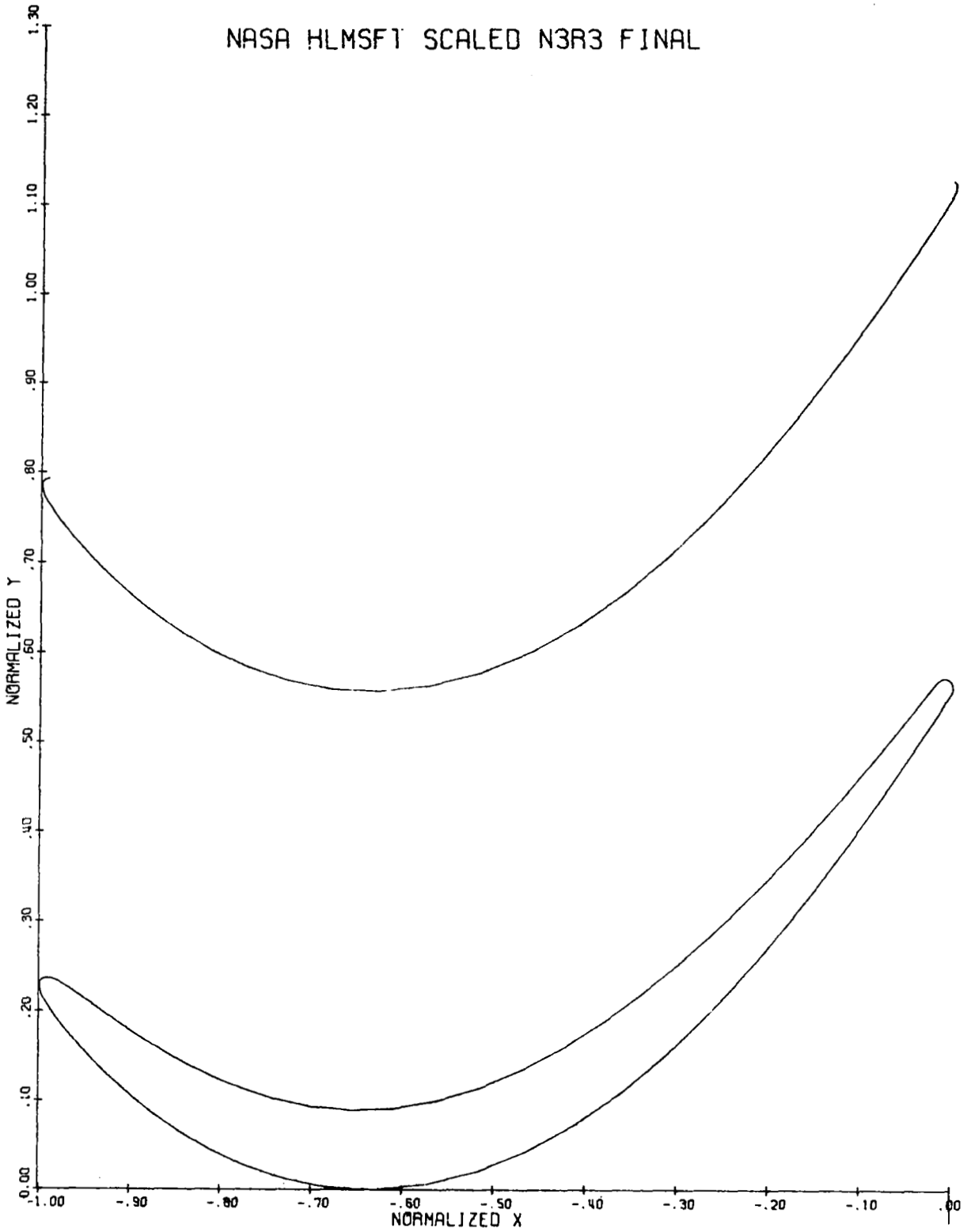


Figure 32. Stage Three Vane Hub Airfoil Flowpath.

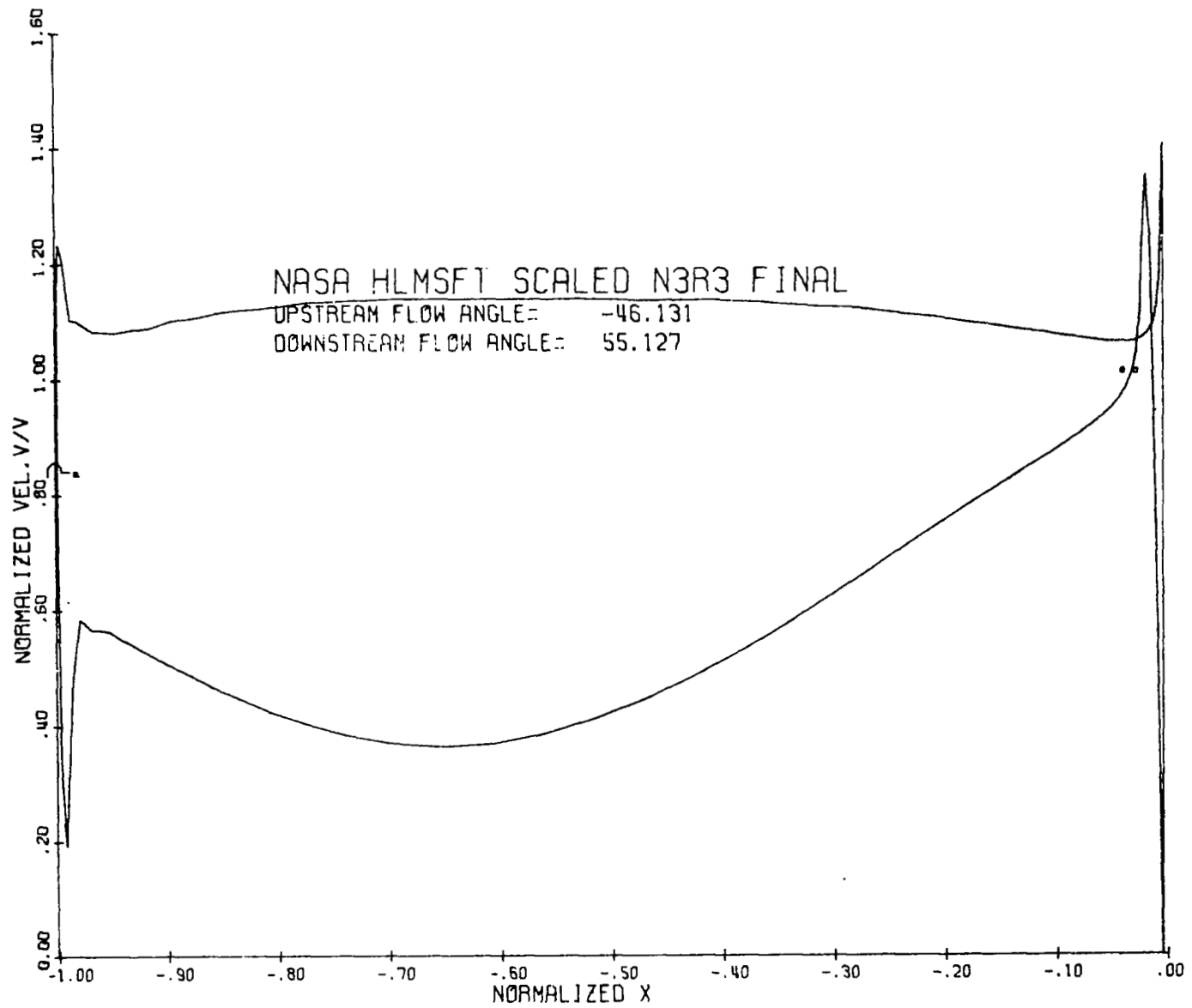


Figure 33. Stage Three Vane Hub Velocity Distribution.

NASA HLMSFT SCALED N3P2 FINAL

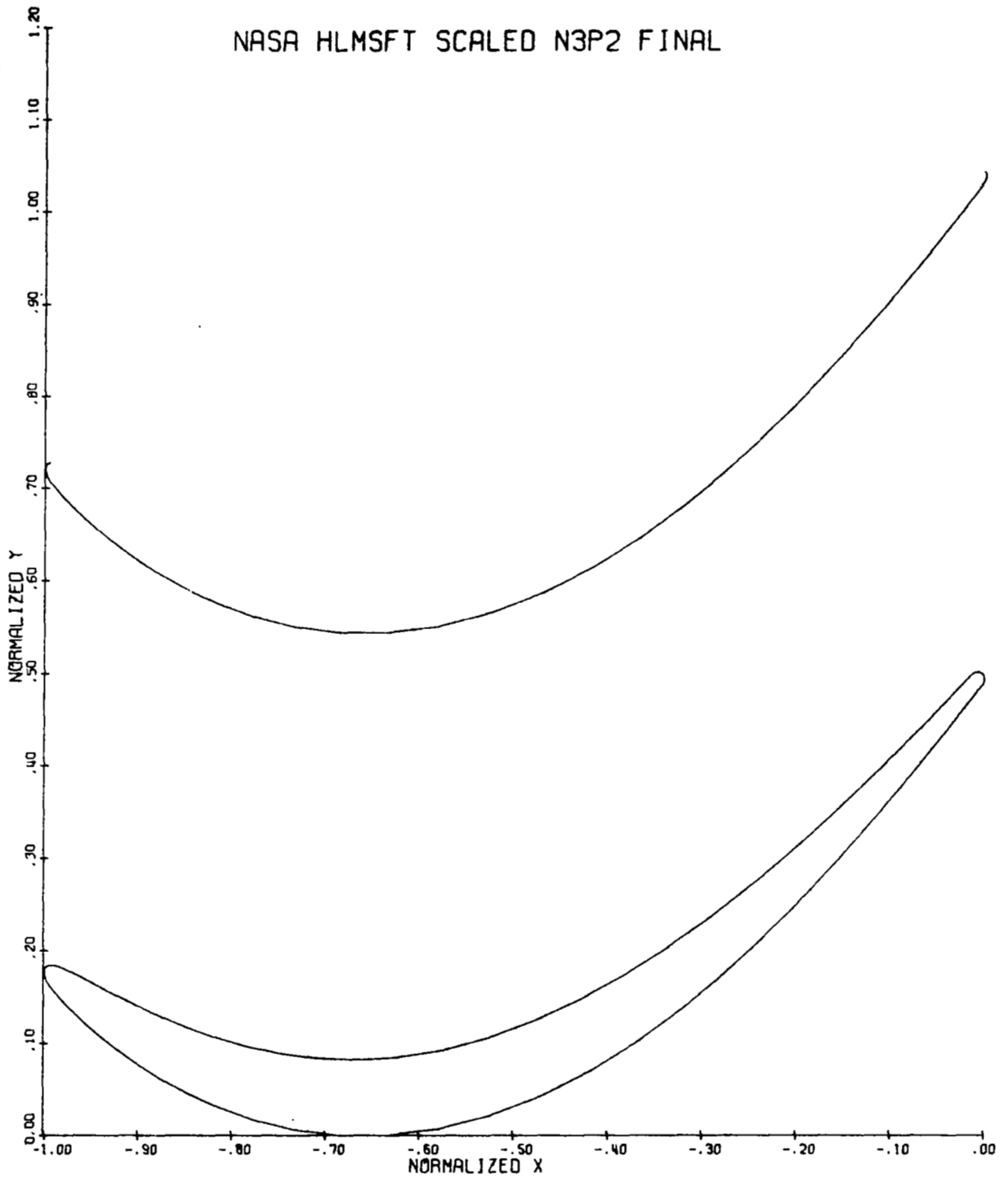


Figure 34. Stage Three Vane Pitch Airfoil Flowpath.



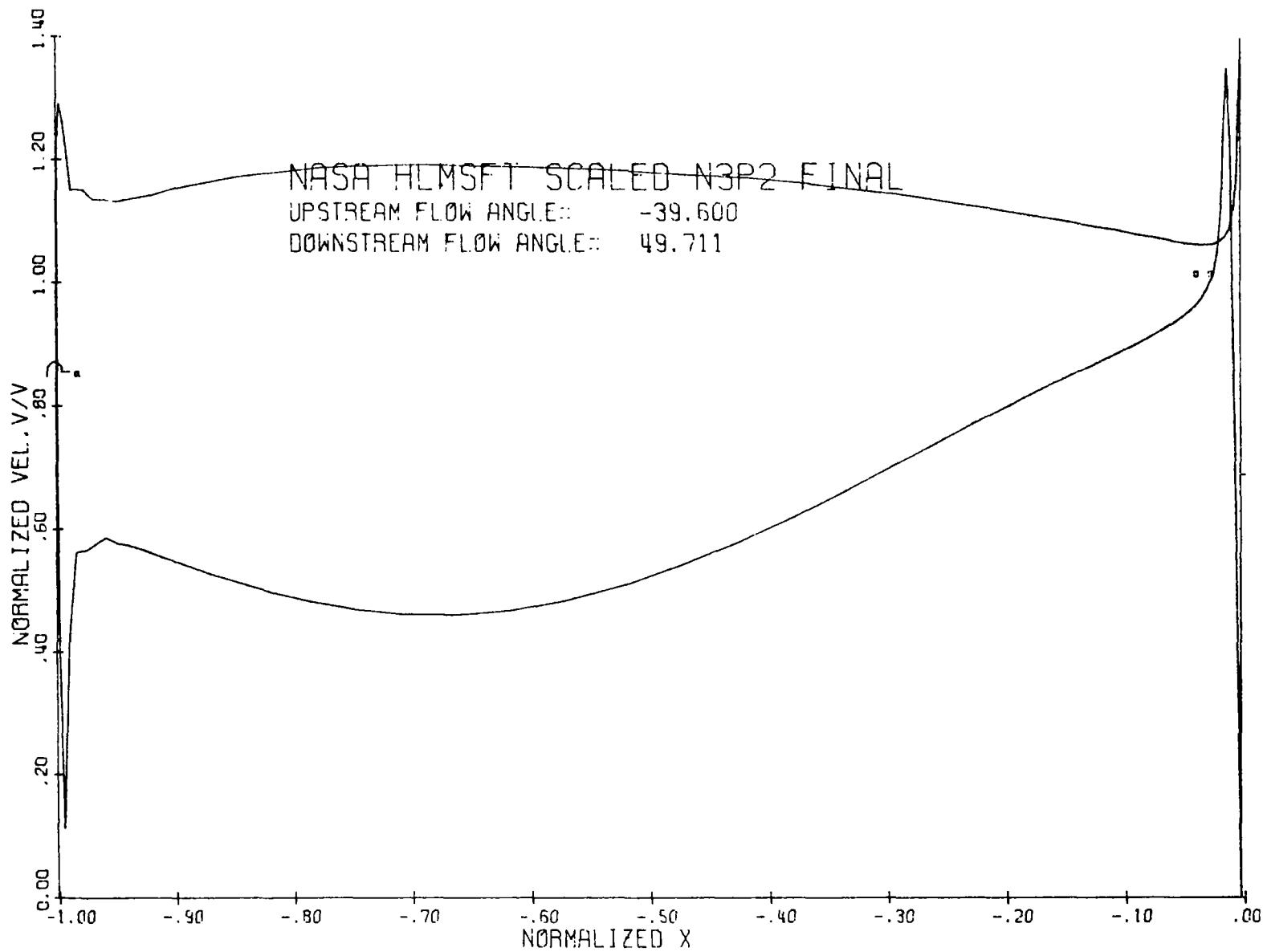


Figure 35. Stage Three Vane Pitch Velocity Distribution.

NASA HLMSFT SCALED N3T3 FINAL

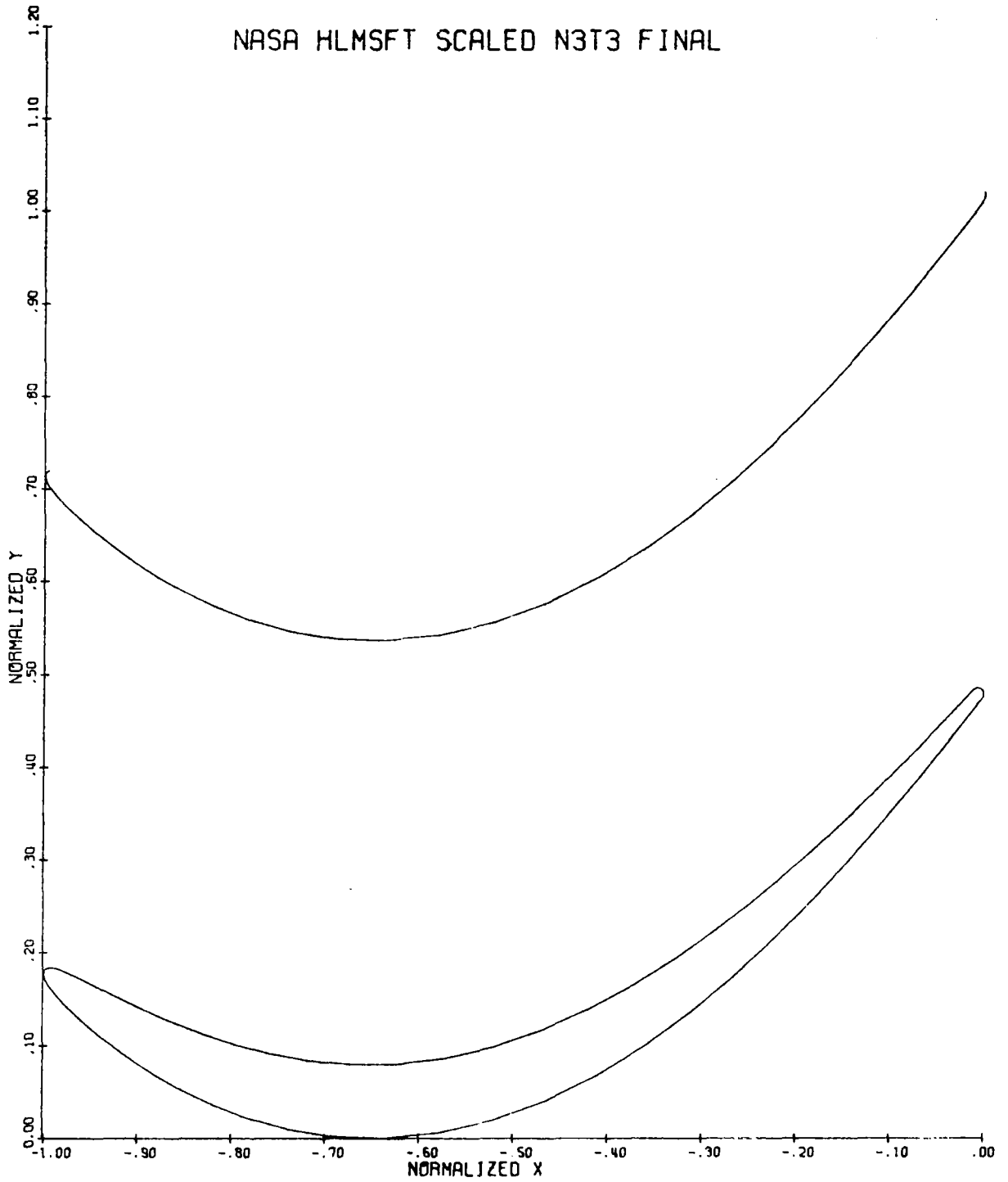


Figure 36. Stage Three Vane Tip Airfoil Flowpath.

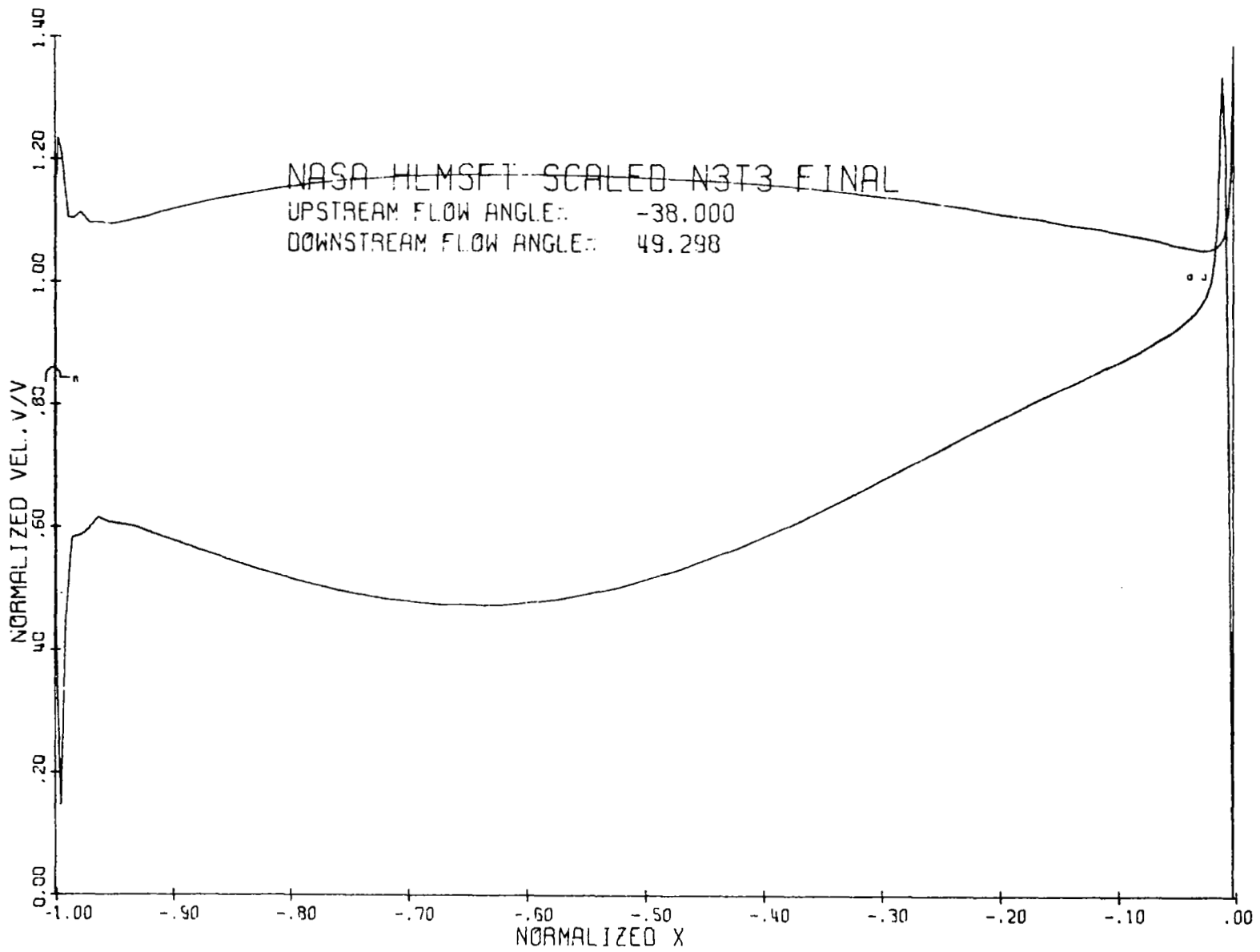


Figure 37. Stage Three Vane Tip Velocity Distribution.

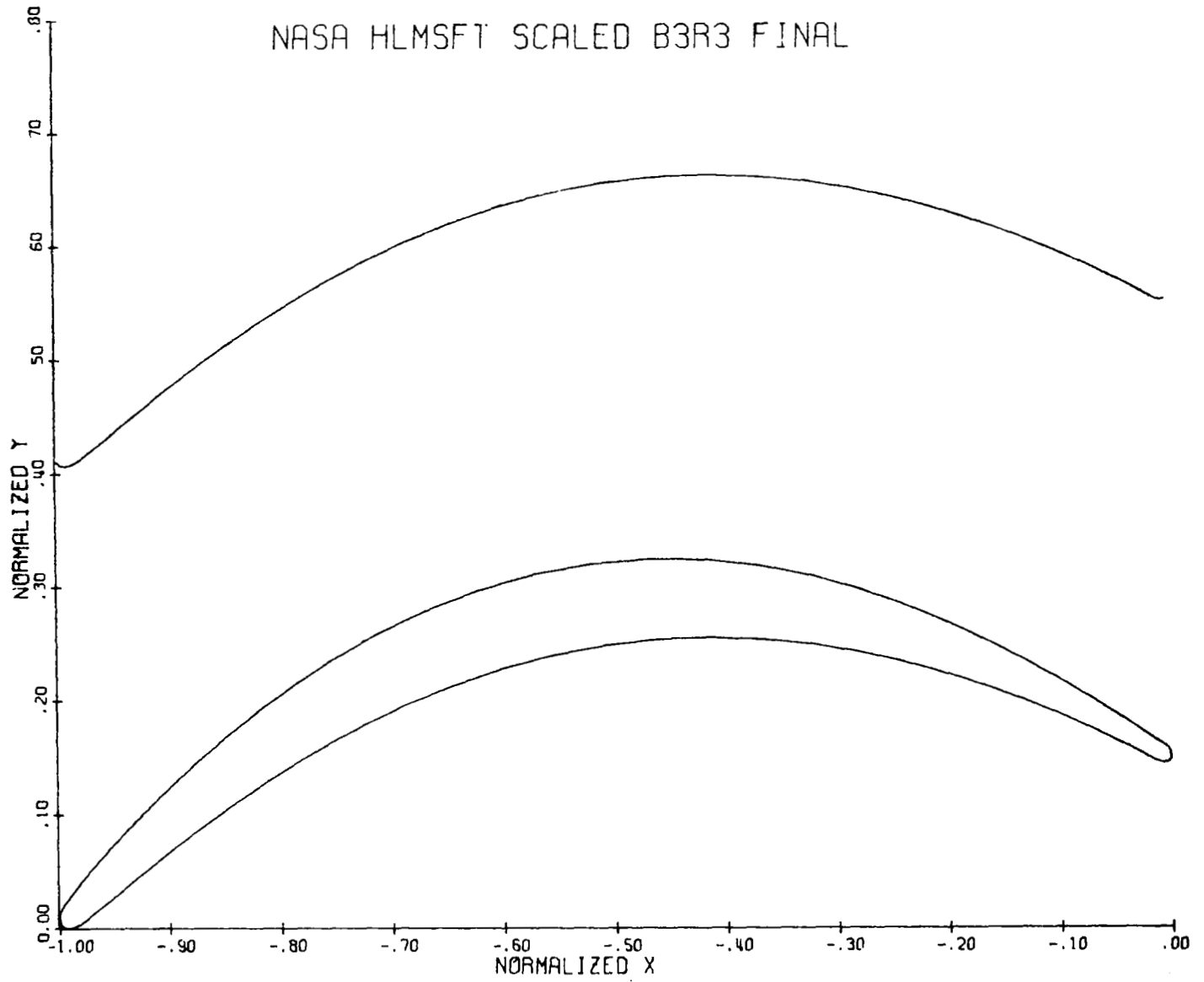


Figure 38. Stage Three Blade Hub Airfoil Flowpath.

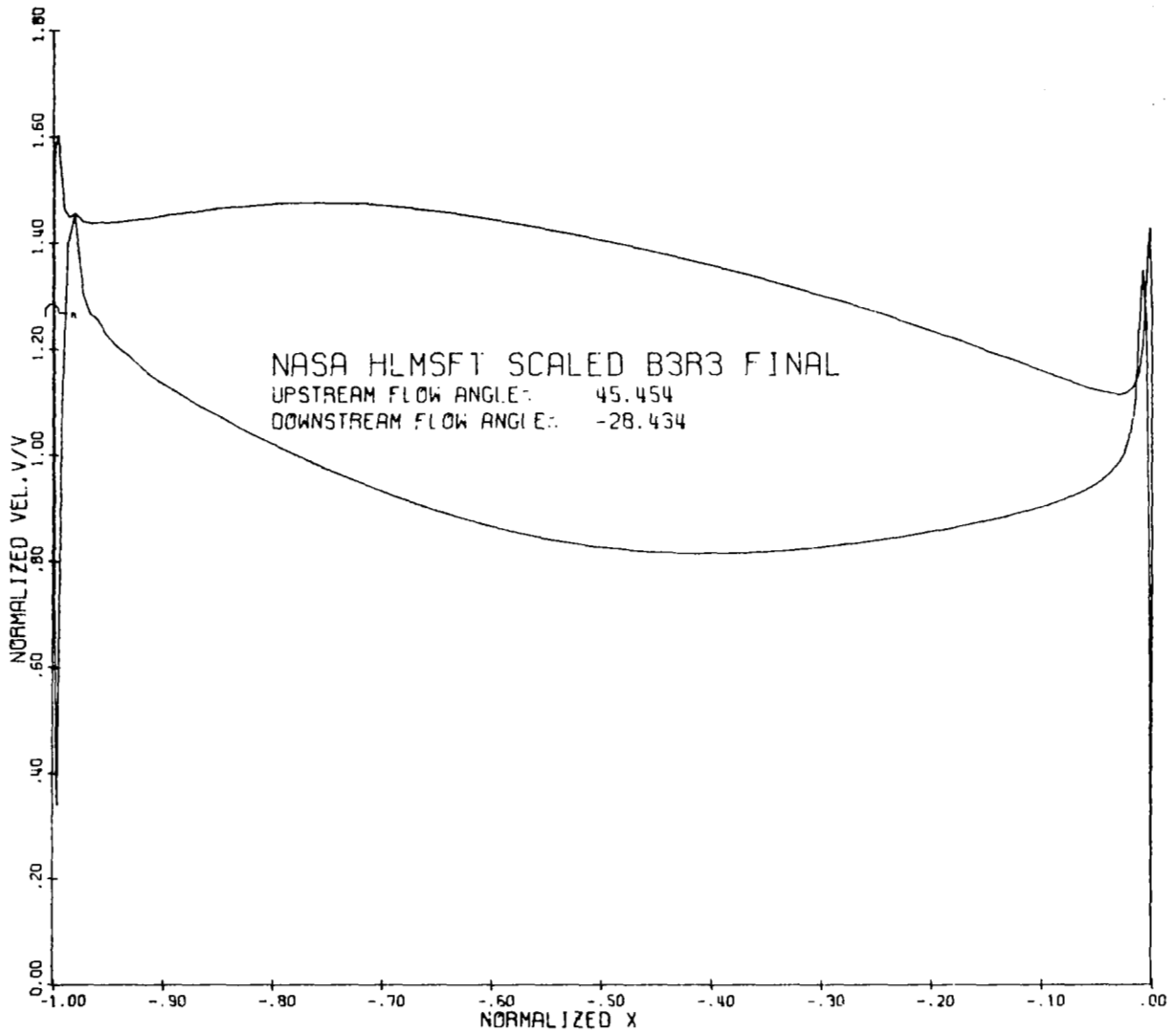
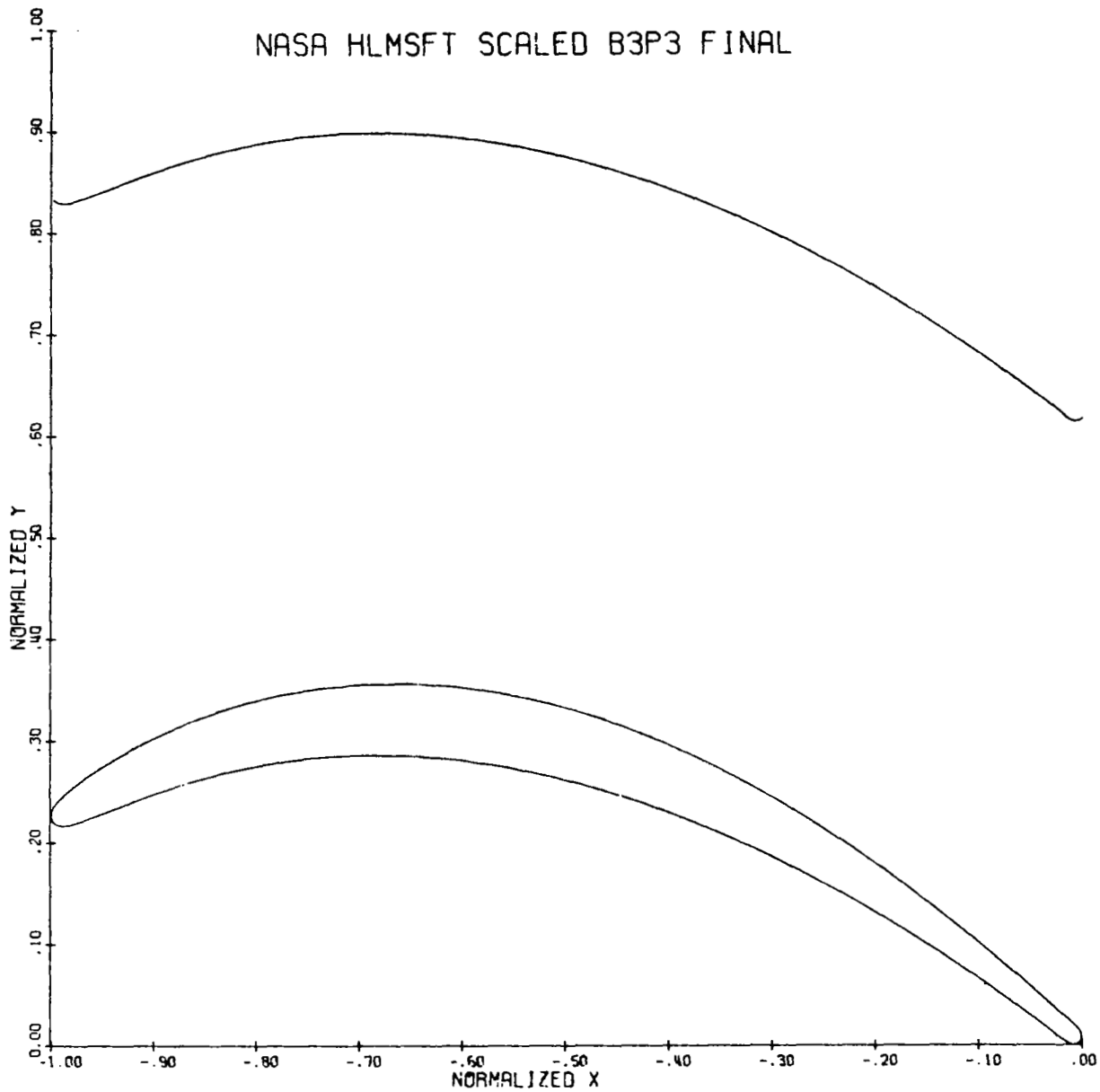


Figure 39. Stage Three Blade Hub Velocity Distribution.



**Figure 40. Stage Three Blade Pitch Airfoil Flowpath.**

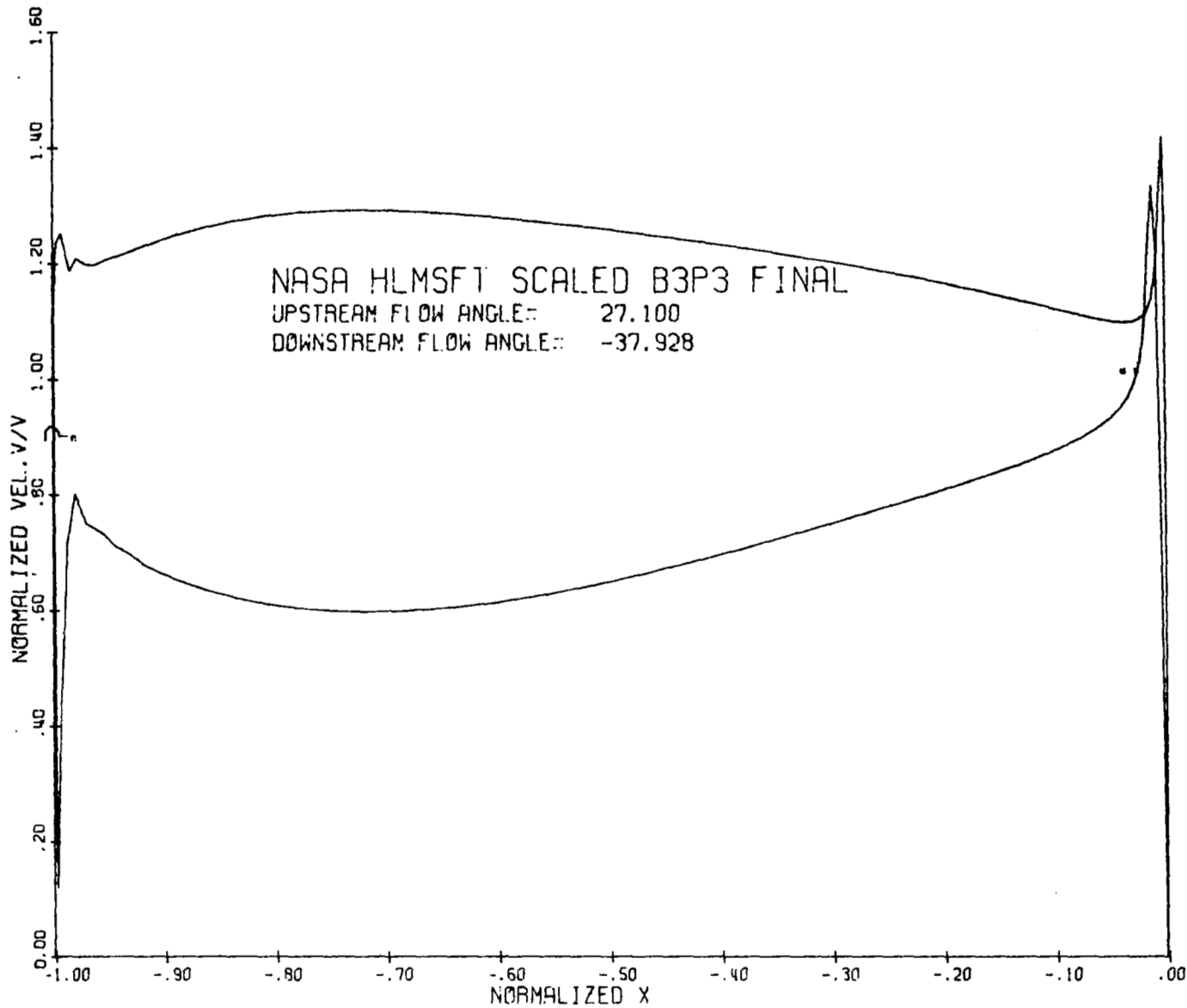
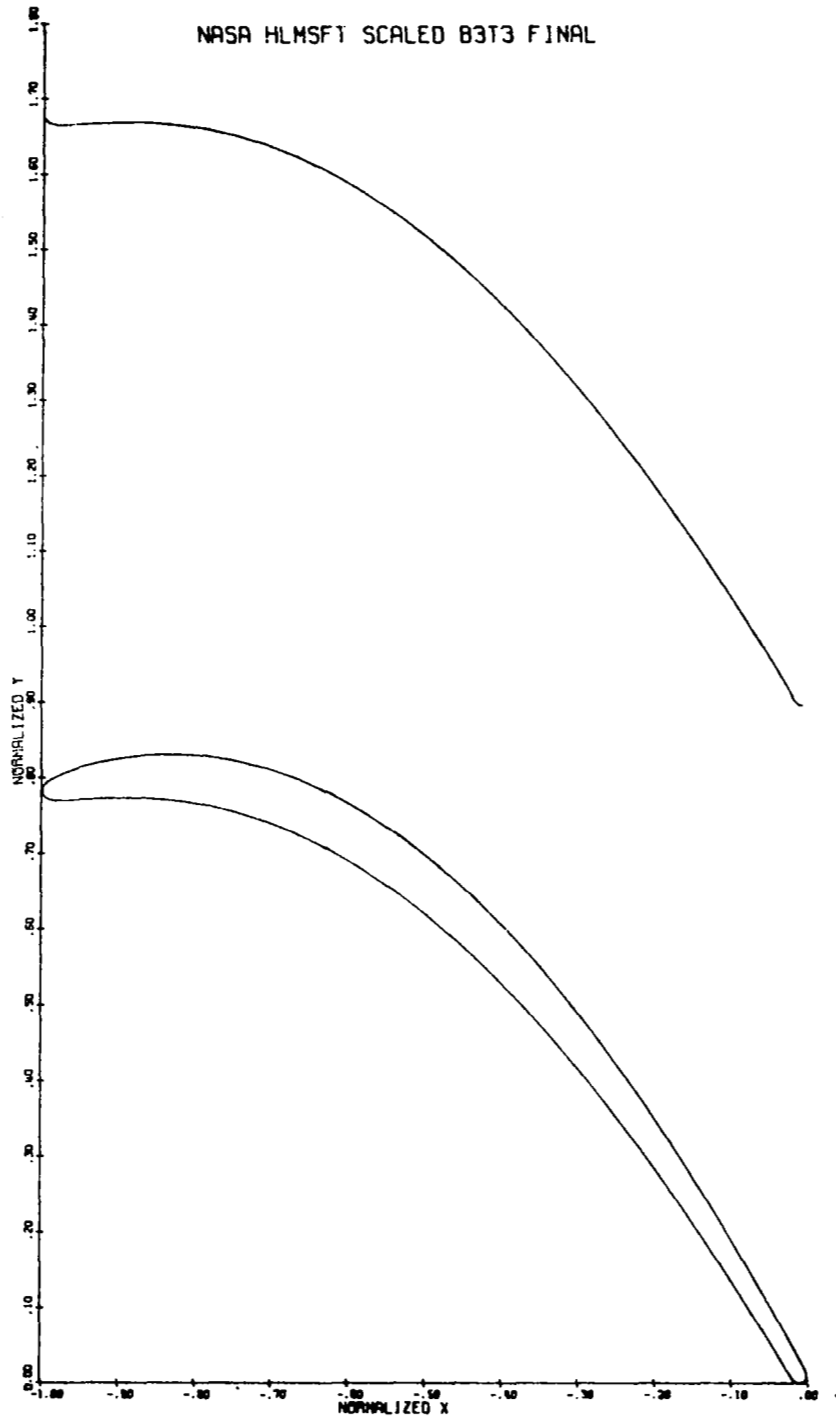


Figure 41. Stage Three Blade Pitch Velocity Distribution.



**Figure 42. Stage Three Blade Tip Airfoil Flowpath.**



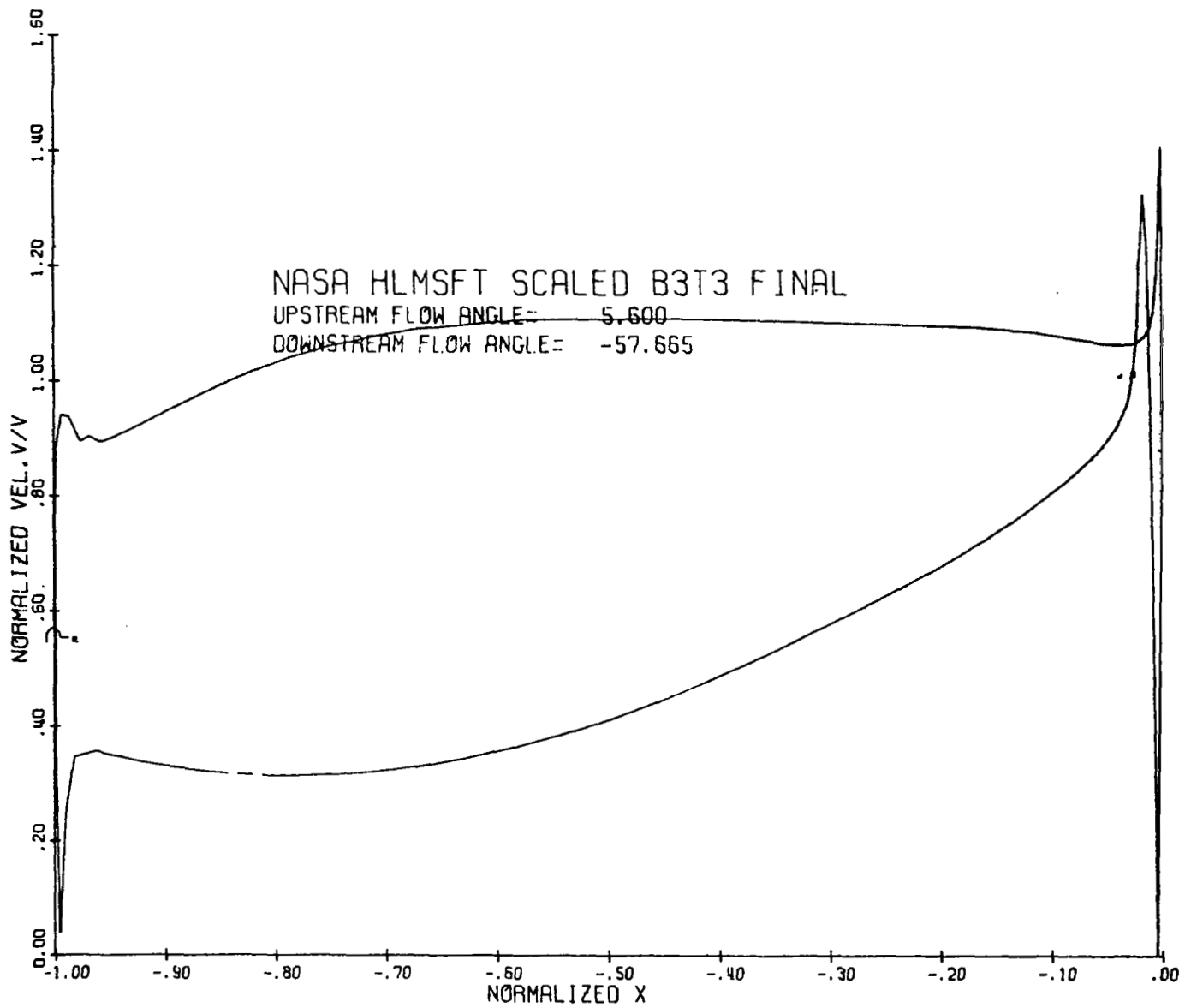


Figure 43. Stage Three Blade Tip Velocity Distribution.

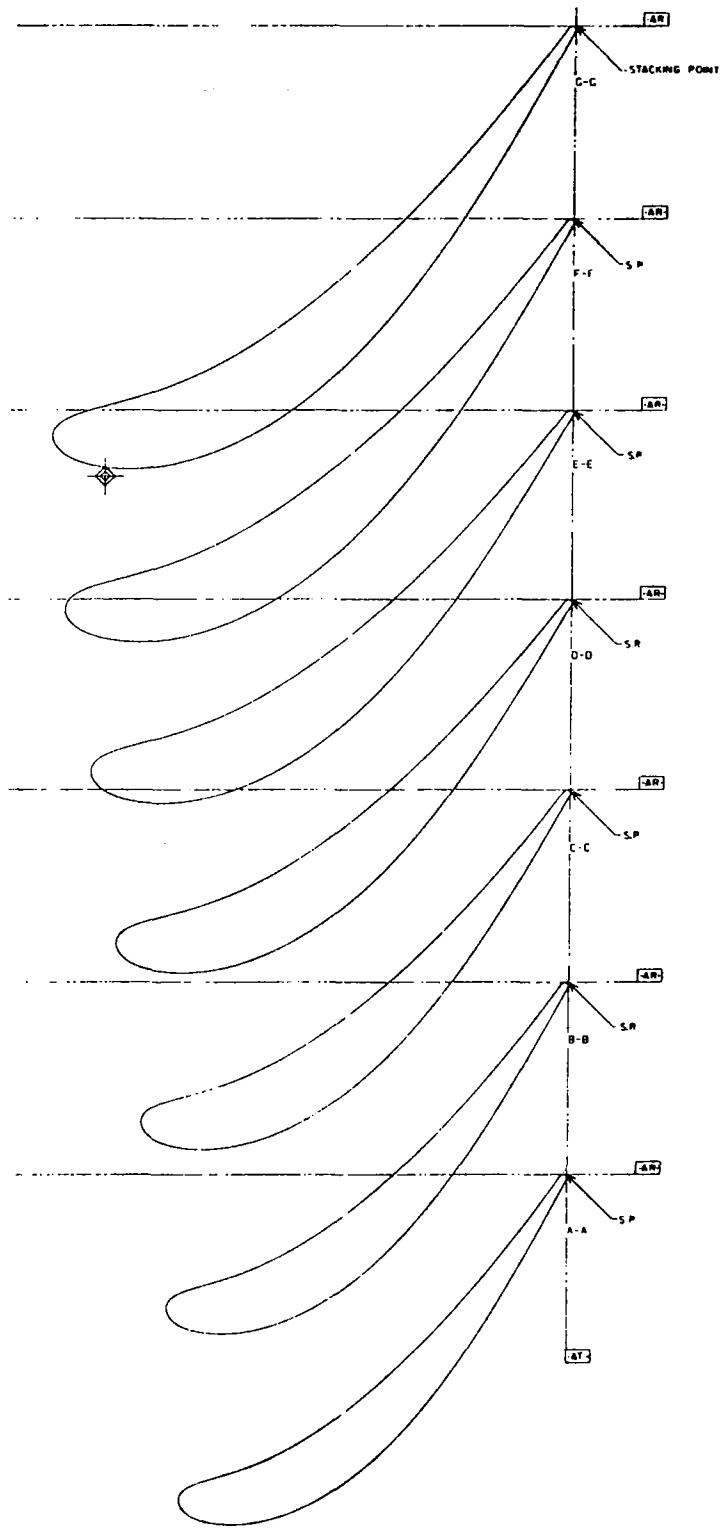


Figure 44. Stage One Vane Precision Master (4012241-942).

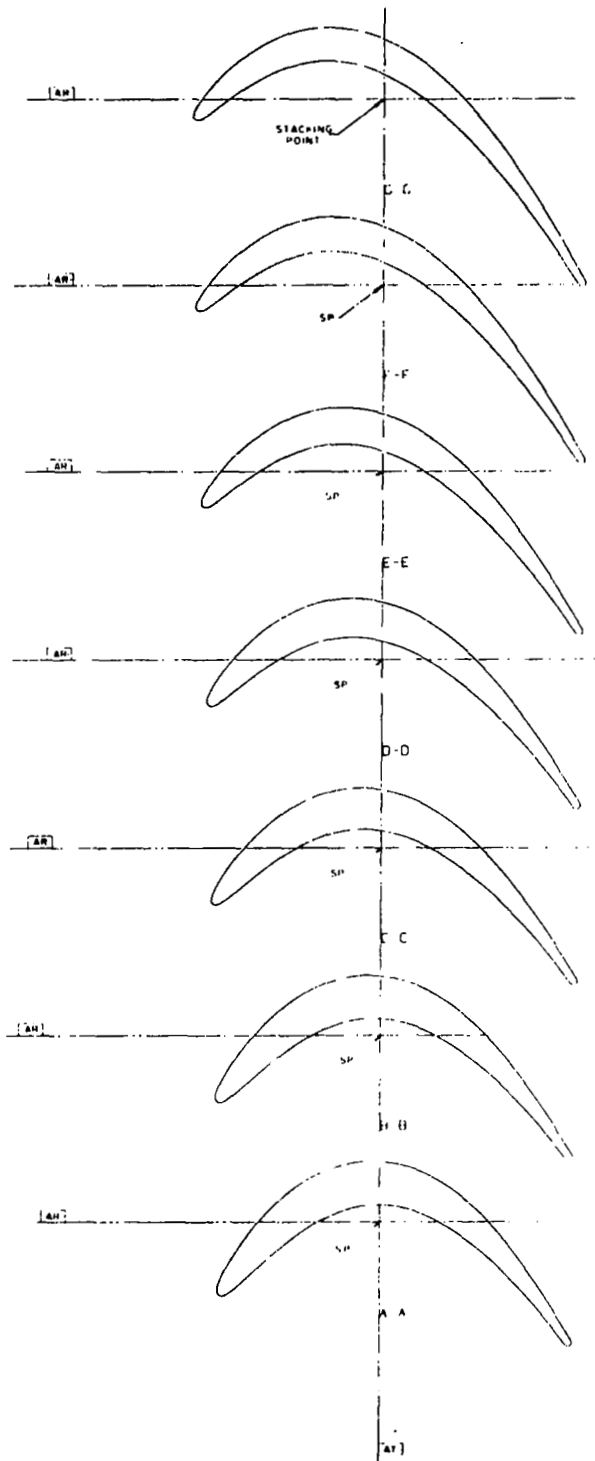


Figure 45. Stage One Blade Precision Master (4012241-948).

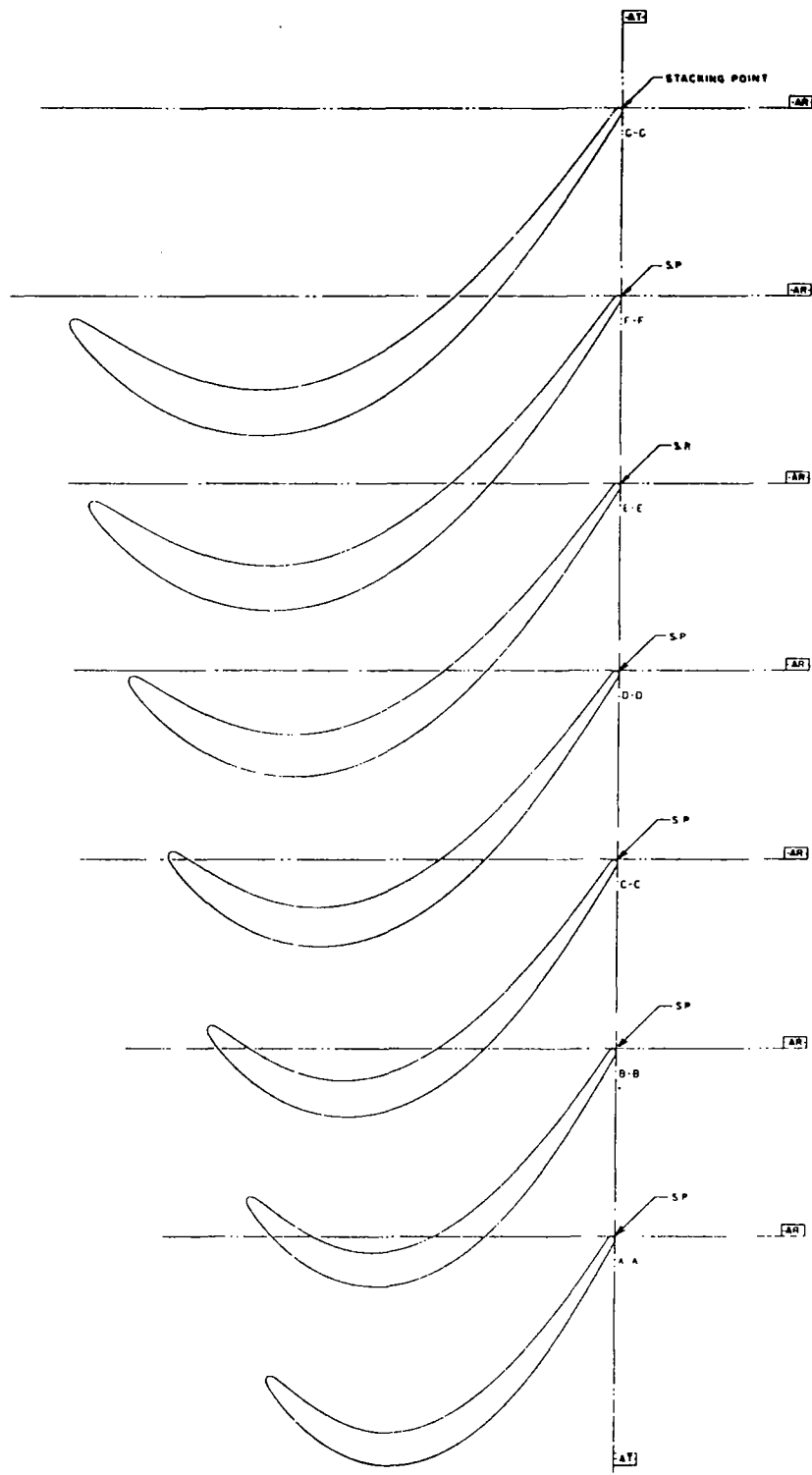


Figure 46. Stage Two Vane Precision Master (4012241-944).

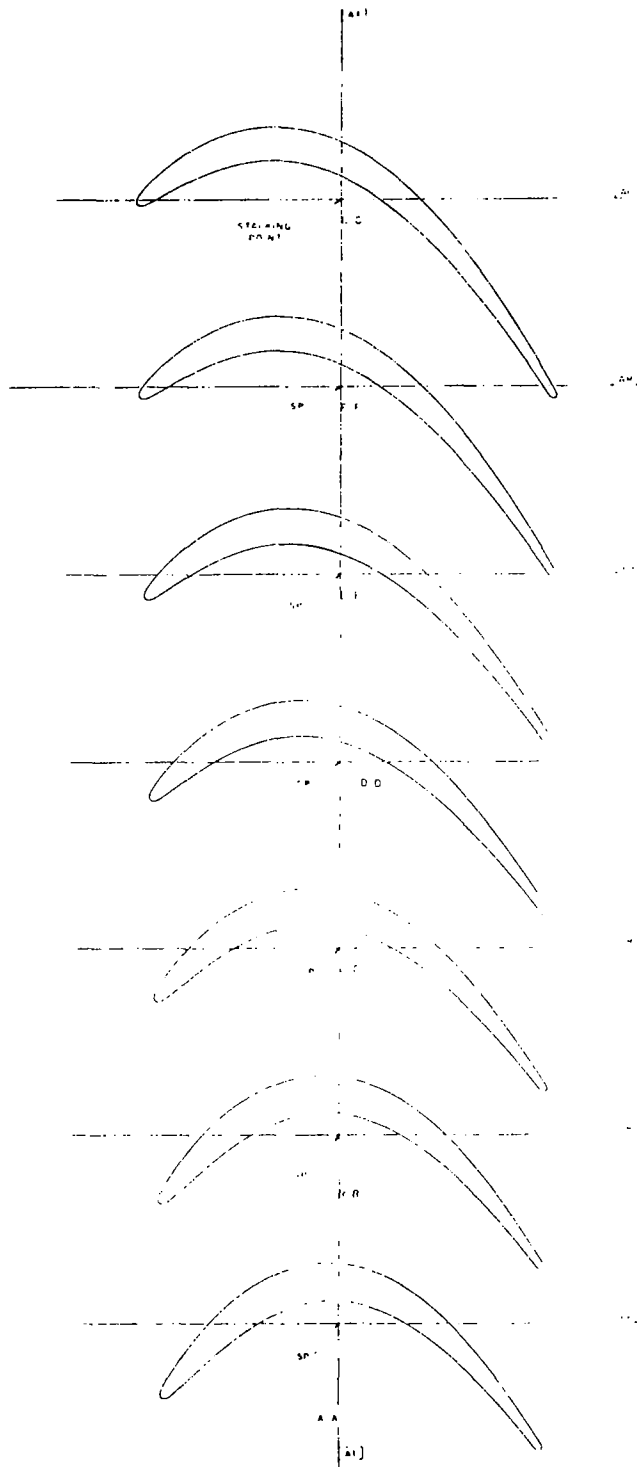
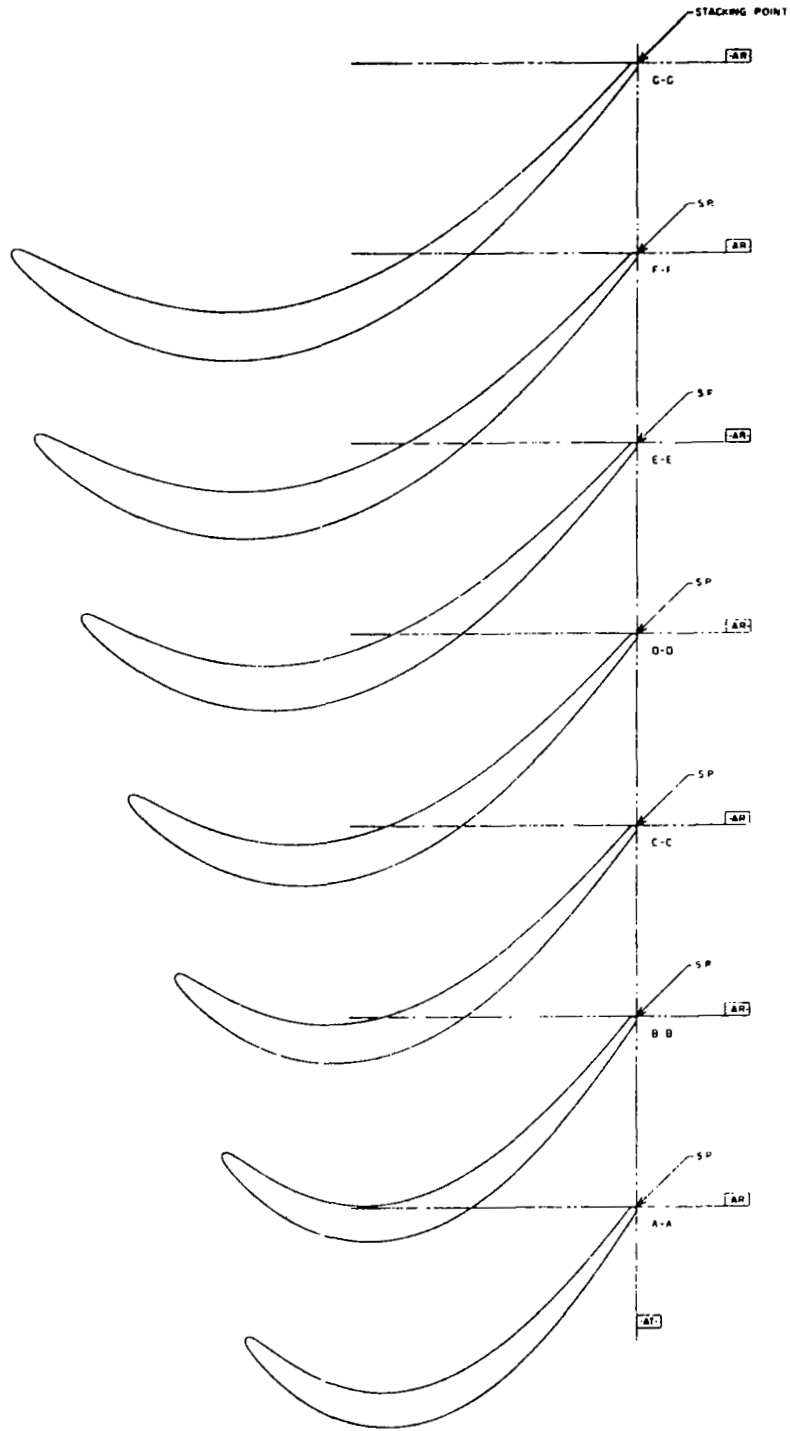


Figure 47. Stage Two Blade Precision Master (4012241-950).



**Figure 48. Stage Three Vane Precision Master (4012241-946).**

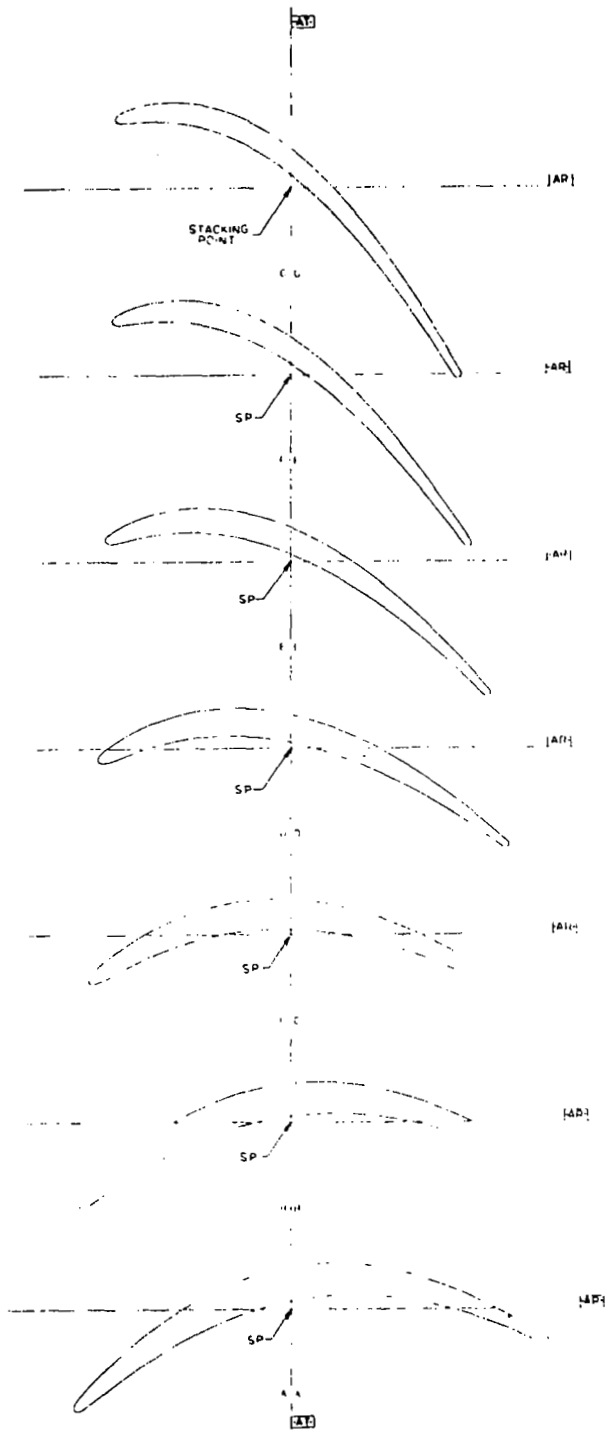


Figure 49. Stage Three Blade Precision Master (4012241-952).

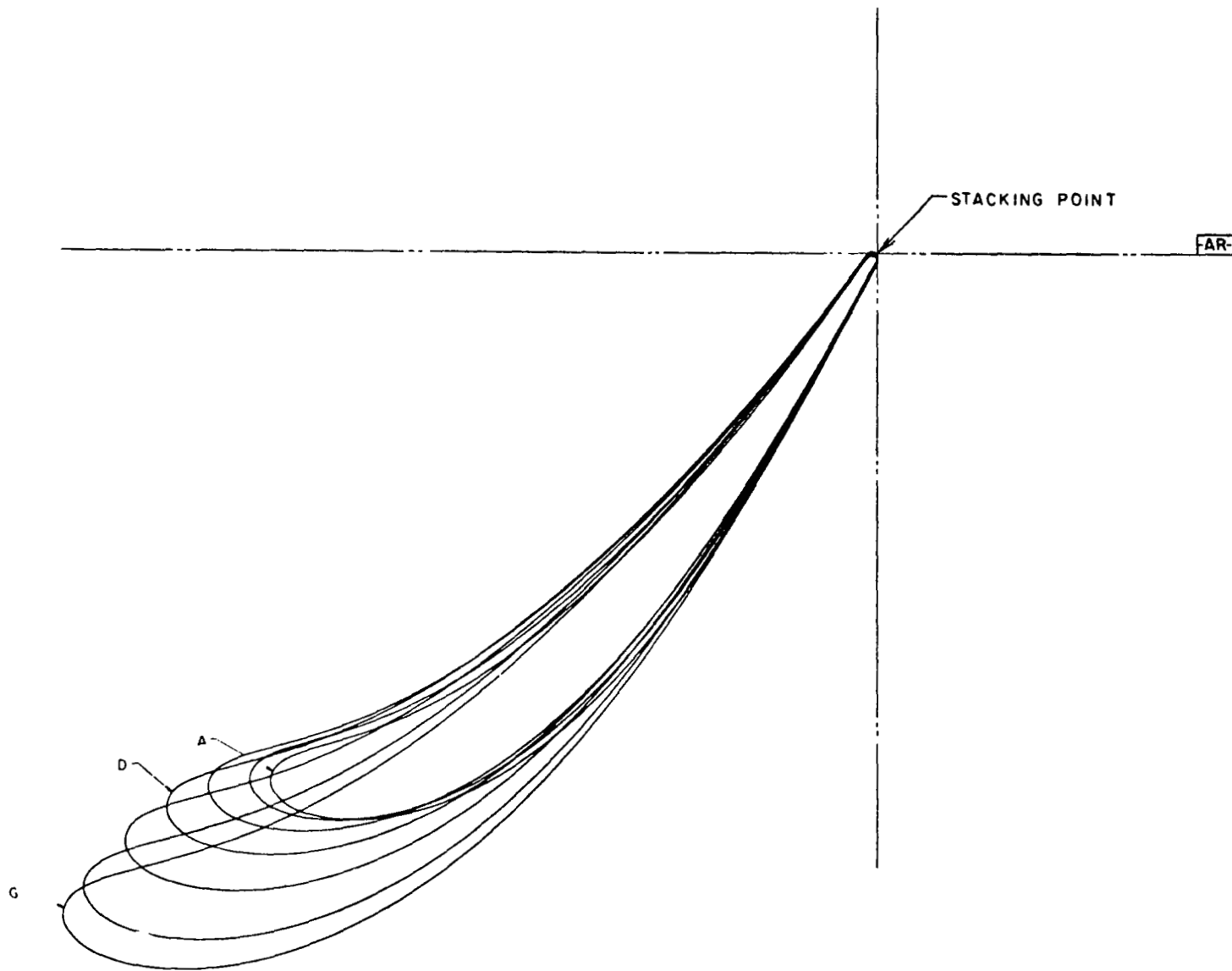


Figure 50. Stake One Vane Stackup (4012241-943).



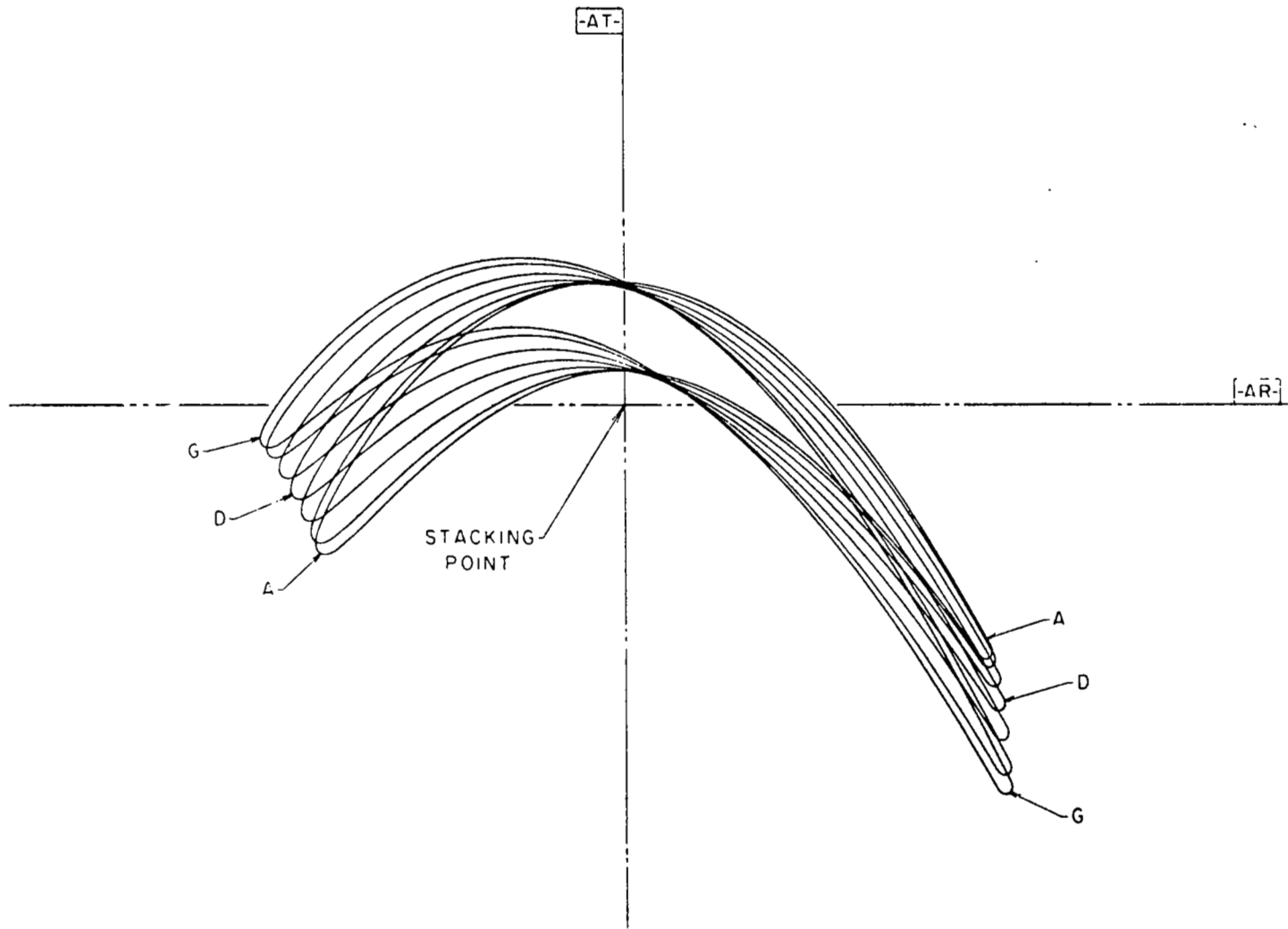


Figure 51. Stage One Blade Stackup (4012241-949).

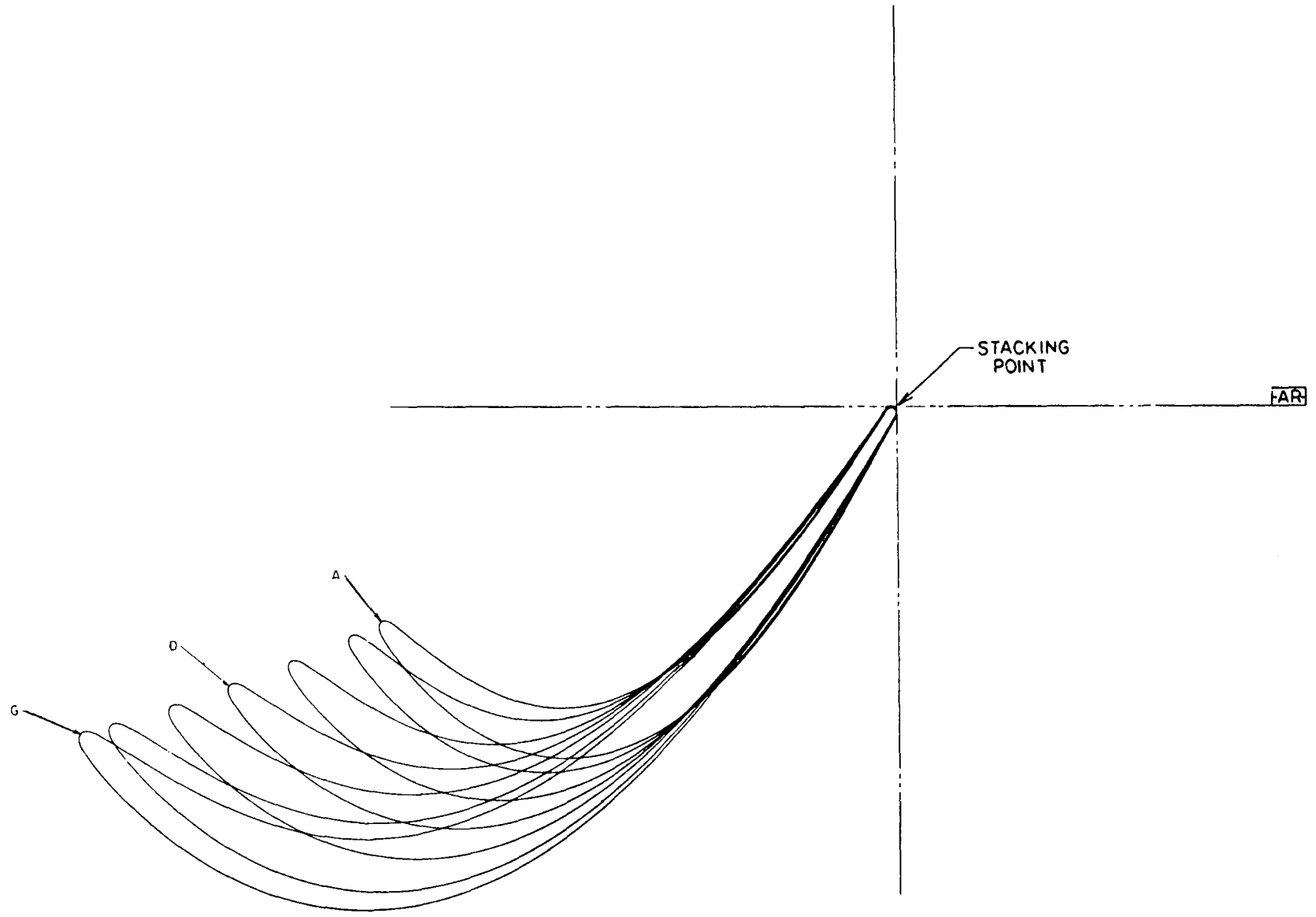


Figure 52. Stage Two Vane Stackup (4012241-945).

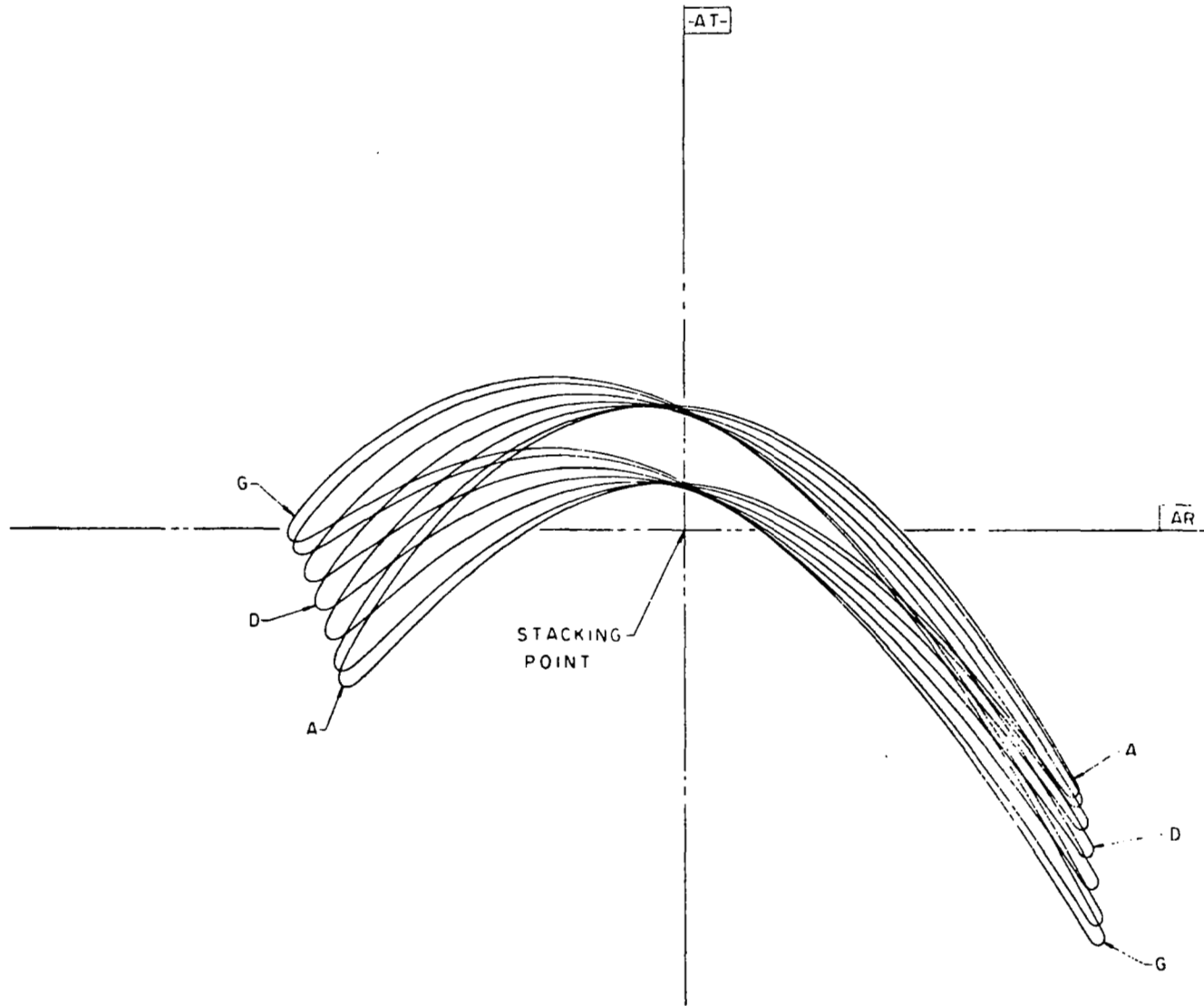


Figure 53. Stage Two Blade Stackup (4012241-951).

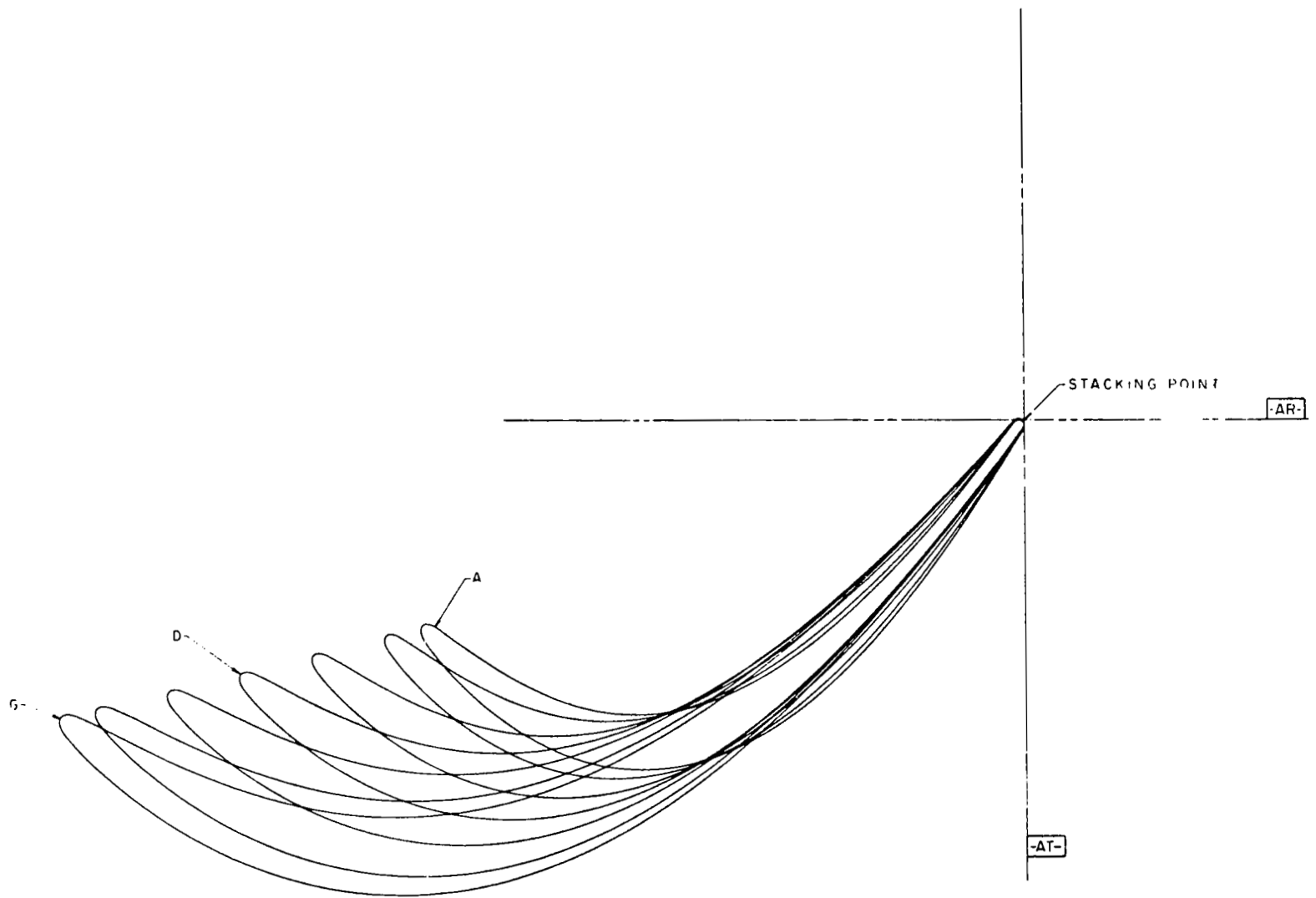


Figure 54. Stage Three Vane Stackup (4012241-947).

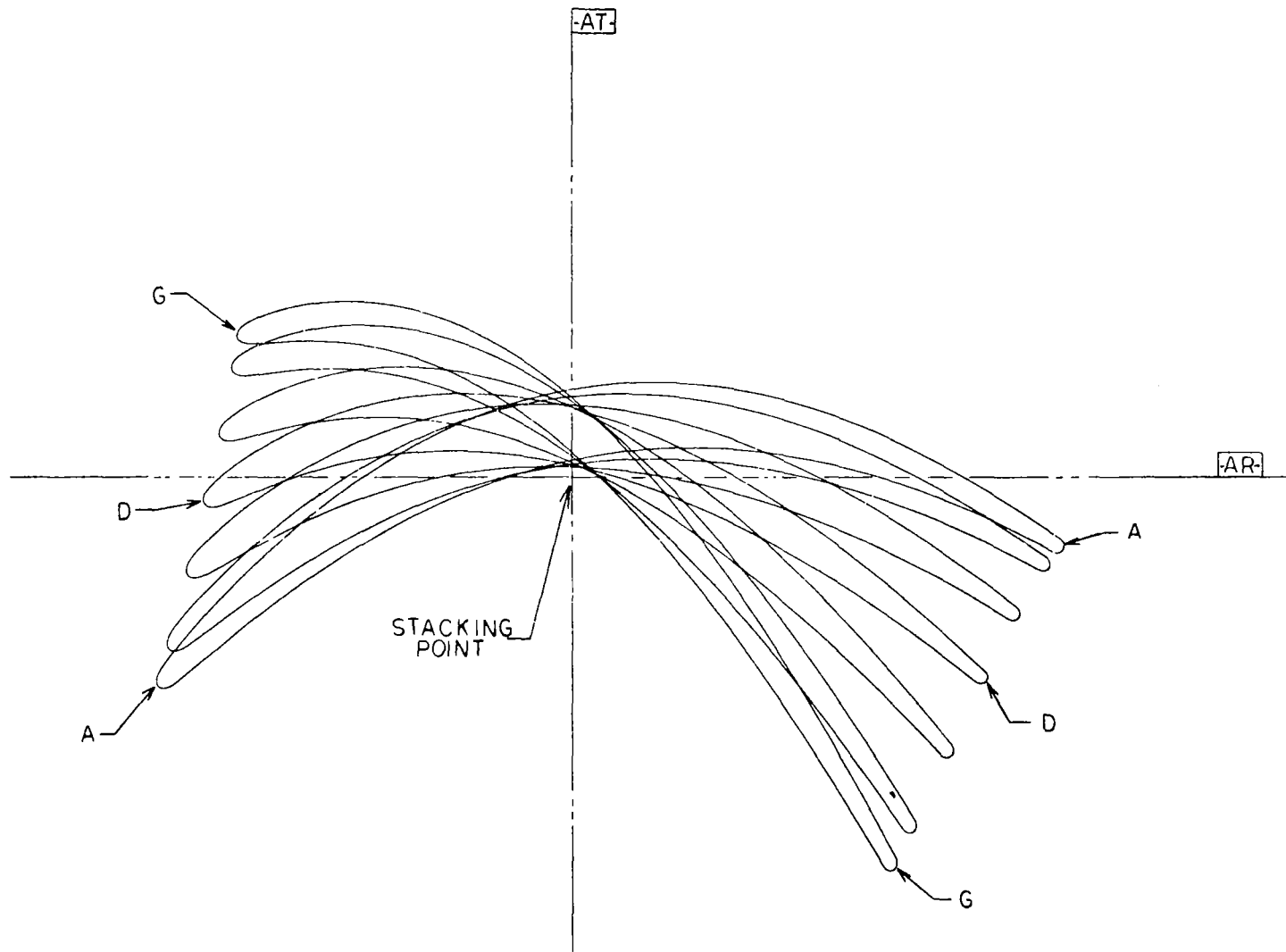


Figure 55. Stage Three Blade Stackup (4012241-953).

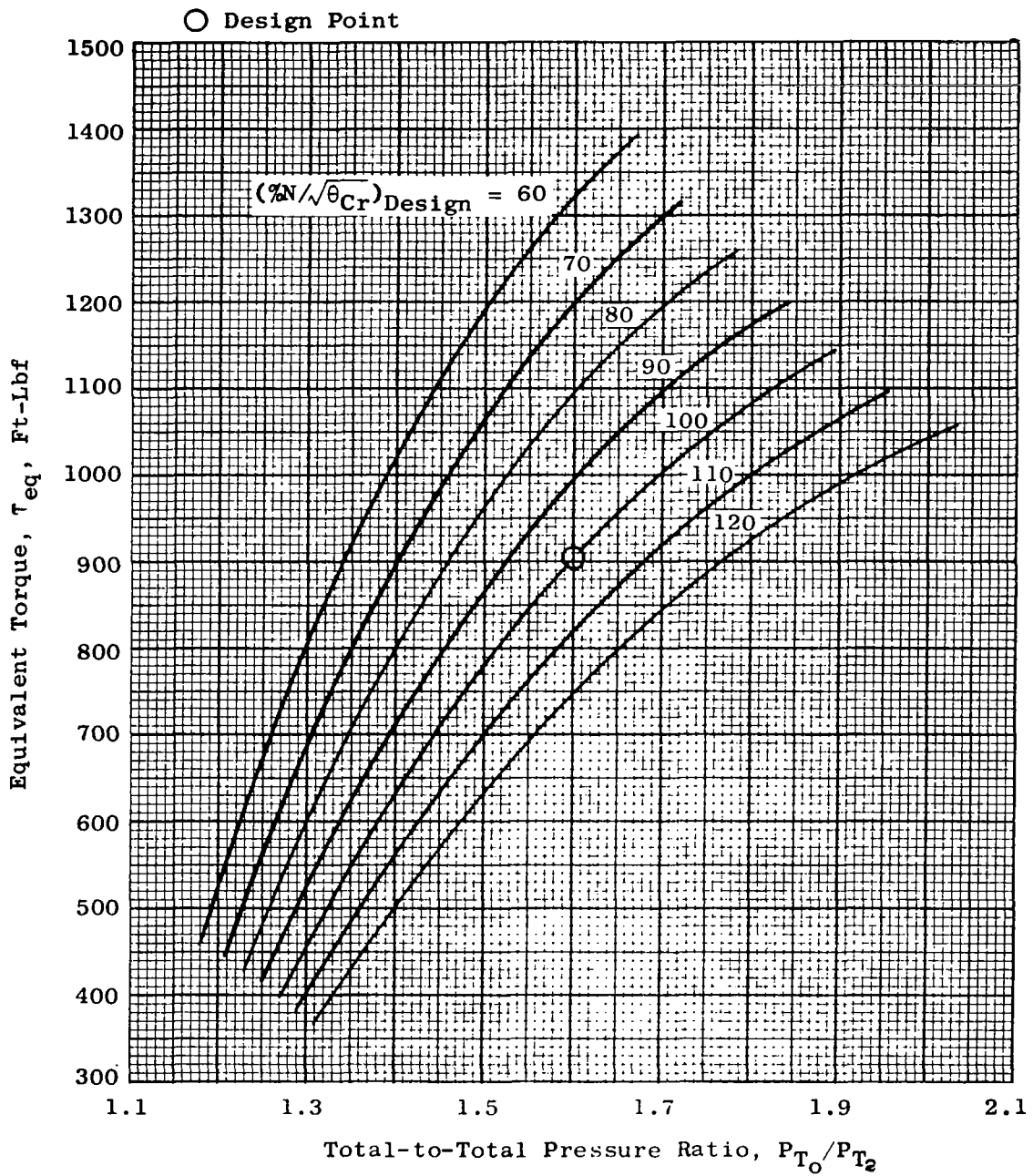


Figure 56. Equivalent Torque vs. Total-to-Total Pressure Ratio, One-Stage Configuration.

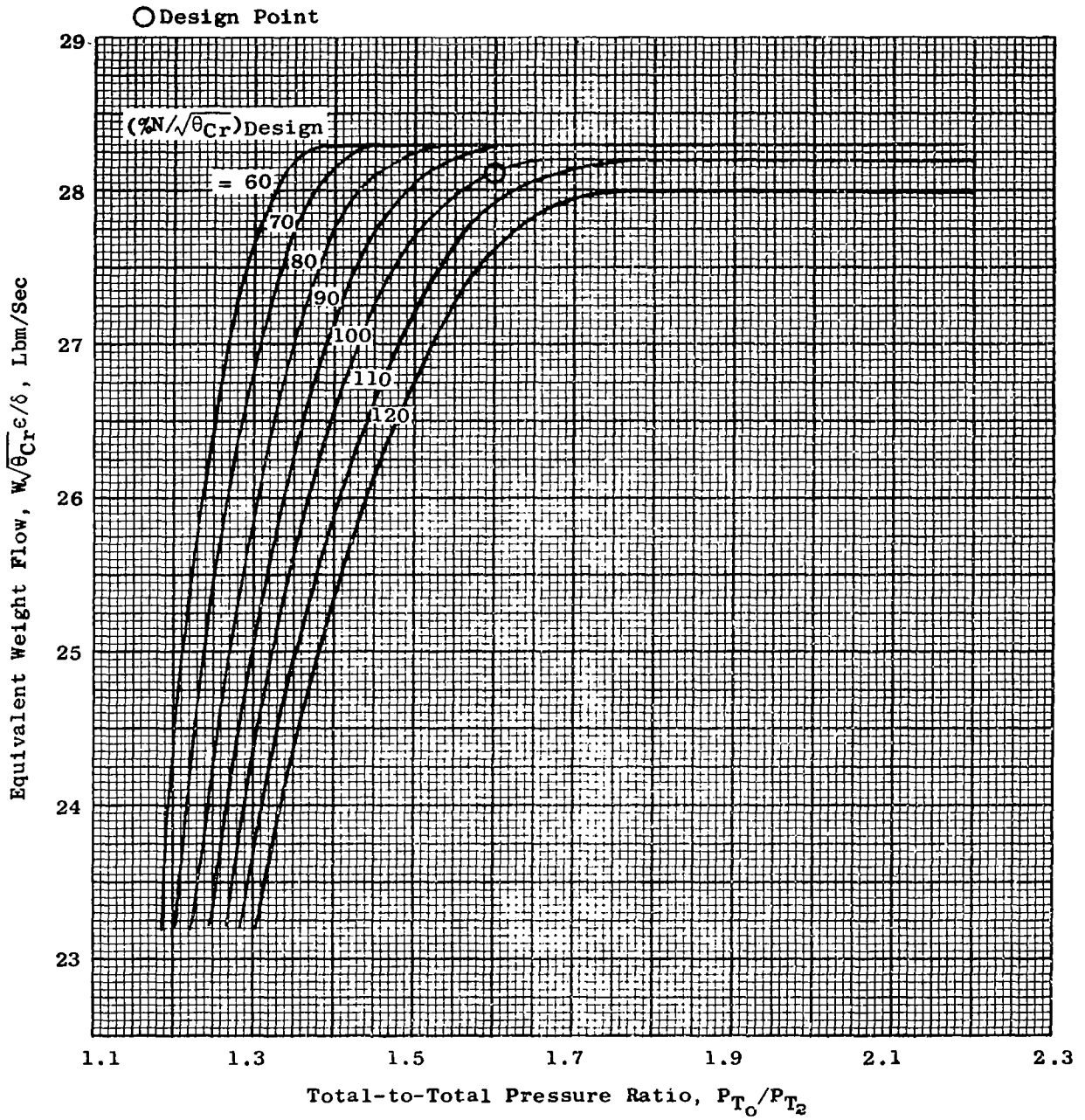


Figure 57. Equivalent Weight Flow vs. Total-to-Total Pressure Ratio, One-Stage Configuration.

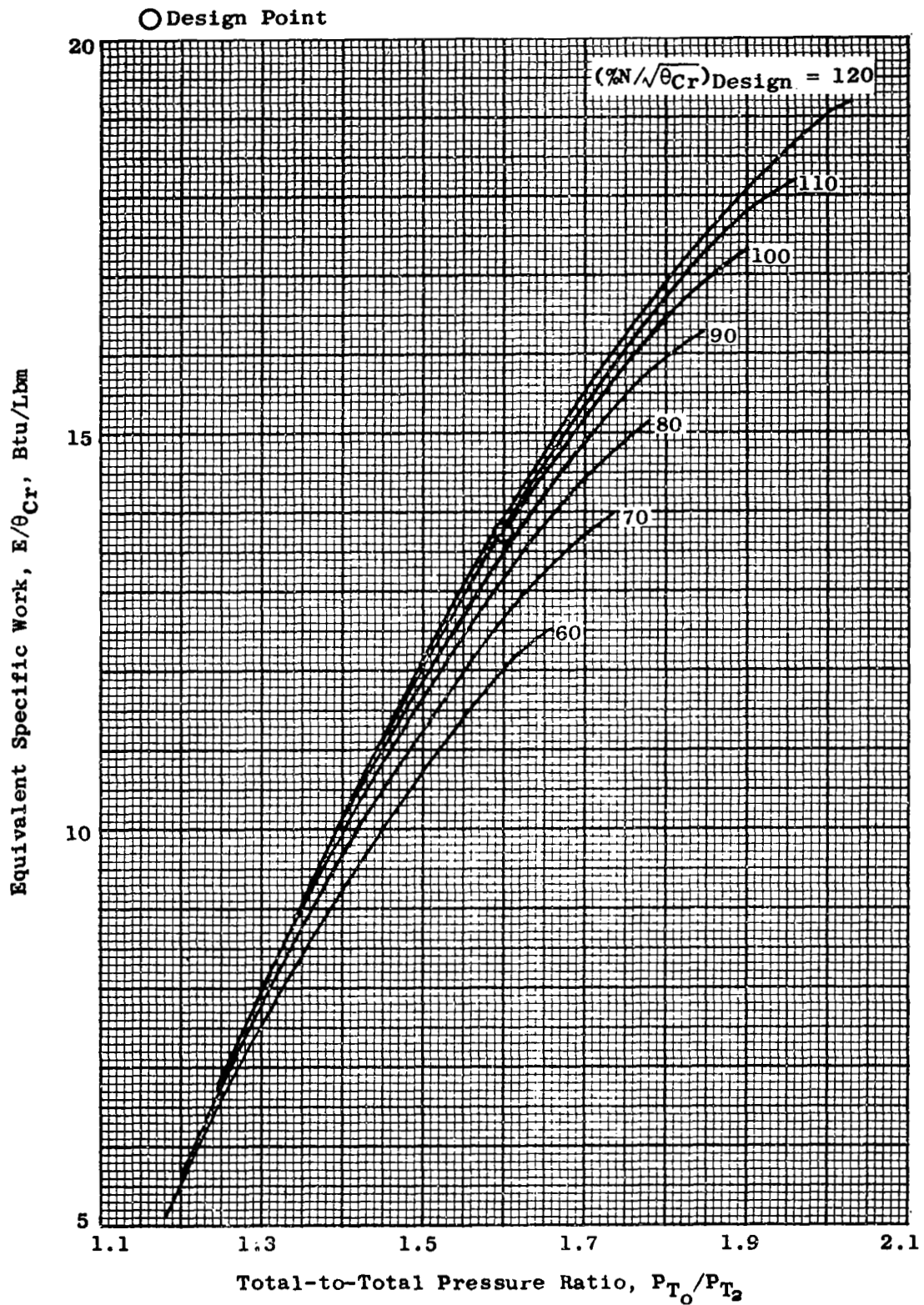


Figure 58. Equivalent Specific Work vs. Total-to-Total Pressure Ratio, One-Stage Configuration.



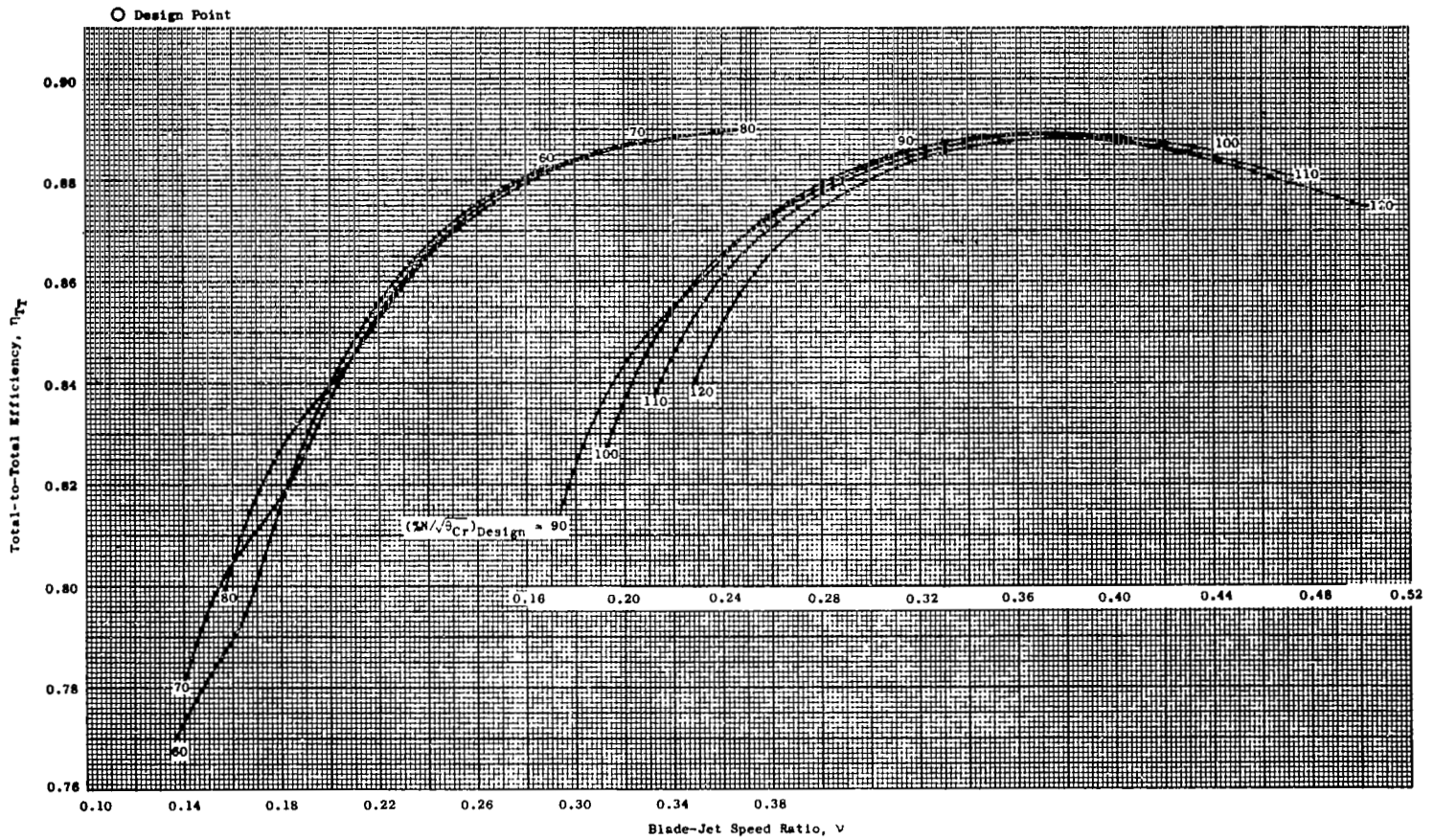


Figure 59. Total-to-Total Efficiency vs. Blade-Jet Speed Ratio, One-Stage Configuration.

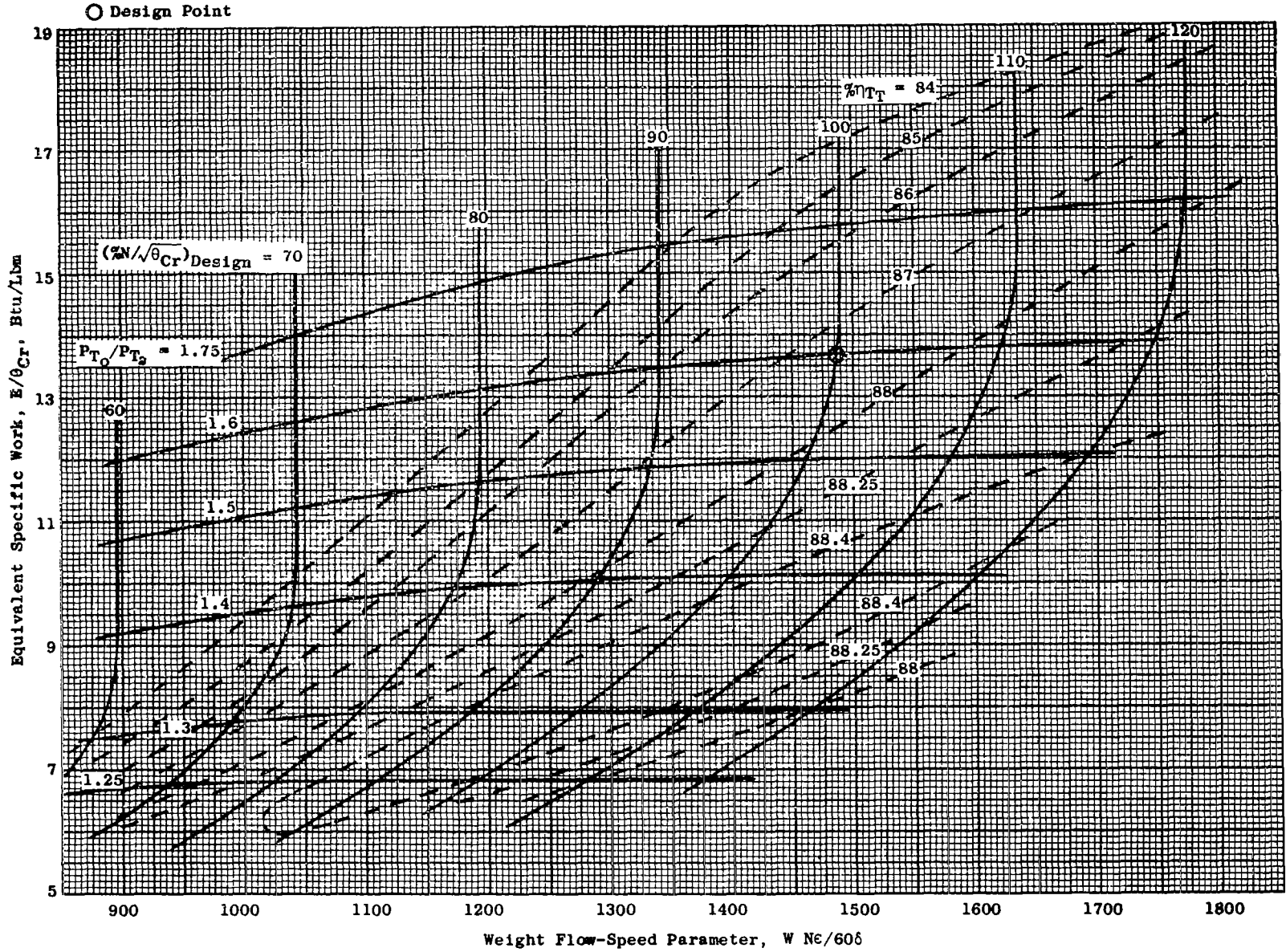


Figure 60. Equivalent Specific Work vs. Weight Flow-Speed Parameter, One-Stage Configuration.

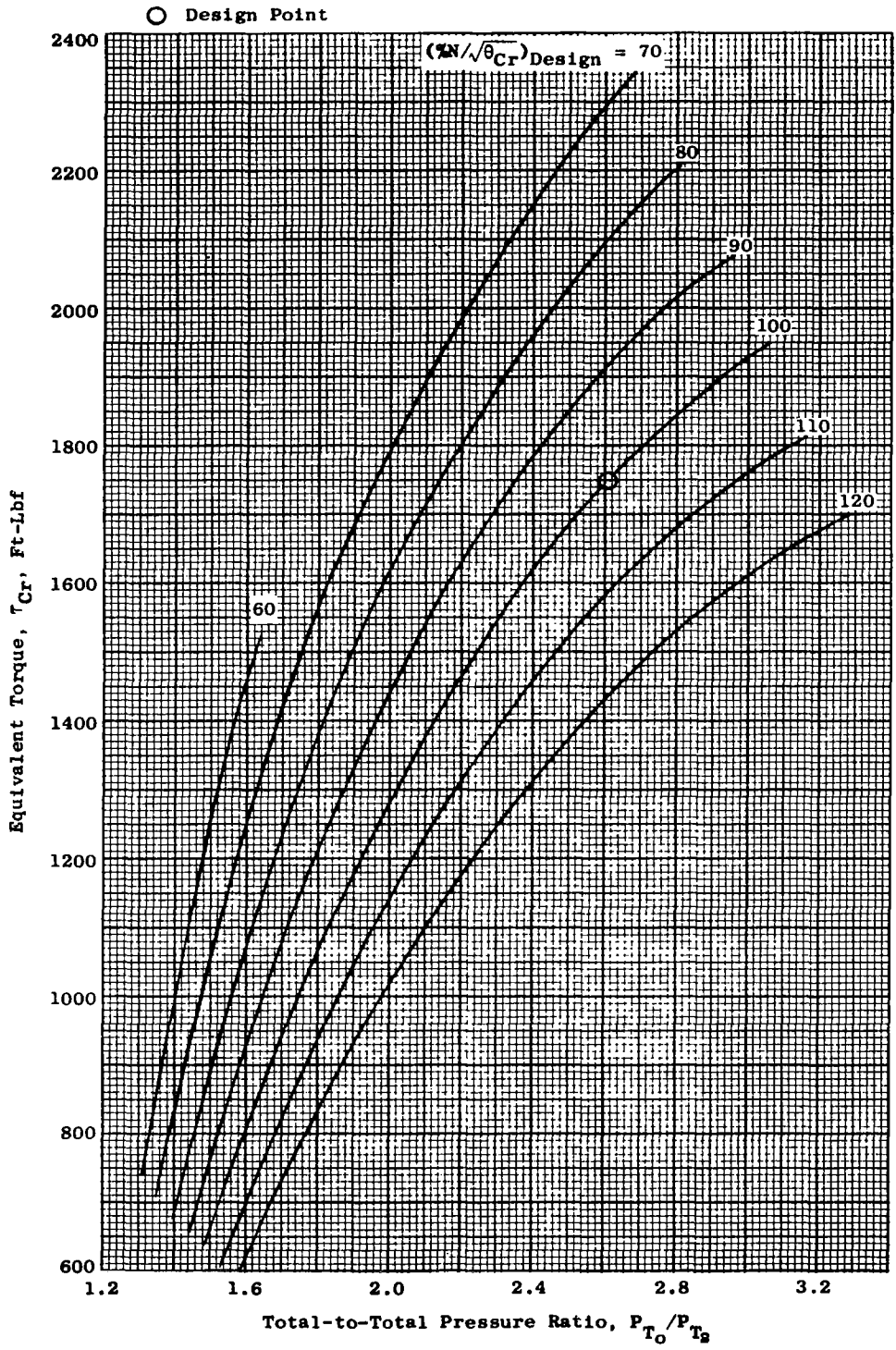


Figure 61. Equivalent Torque vs. Total-to-Total Pressure Ratio, Two-Stage Configuration.

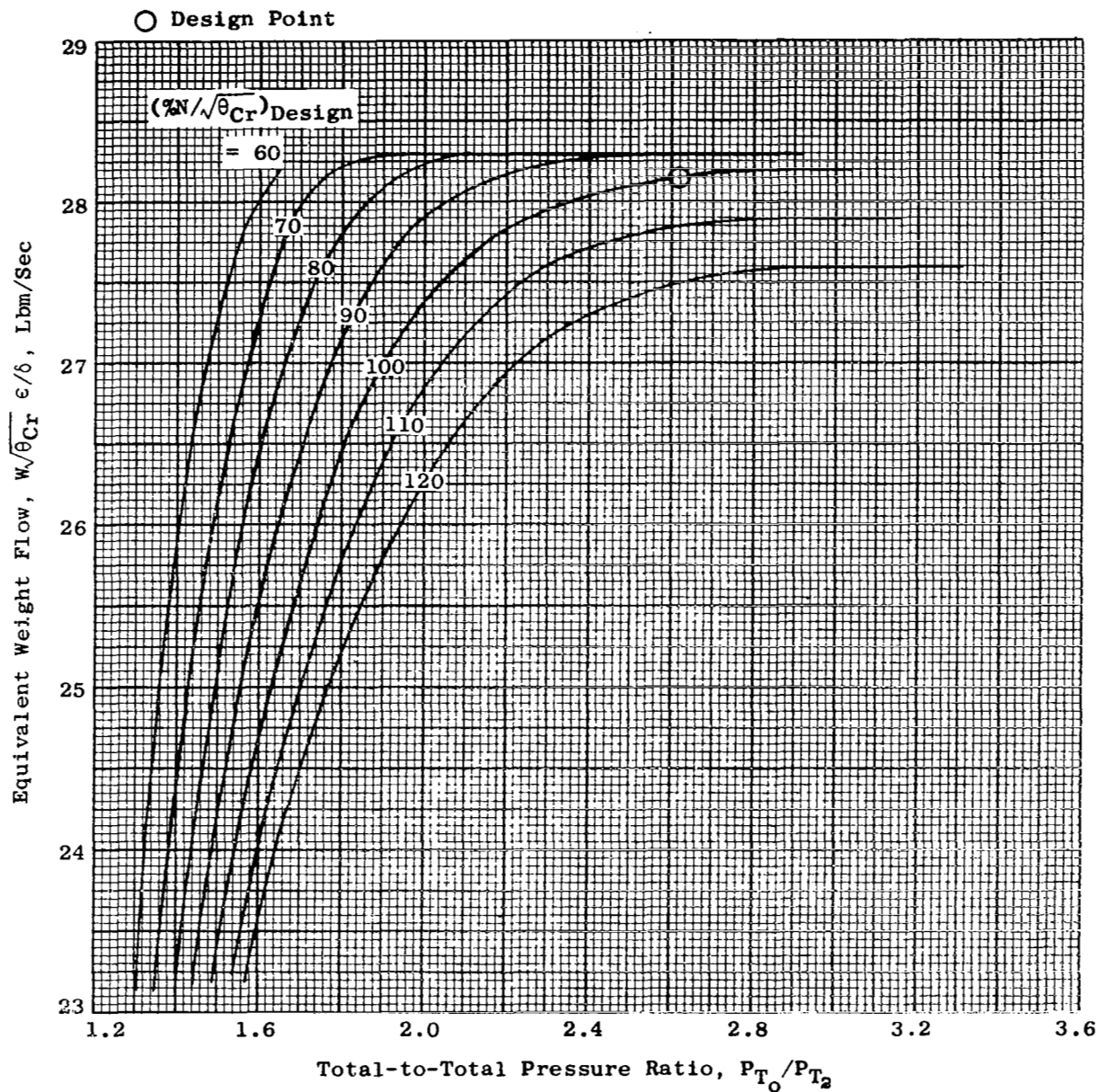


Figure 62. Equivalent Weight Flow vs. Total-to-Total Pressure Ratio, Two-Stage Configuration.

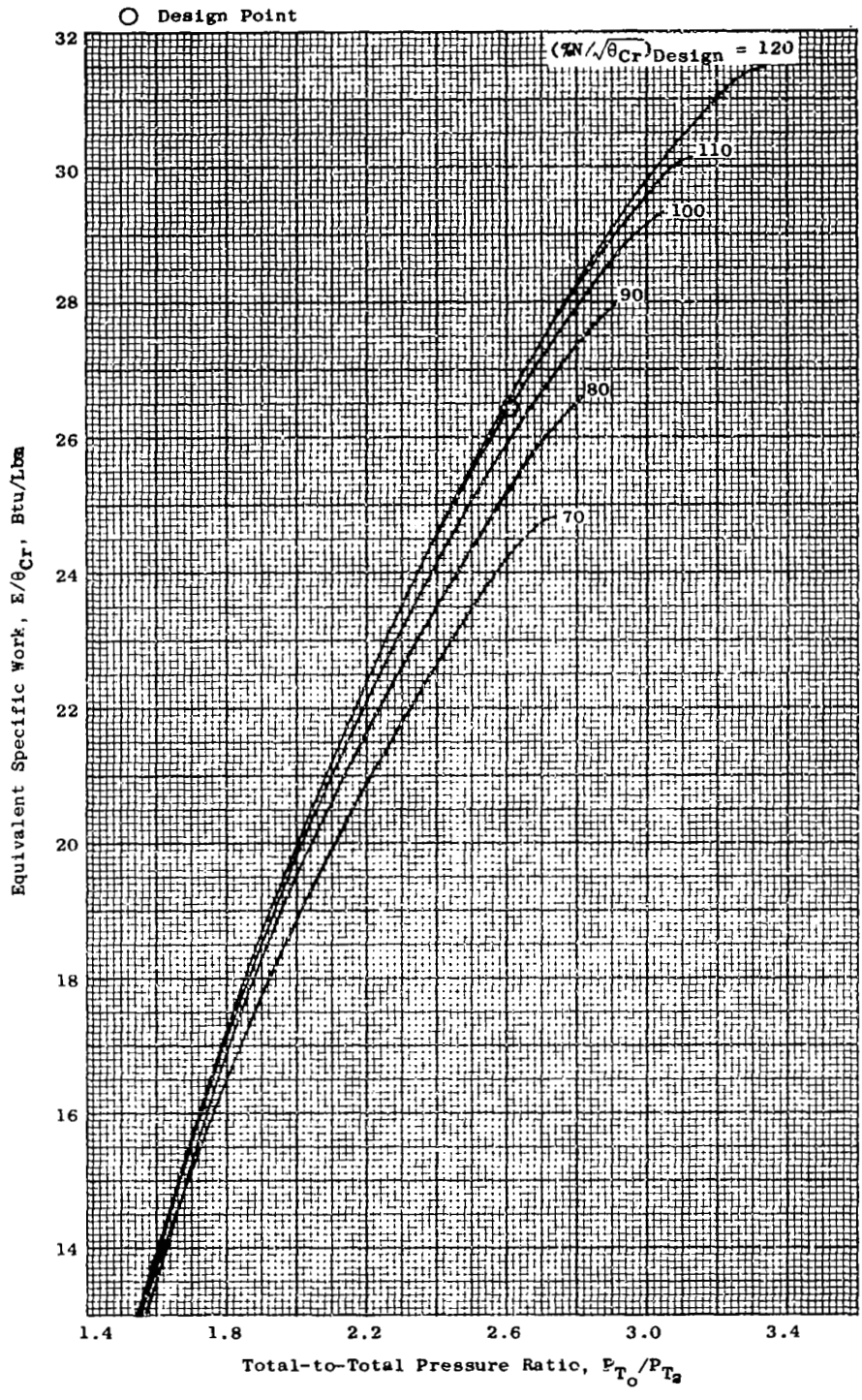


Figure 63. Equivalent Specific Work vs. Total-to-Total Pressure Ratio, Two-Stage Configuration.

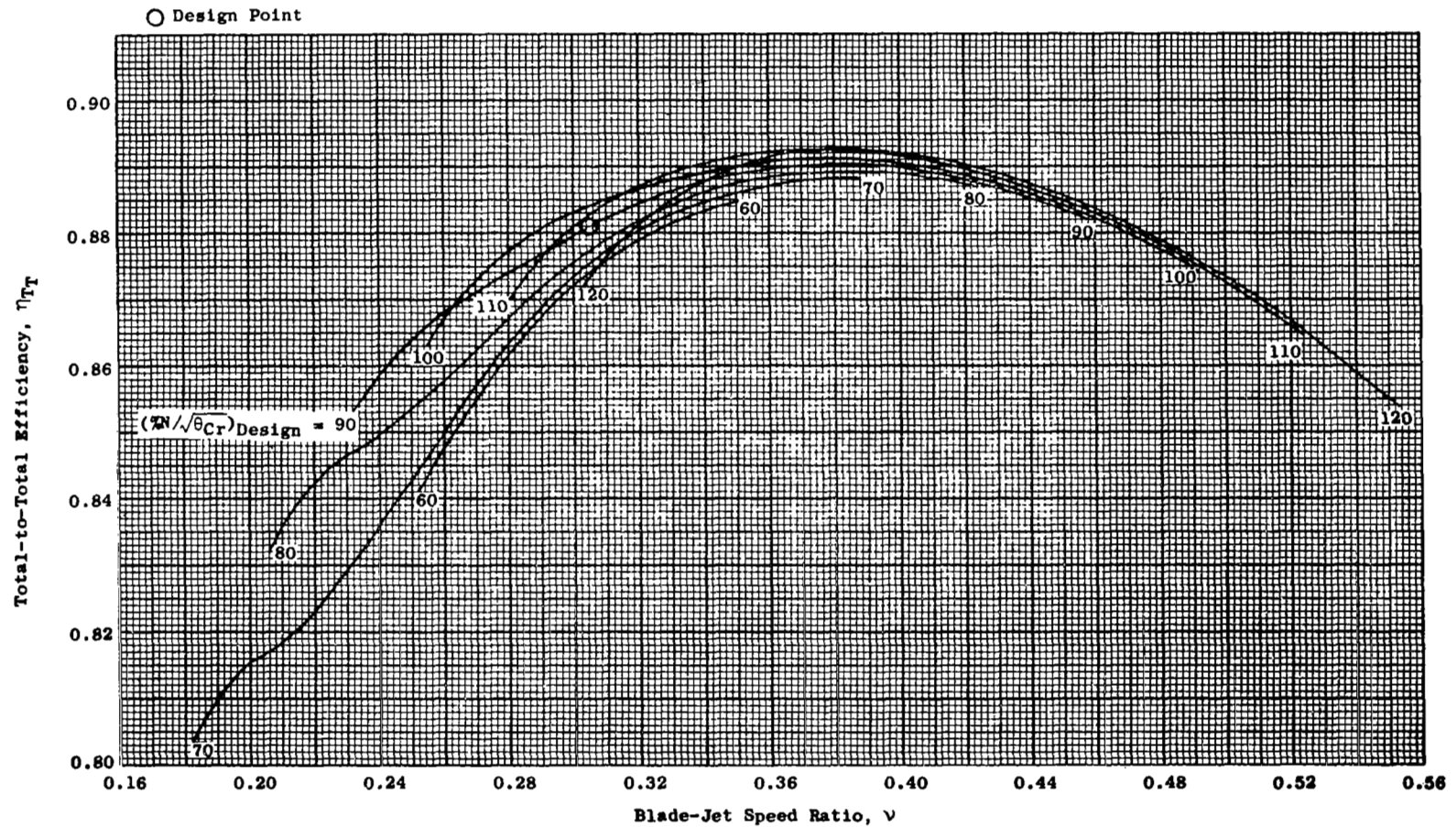


Figure 64. Total-to-Total Efficiency vs. Blade-Jet Speed Ratio, Two-Stage Configuration.

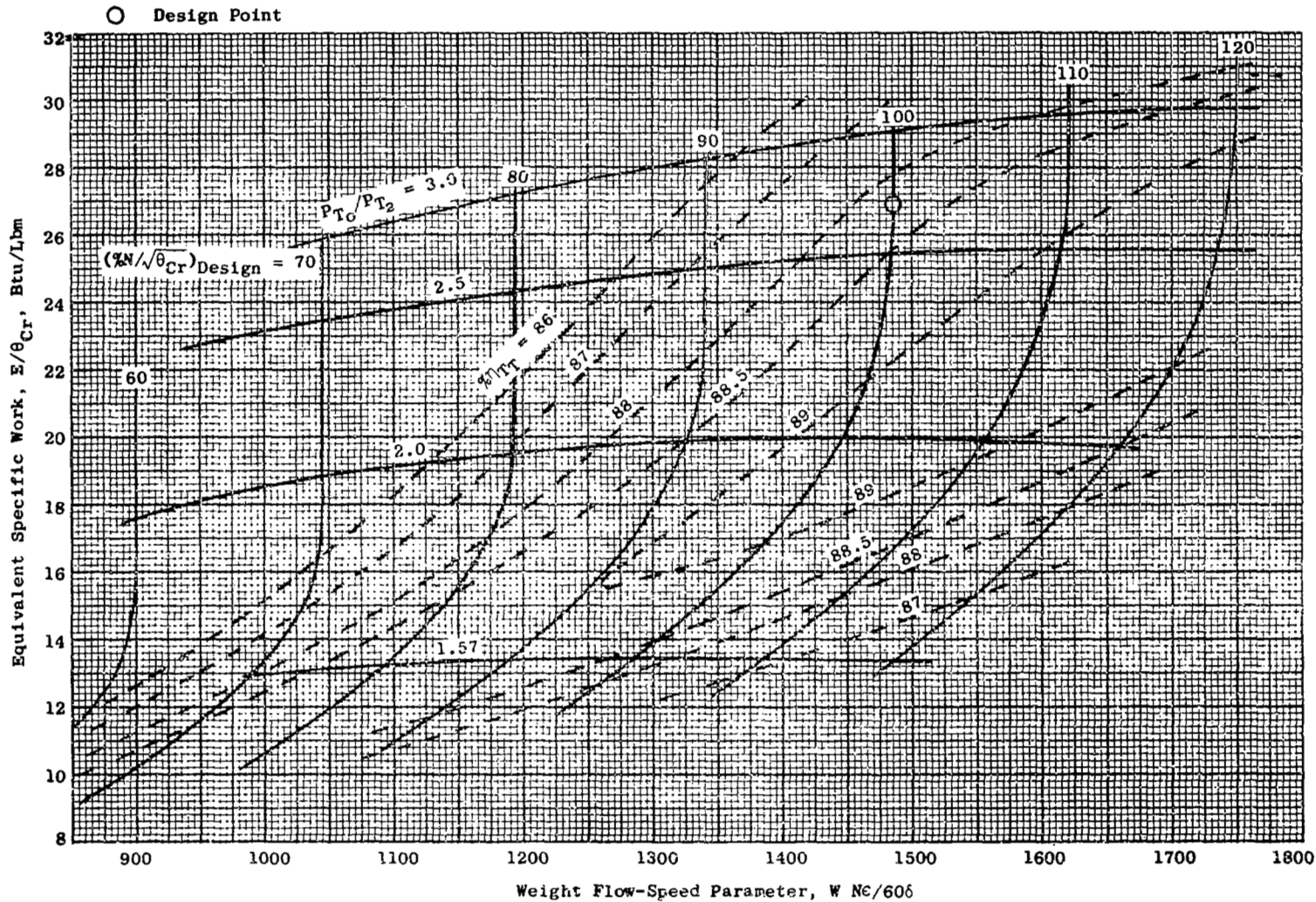


Figure 65. Equivalent Specific Work vs. Weight Flow - Speed Parameter, Two-Stage Configuration.

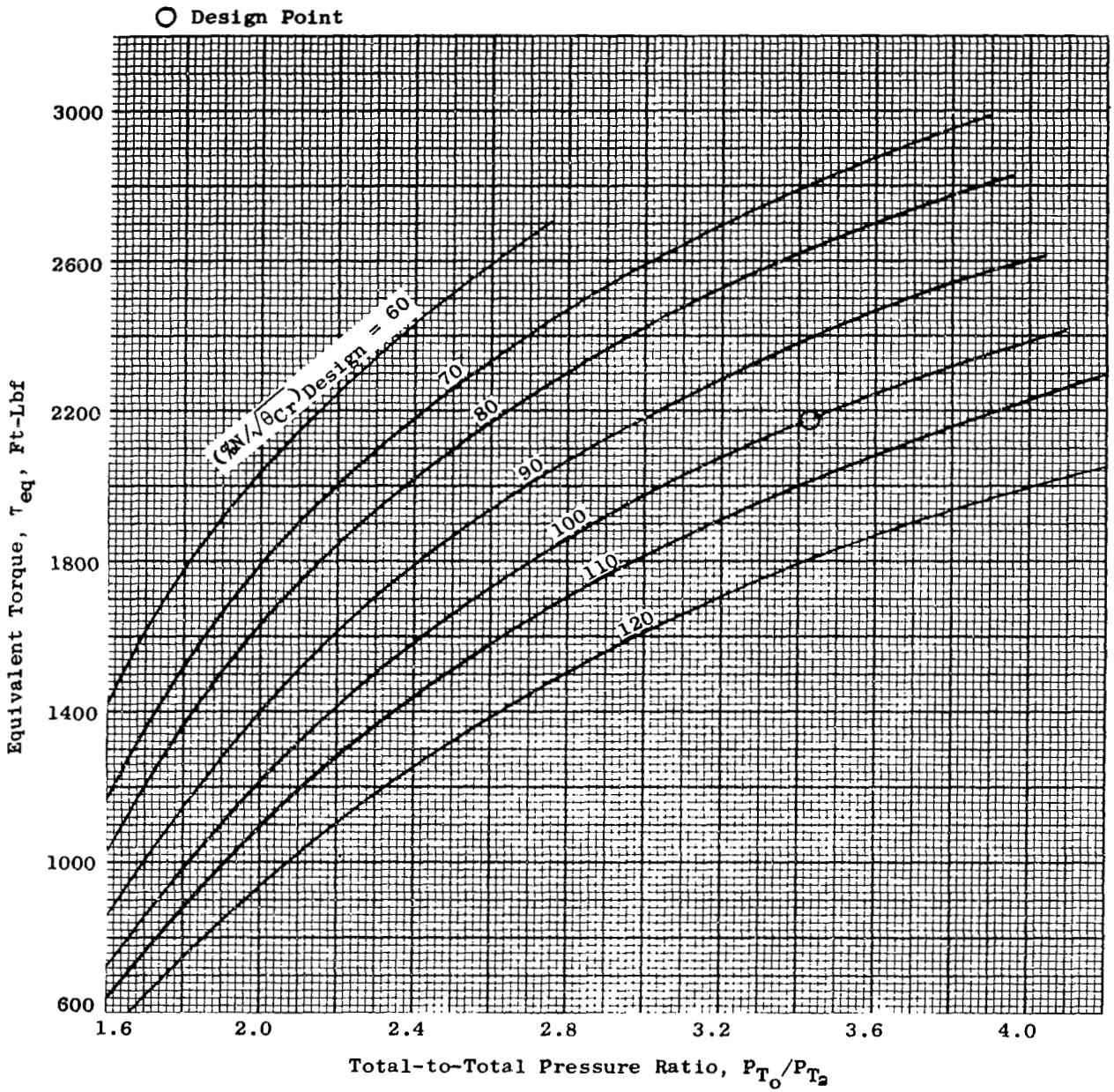


Figure 66. Equivalent Torque vs. Total-to-Total Pressure Ratio, Three-Stage Configuration.



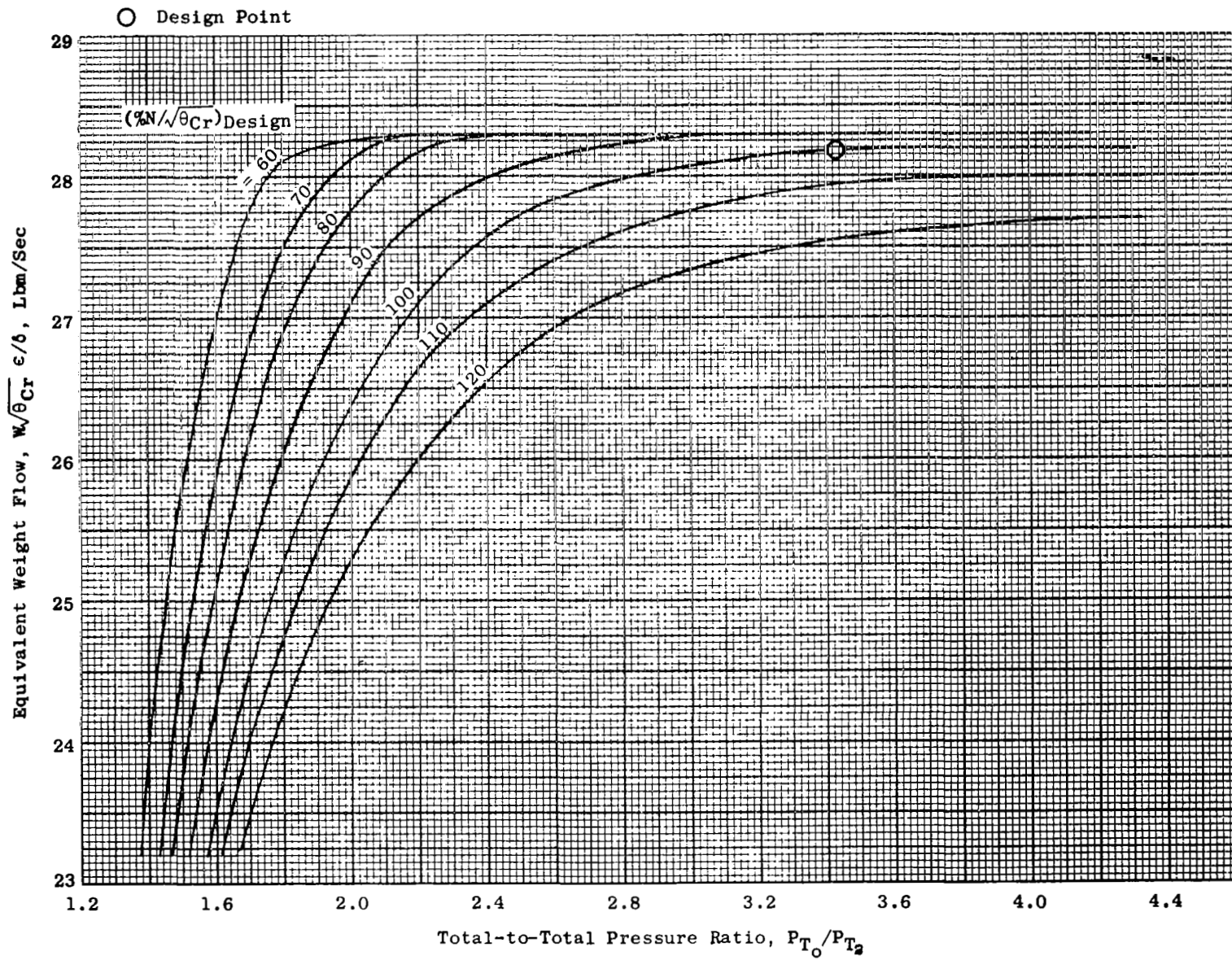


Figure 67. Equivalent Weight Flow vs. Total-to-Total Pressure Ratio, Three-Stage Configuration.

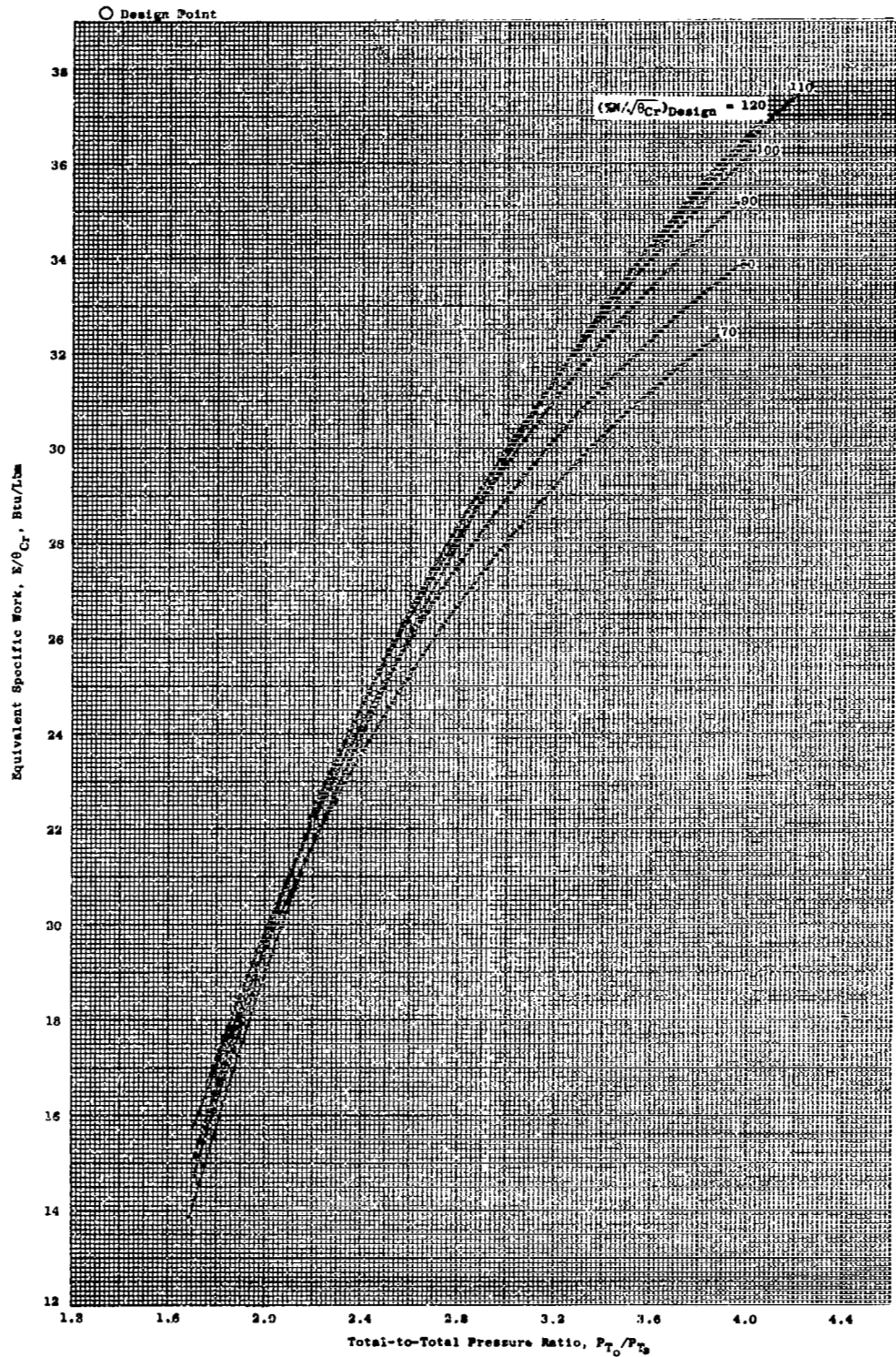


Figure 68. Equivalent Specific Work vs. Total-to-Total Pressure Ratio, Three-Stage Configuration.

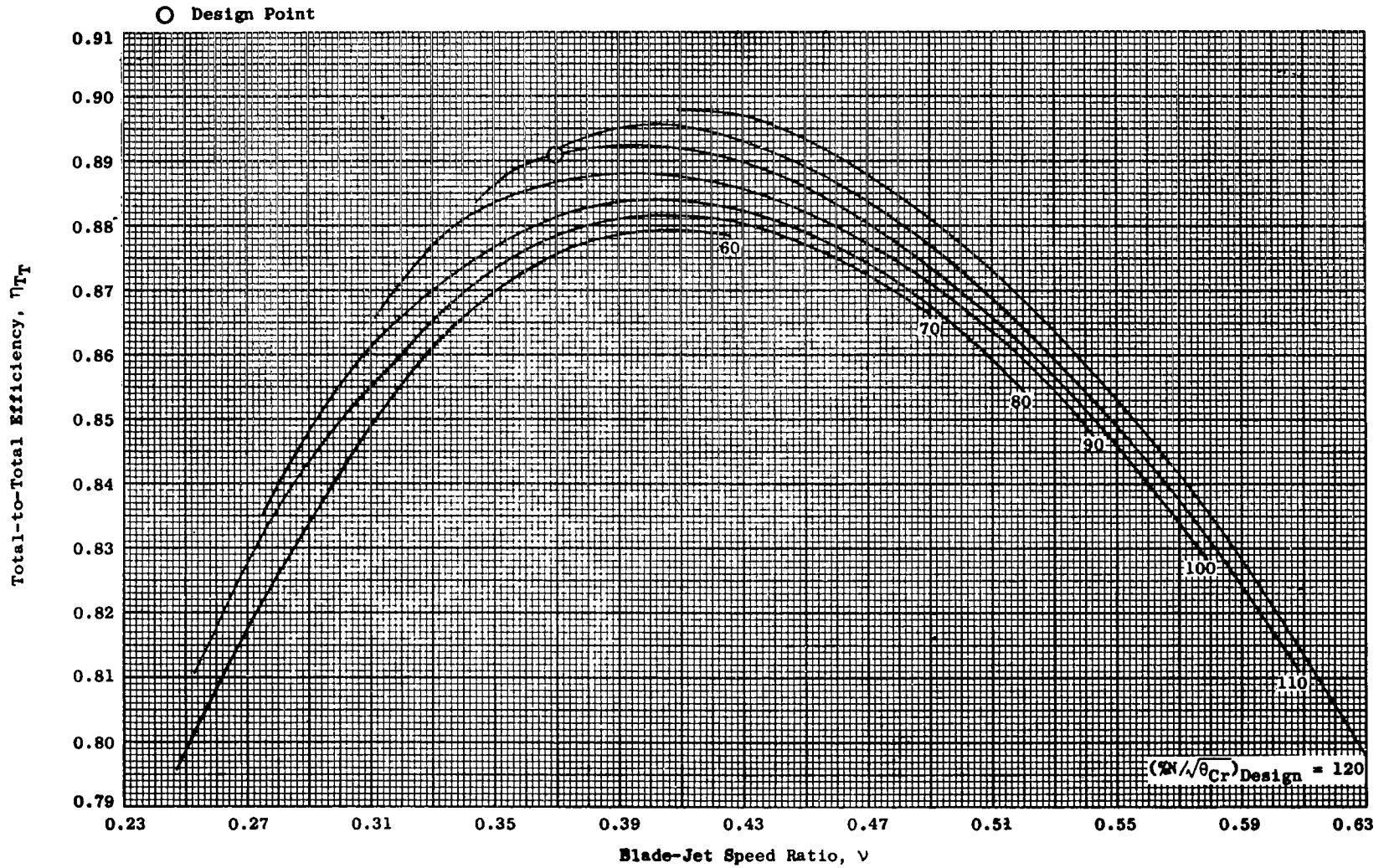


Figure 69. Total-to-Total Efficiency vs. Blade-Jet Speed Ratio, Three-Stage Configuration.

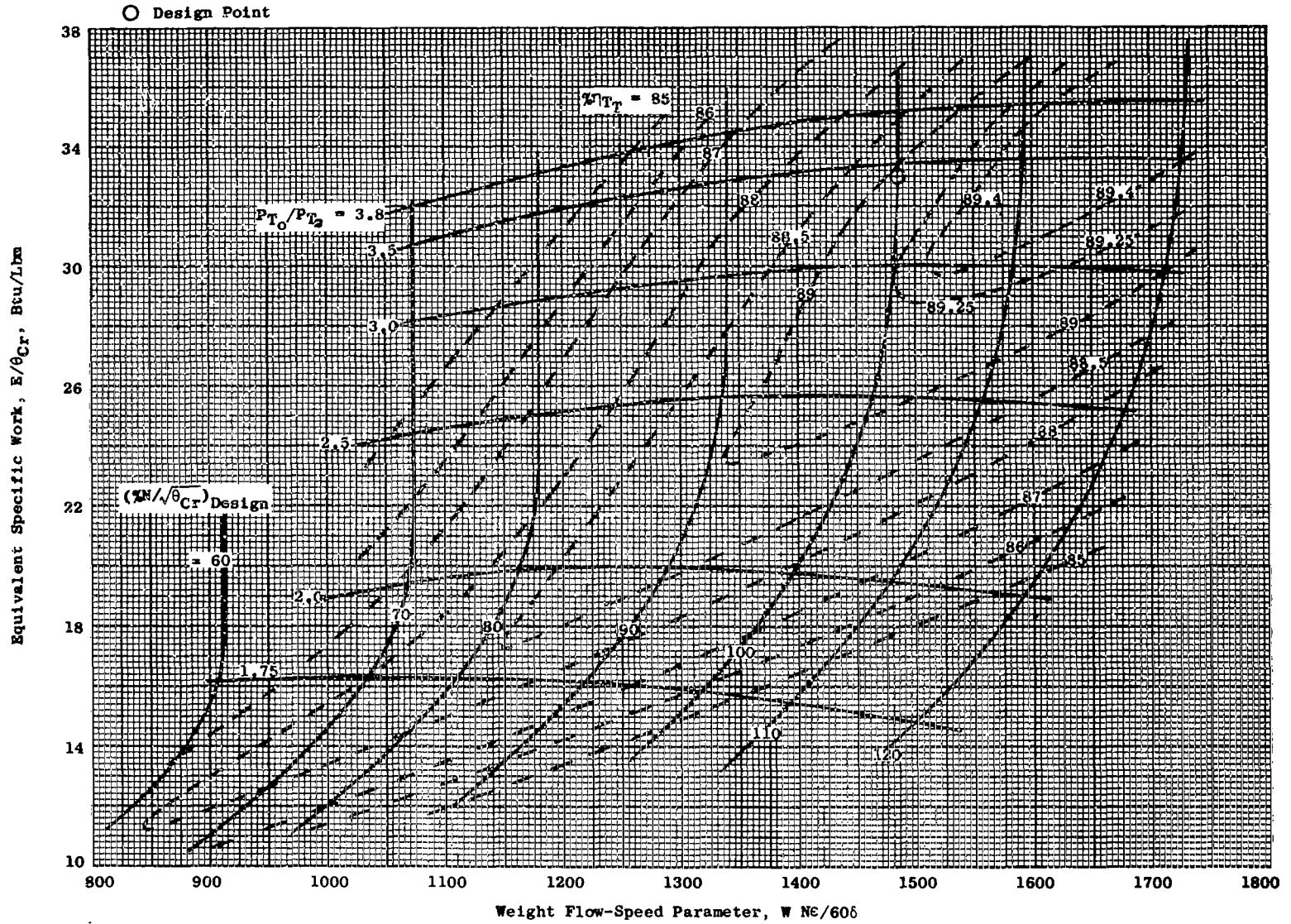


Figure 70. Equivalent Specific Work vs. Flow-Speed Parameter, Three-Stage Configuration.

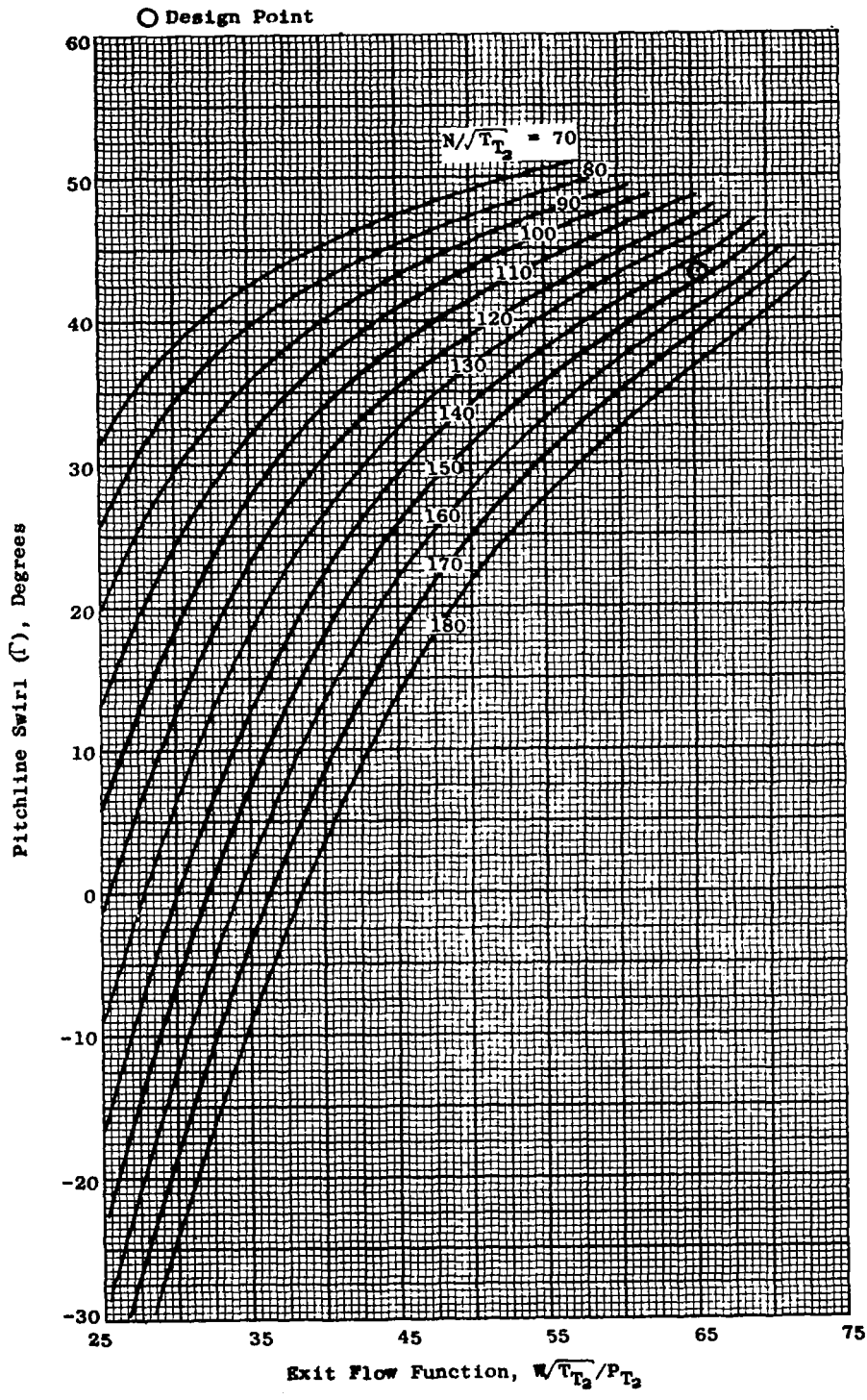


Figure 71. Swirl Map, One-Stage Configuration.

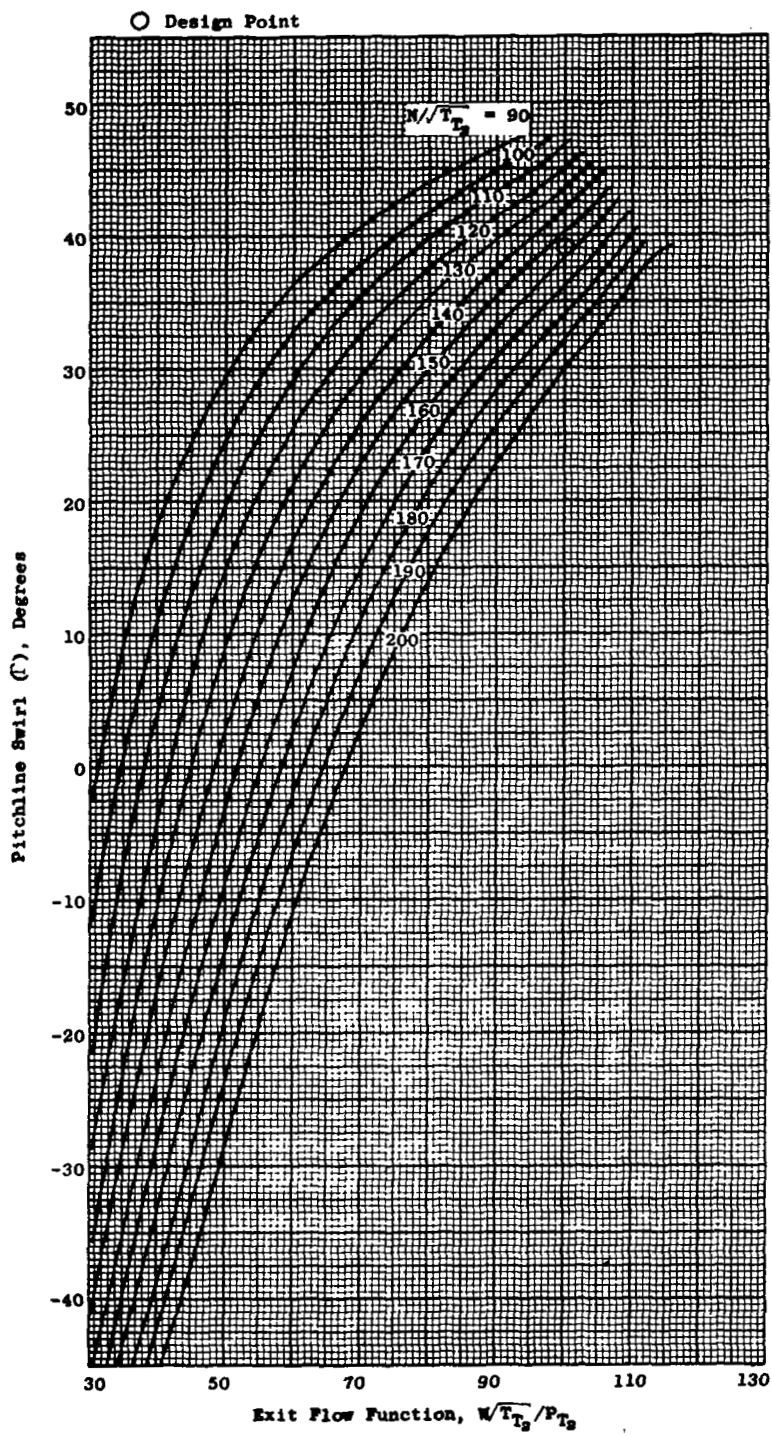


Figure 72. Swirl Map, Two-Stage Configuration.

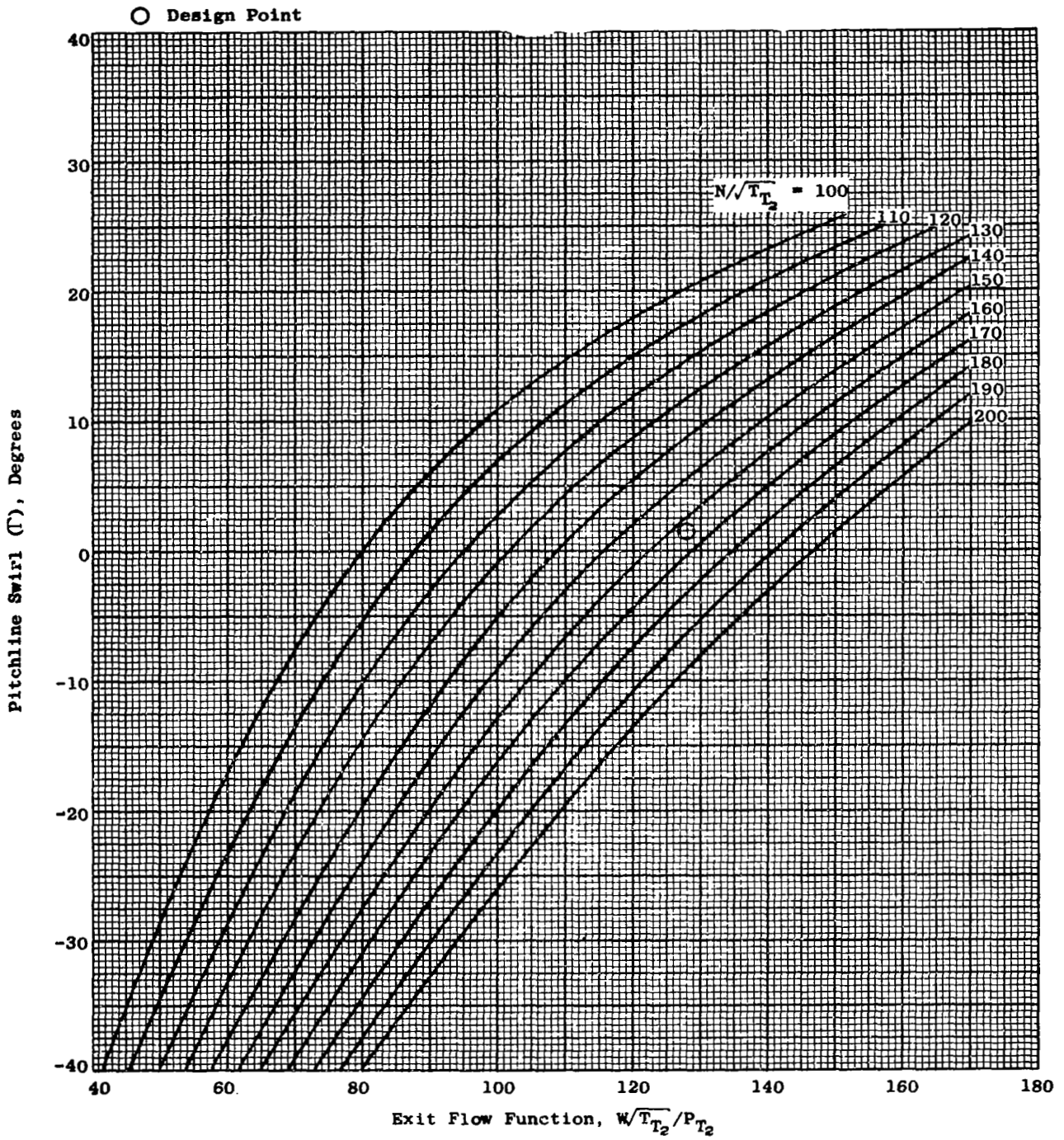


Figure 73. Swirl Map, Three-Stage Configuration.

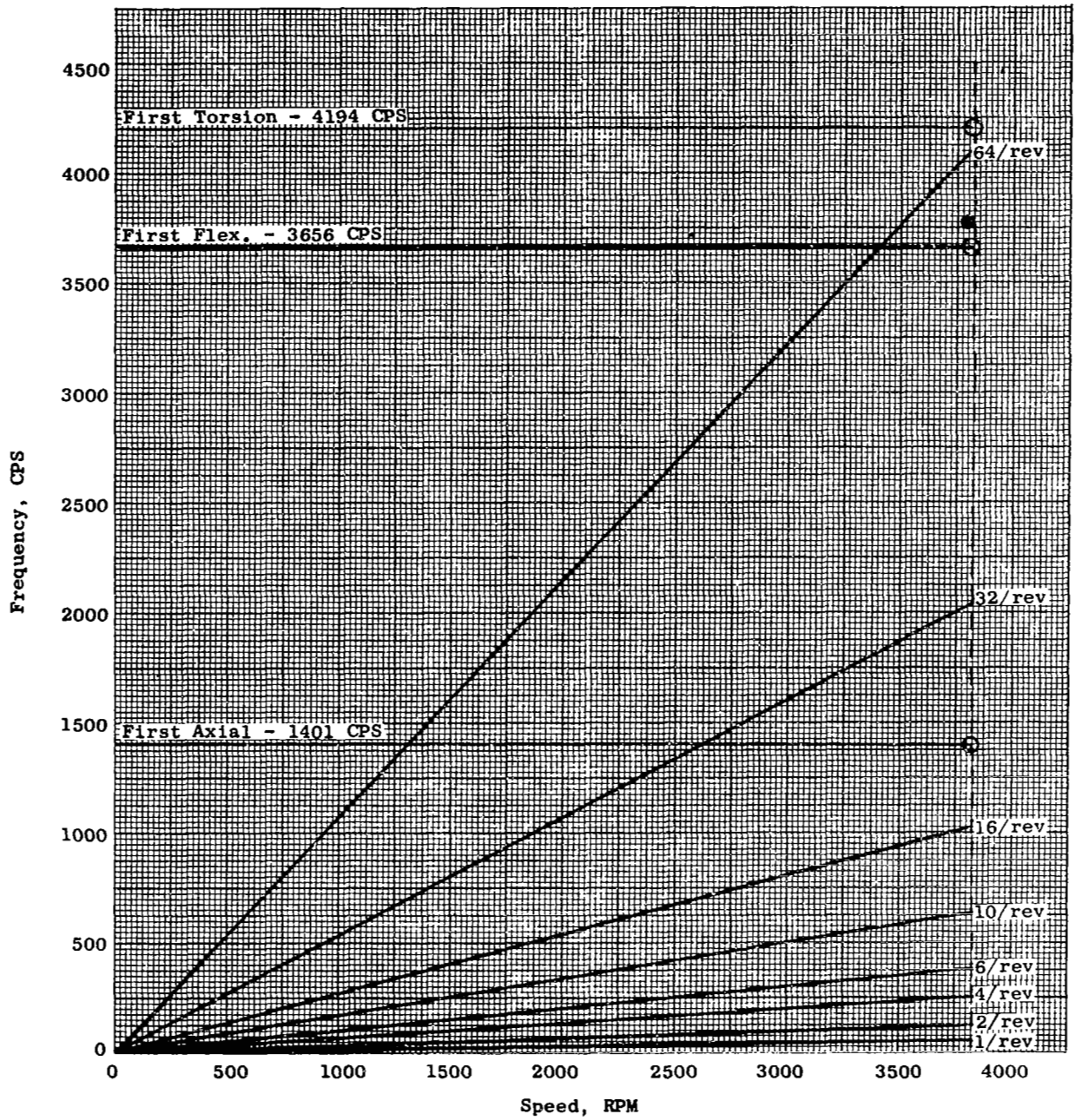


Figure 74. Most Probable Modes of Vibration, Stage One Blade.



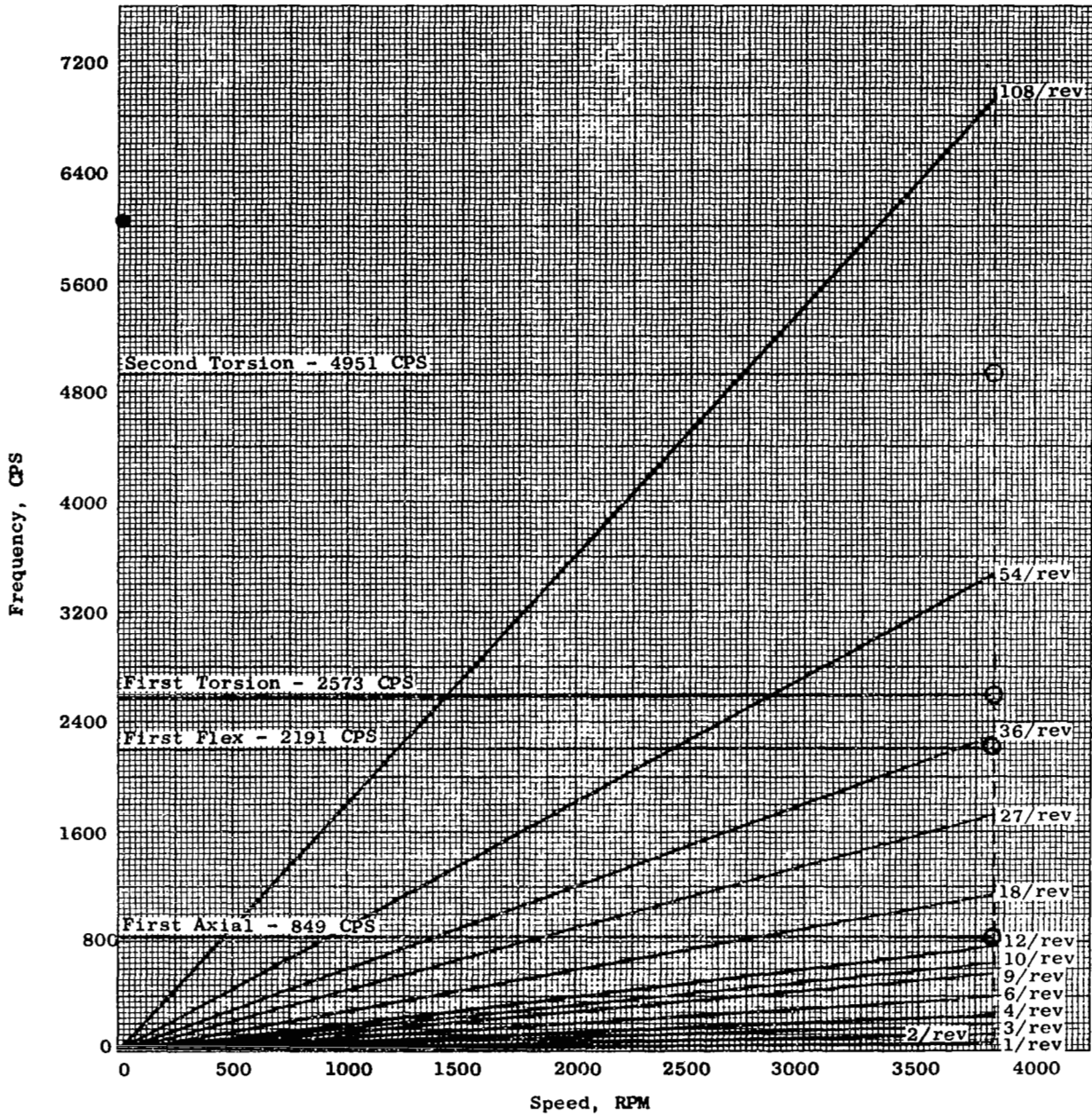


Figure 75. Most Probable Modes of Vibration, Stage Two Blade.

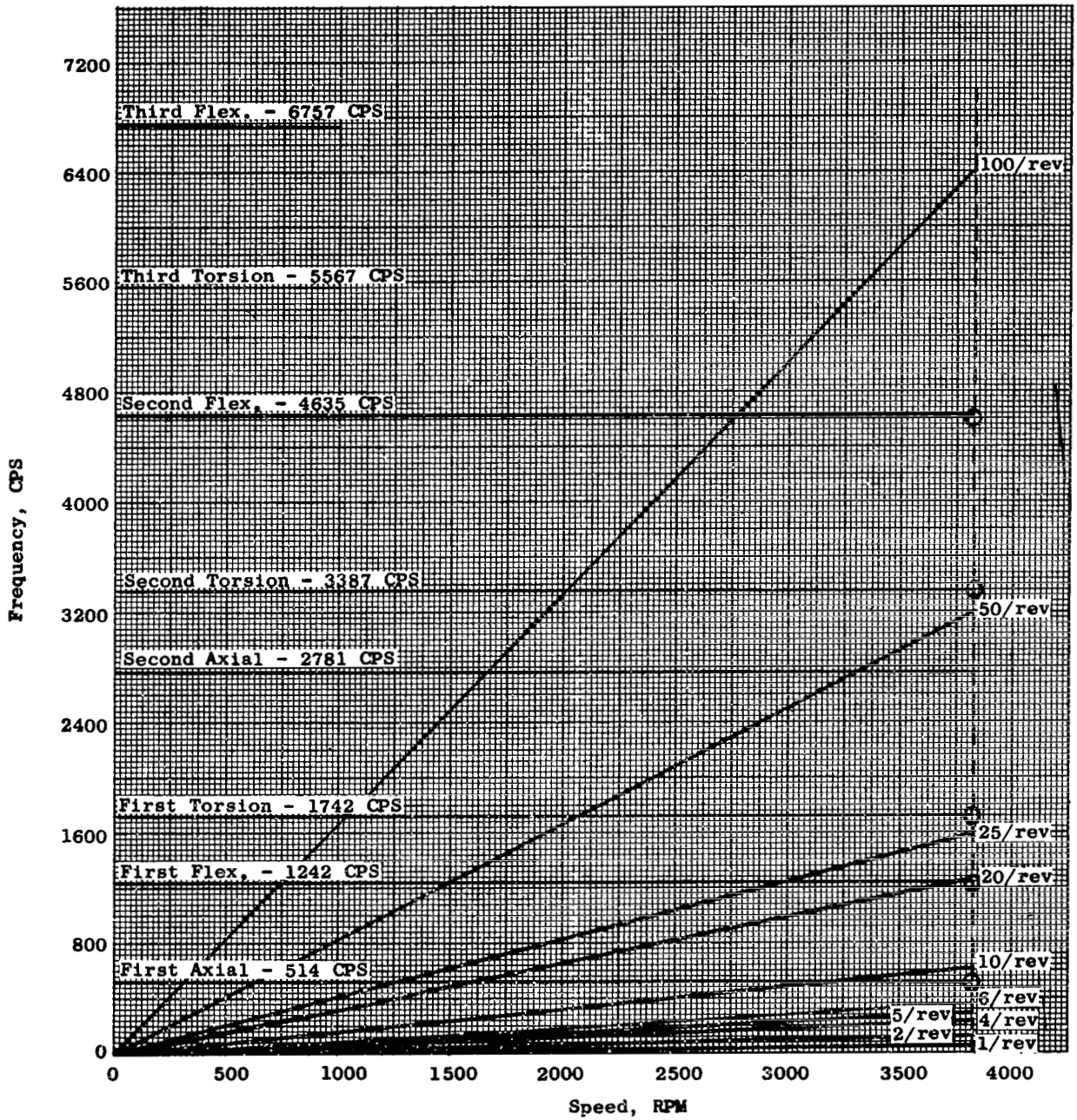


Figure 76. Most Probable Modes of Vibration, Stage Three Blade.

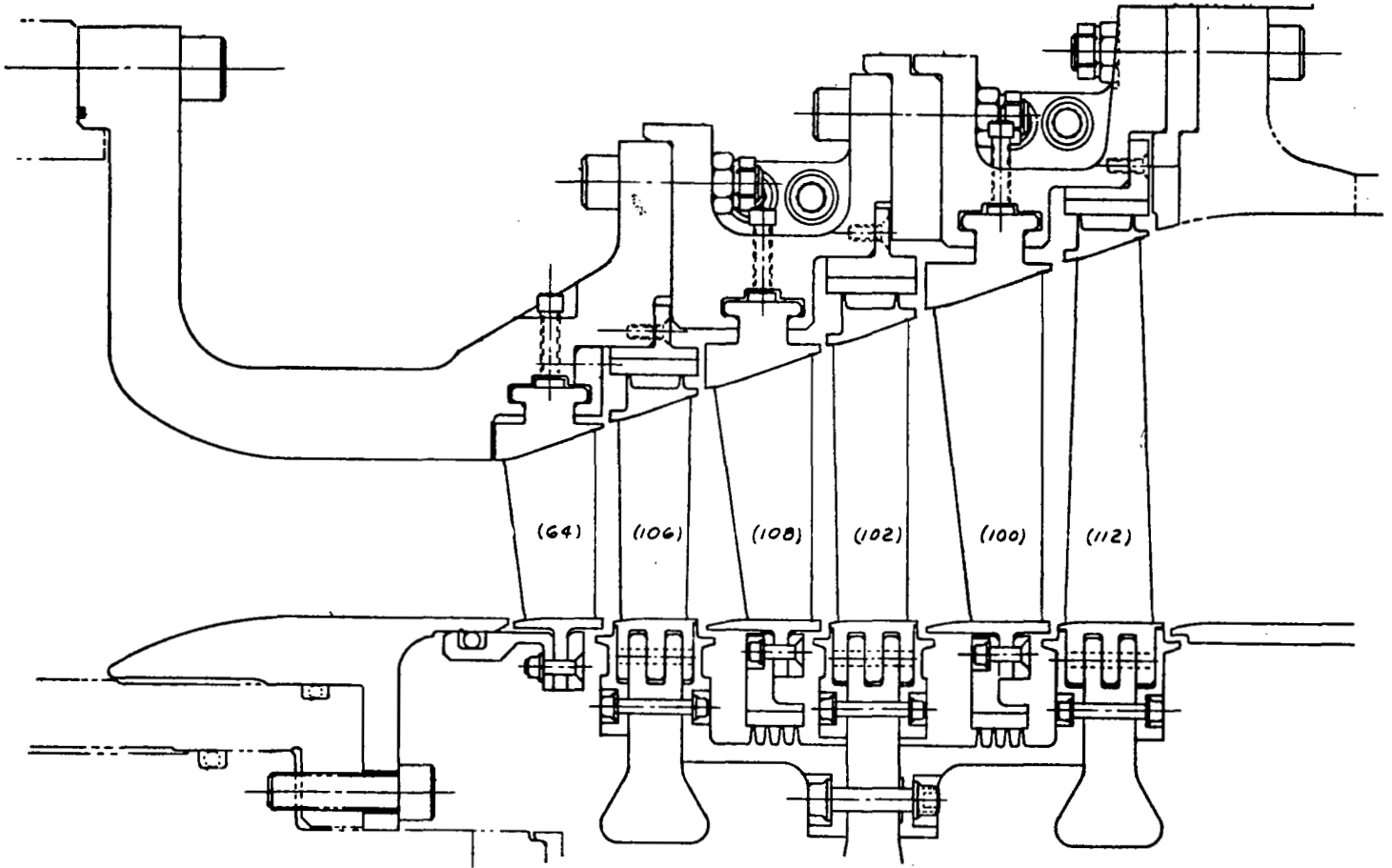


Figure 77. Mechanical Design Flowpath.